

THE REGULATION OF INTEGRIN ACTIVATION AND RECYCLING BY RSK2

PROMOTES CANCER MIGRATION AND INVASION

A DISSERTATION SUBMITTED TO THE GRADUATE DIVISION OF THE  
UNIVERSITY OF HAWAI'I AT MĀNOA IN PARTIAL FULFILLMENT  
OF THE REQUIREMENTS FOR THE DEGREE OF

DOCTOR OF PHILOSOPHY  
IN  
CELL AND MOLECULAR BIOLOGY

AUGUST 2016

BY  
SHIRLEY SUMI YOUNG

DISSERTATION COMMITTEE:

JOE W. RAMOS (CHAIRPERSON)

PETER HOFFMAN

MICHELLE L. MATTER

JAMES TURKSON

PHILIP WILLIAM

© Copyright by  
Shirley Sumi Young  
All Rights Reserved  
August 2016

To my family

## ACKNOWLEDGMENTS

I owe a debt of gratitude to my advisor, Dr. Joe Ramos, for the continuous support of my doctoral research and his patience, encouragement, and knowledge. His guidance was invaluable in the completion of this degree, and it was a privilege to be led by an advisor who possesses a genuine passion for science.

I would like to acknowledge the rest of my committee, Dr. Peter Hoffman, Dr. Michelle Matter, Dr. James Turkson, and Dr. Philip Williams for their thought-provoking questions and insightful comments that helped shaped my dissertation. I sincerely thank you for your time and support.

I am deeply thankful to all the members of the Ramos and Matter Labs for the inspiring discussions and fun we had throughout the years. I would particularly like to thank Chena Bryan, Maisel Caliva, Florian Sulzmaier, Paul Anastasiadis, Mayumi Jijiwa, and Laura Halpin-Garcia for making my Ph.D. experience so memorable. Also, I am grateful to interns Maveric Abella and Jeffery Sakamoto for their assistance in my project.

My sincere thanks also goes to Dr. Chris Farrar for the training and support on live imaging and confocal microscopy conducted in this research. Her expertise was instrumental in the success of the brain slice invasion assay.

Last but not the least, I would like to thank my husband, Mark, for believing in my education and my sister, Sally for being my biggest cheerleader.

## ABSTRACT

Integrins are cell-surface receptors that mediate cellular processes that occur during development and in the progression of disease such as cancer. Integrins signal bidirectionally across the plasma membrane. Outside-in signaling is activated upon ligation of integrins to ECM molecules and elicits intracellular responses to environmental cues. Inside-out signaling cascades, such as the RAS MAPK pathway, modulate the affinity of integrins for their ligands and therefore, regulate integrin activation. RSK2 functions downstream of the RAS and mediates several biological functions of the RAS MAPK pathway, such as the cell cycle, proliferation, and survival. We investigated RSK2 effects on integrin function and found that RSK2 mediates H-RAS inactivation of integrins. As a consequence, RSK2 impairs cell adhesion and promotes cell migration. RSK2 co-precipitated with talin and filaminA from  $\beta$ -integrin tail complexes, and thereby, we conclude in a position to modulate talin activation of integrins and inactivation by filaminA. RSK2 phosphorylation of filaminA at S2152 enhanced filaminA association with  $\beta$ -integrin tails and regulated filaminA-mediated migration. Furthermore, we find that PEA-15 (Phosphoprotein enriched in astrocytes of 15 kDa) is a requirement for efficient recycling of internalized  $\alpha_5\beta_1$  integrins in a manner dependent on RSK2 activity. We propose that RSK2 promotes a highly migratory phenotype as a consequence of filaminA inactivation and subsequent recycling of integrins from the trailing edge of a cell to the advancing leading edge. We also observed that RSK2 promotes invasion and migration in established glioblastoma cell lines U87MG and U373MG and migration in fresh human-derived GBM cells and into cultured mouse brain slices. We present data that indicates inhibition of RSK2 can sensitize GBM cells to chemotherapy

treatment with temozolomide. In agreement with our *in vitro* data, using public datasets, we find that RSK2 expression is significantly upregulated in human GBM patients and correlates with advanced tumor stage and poor prognosis. Taken together, these results reveal RSK2 as a key regulator of integrin activity and provide a novel mechanism by which RSK2 promotes invasion and migration.

# TABLE OF CONTENTS

<b>DEDICATION</b> .....	<b>iii</b>
<b>ACKNOWLEDGMENTS</b> .....	<b>iv</b>
<b>ABSTRACT</b> .....	<b>v</b>
<b>Table of Contents</b> .....	<b>vii</b>
<b>List of Tables</b> .....	<b>x</b>
<b>List of Figures</b> .....	<b>xi</b>
<b>List of Abbreviations</b> .....	<b>xiii</b>
<b>List of Publications</b> .....	<b>xvii</b>
<b>Chapter 1</b> .....	<b>1</b>
<b>Introduction</b> .....	<b>1</b>
<b>1.1 Integrins</b> .....	<b>2</b>
History .....	2
Structure .....	3
Regulation of integrin activation.....	4
Integrin-mediated cell migration.....	7
<b>1.2 RSK2</b> .....	<b>8</b>
Ribosomal protein s6 kinase alpha -3.....	8
RSK2 structure and the regulation of RSK2 activation.....	9
RSK2 substrates.....	12
RSK2 phenotype and RSK expression.....	15
Chemical inhibitors of RSK .....	16
<b>1.3 Tables</b> .....	<b>19</b>
<b>1.4 Figures</b> .....	<b>23</b>
<b>Chapter 2</b> .....	<b>36</b>
<b>RSK2 suppresses integrin activation and promotes cell migration</b> .....	<b>36</b>
<b>2.1 Introduction</b> .....	<b>37</b>
<b>2.2 Results</b> .....	<b>39</b>
RSK2 inhibits integrin activation .....	39
RSK2 enhances integrin-mediated cell migration .....	39
RSK2 associates with integrin cytoplasmic tails .....	40
RSK2 phosphorylates filaminA and promotes its binding to integrin tails .....	41
FilaminA and RSK2 colocalize at the plasma membrane.....	41
RSK2 and filaminA are enriched in the trailing edge of a migrating cell .....	43
UniRapR RSK2 .....	43
RSK2 induces focal adhesion disassembly in a microtubule-independent manner .....	45
RSK2 regulates filaminA-mediated cell migration .....	46

2.3	<b>Discussion</b> .....	47
2.4	<b>Materials and Methods</b> .....	49
	Antibodies, inhibitors, and plasmids .....	49
	UniRapR RSK2 construction.....	49
	Cell culture and transfections.....	50
	Immunoblotting.....	51
	Generation of M2 melanoma cell lines.....	51
	Immunostaining and microscopy .....	52
	Nocodazole washout assay .....	52
	Migrations assays.....	52
	Integrin pull-down assays.....	53
	Integrin activation assay.....	54
	<i>In vitro</i> kinase Assays .....	55
	ADP-Glo kinase assay .....	55
2.5	<b>Figures</b> .....	57
<b>Chapter 3</b> .....		<b>86</b>
<b>RSK2 activity mediates glioblastoma invasiveness and is a potential target for new therapeutics.</b> .....		<b>86</b>
3.1	<b>Introduction</b> .....	87
3.2	<b>Results</b> .....	89
	RSK2 activity is required for GBM cell migration and invasion.....	89
	RSK2 modulates cellular adhesion and is required for migration into mouse brain slices.....	89
	RSK2 activity drives patient-derived GBM cell migration and invasion .....	90
	RSK inhibition enhances the effectiveness of standard GBM therapy .....	91
	RSK2 expression is elevated in human glioma tissue, correlates with high tumor grade, and is prognostic for poor patient outcome .....	92
3.3	<b>Discussion</b> .....	94
3.4	<b>Materials and Methods</b> .....	96
	Human cell lines and reagents .....	96
	Brain slice invasion assay.....	96
3.5	<b>Figures</b> .....	98
<b>Chapter 4</b> .....		<b>113</b>
<b>PEA-15 is an endosomal-associated and microtubule-binding phosphoprotein that regulates <math>\alpha_5\beta_1</math> integrin recycling</b> .....		<b>113</b>
4.1	<b>Introduction</b> .....	114
4.2	<b>Results</b> .....	116
	Phosphorylated PEA-15 regulates $\alpha_5\beta_1$ integrin recycling.....	116
	PEA-15 is required for cell migration in U87MG Cells.....	117
	PEA-15 complexes with $\beta$ -integrin tails and sorts integrins to endosomes.....	118
	PEA-15 directly interacts with polymerized microtubules and is required for .....	119

microtubule-dependent cell morphology.....	119
RSK2 activity is required for PEA-15 mediated recycling of integrins.....	119
<b>4.5 Discussion .....</b>	<b>121</b>
<b>4.4 Material and Methods .....</b>	<b>124</b>
Cell culture and reagent .....	124
Migration assay.....	124
Tumor spheroid invasion assay.....	125
Integrin tail pulldown .....	125
Microtubule regrowth assay .....	125
Degradation assay.....	126
Integrin recycling assay.....	126
Capture ELISA.....	127
<b>4.5 Figures.....</b>	<b>128</b>
<b>Chapter 5 .....</b>	<b>141</b>
<b>Future Direction .....</b>	<b>141</b>
<b>5.1 Discussion .....</b>	<b>142</b>
<b>5.2 Materials and Methods .....</b>	<b>147</b>
Immunoprecipitation .....	147
Immunostaining and microscopy .....	147
ADP-Glo kinase assay .....	147
<b>5.3 Figures.....</b>	<b>149</b>
<b>Appendix .....</b>	<b>156</b>
<b>References .....</b>	<b>159</b>

## LIST OF TABLES

1.1	The integrin family of cell adhesion receptors	20
1.2	RSK2 substrates	21

## LIST OF FIGURES

FIGURE 1.1 INTEGRINS ARE HETERODIMERIC CELL ADHESION RECEPTORS	24
FIGURE 1.2 INTEGRINS ARE ACTIVATED BY INSIDE-OUT SIGNALING	26
FIGURE 1.3 CELL MIGRATION IS A MULTISTEP CYCLIC PROCESS	28
FIGURE 1.4 THE STRUCTURE AND REGULATION OF RSK2 ACTIVATION	30
FIGURE 1.5 RSK2 SUBSTRATES ARE BOTH CYTOSOLIC AND NUCLEAR	32
FIGURE 1.6 CHEMICAL STRUCTURE OF RSK2 INHIBITORS	34
FIGURE 2.1 RSK2 INHIBITS INTEGRIN ACTIVATION AND IMPAIRS CELL ADHESION	58
FIGURE 2.3 RSK2 ASSOCIATES WITH INTEGRIN TAIL COMPLEXES	62
FIGURE 2.4 RSK2 MODULATES FILAMINA BINDING TO INTEGRIN TAILS	64
FIGURE 2.5 MODEL OF RSK2 MEDIATED TLN/FLNA EXCHANGE ON INTEGRIN TAIL	66
FIGURE 2.6 RSK INHIBITOR IMPAIRS FLNA DISTRIBUTION AT THE PLASMA MEMBRANE	68
FIGURE 2.7 FILAMINA AND RSK2 COLOCALIZE AT THE PLASMA MEMBRANE	70
FIGURE 2.8 THE LOCALIZATION OF RSK2 IN A MIGRATING CELL.	72
FIGURE 2.9 RSK2 AND FLNA COLOCALIZE AT THE TRAILING EDGE OF A MIGRATING CELL	74
FIGURE 2.10 UNIRAPR RSK2	76
FIGURE 2.11 UNIRAPR RSK2 PHOSPHORYLATES SP6 AND PROMOTES MIGRATION	78
FIGURE 2.12 IMMUNOFLOUORESCENT MICROGRAPH OF UNIRAPR RSK2	80
FIGURE 2.13 RSK2 STIMULATES FOCAL ADHESION DISASSEMBLY	82
FIGURE 2.14 RSK2 REGULATES FLNA-MEDIATED MIGRATION	84
FIGURE 3.1 RSKS ARE REQUIRED FOR GBM MIGRATION AND INVASION	99
FIGURE 3.2 RSK2 ACTIVITY REDUCES CELL ADHESION TO FIBRONECTIN AND PROMOTES MIGRATION INTO MOUSE BRAIN SLICES	101
FIGURE 3.3 PATIENT-DERIVED GBM REQUIRE RSK2 FOR INVASION AND MIGRATION	103
FIGURE 3.4 INHIBITION OF RSK2 SENSITIZES RESISTANT PATIENT-DERIVED GBM TO TEMOZOLOMIDE	105
FIGURE 3.5 RSK2 MRNA EXPRESSION IS HIGHER IN HUMAN GLIOMA THAN IN NORMAL BRAIN TISSUE	107
FIGURE 3.6 RSK2 MRNA EXPRESSION CORRELATES WITH HIGH HUMAN GLIOMA TUMOR STAGE	109

FIGURE 3.7 RSK2 MRNA EXPRESSION IS PROGNOSTIC FOR POOR GLIOMA PATIENT PROGNOSIS	111
FIGURE 4.1 PHOSPHORYLATED PEA-15 REGULATES $\alpha_5\beta_1$ INTEGRIN RECYCLING	129
FIGURE 4.2 PEA-15 IS REQUIRED FOR CELL MIGRATION	131
FIGURE 4.3 PEA-15 SORTS $\beta_1$ INTEGRINS TO ENDOSOMES	133
FIGURE 4.4 PEA-15 REGULATES CELL MORPHOLOGY IN A MICROTUBULE DEPENDENT MANNER	135
FIGURE 4.5 PEA-15 MEDIATED RECYCLING OF $\alpha_5\beta_1$ INTEGRINS REQUIRES RSK2 ACTIVITY	137
FIGURE 4.6 MODEL OF RSK2-PEA-15 AXIS REGULATING RECYCLING OF $\alpha_5\beta_1$ INTEGRINS	139
FIGURE 5.1 PIPK1 $\gamma$ 90 IS A SUBSTRATE OF RSK2	150
FIGURE 5.2 COLOCAZIATION OF PIPK1 $\gamma$ 90 AND RSK2	152
FIGURE 5.3 RSK2 REGULATES CELL ADHESION TO PROMOTE MIGRATION THROUGH PHOSPHORYLATON OF FILAMINA AND PIPK1 $\gamma$ 90.	154

## LIST OF ABBREVIATIONS

ADP	Adenosine diphosphate
AKT	Protein kinase B
ATP	Adenosine triphosphate
BSA	Bovine serum albumin
CAMK	Ca <sup>2+</sup> /calmodulin-dependent protein kinase
CDC42	Cell division control protein 42 homolog
CDK	Cyclin-dependent kinase
CLS	Coffin Lowery Syndrome
cScr	Cytoplasmic sarcoma
CTKD	C-terminal kinase domain
DA	Dominant active
DED	Death effector domain
DN	Dominant negative
DOCK	Dedicator of cytokinesis 3
DPBS	Dulbecco's phosphate-buffered saline
ECM	Extracellular matrix
EDTA	Ethylenediaminetetraacetic acid
EGF	Extracellular growth factor
EGTA	Ethylene glycol-bis( $\beta$ -aminoethyl ether)-N,N,N',N'-tetraacetic acid
ELISA	Enzyme-linked immunosorbent assay
ERK	Extracellular signal-regulated kinase

FA	Focal adhesion
FAK	Focal adhesion kinase
FBS	Fetal bovine serum
FLNa	FilaminA
FN9.11	Recombinant fibronectin comprised of RGDS repeats
GAP	GTPase activating protein
GBM	Glioblastoma multiforme
GDI	Guanosine nucleotide dissociation inhibitor
GDP	Guanosine diphosphate
GEF	Guanosine exchange factor
GFP	Green fluorescence protein
GRB2	Growth factor receptor-bound protein 2
GST	Glutathione <i>S</i> -transferase
GTP	Guanosine triphosphate
HA	Human influenza hemagglutinin
HRP	Horse radish peroxidase
KD	Knock-down
KO	Knock-out
MAPK	Mitogen activated protein kinase
MEK	Mitogen activated protein kinase kinase
MESNA	Sodium 2-sulfanylethanesulfonate
MKP1	Mitogen-activated protein kinase (MAPK) phosphatase 1

MLCK	Myosin light chain kinase
mRNA	Messenger ribonucleic acid
mTOR	Mammalian target of rapamycin
Myc	Myc oncogene
NTKD	N-terminal kinase domain
ntRNA	Nontarget hairpin RNA
OPD	<i>o</i> -phenylenediamine dihydrochloride,
p130Cas	CRK-associated substrate
PAK	p21-activated kinase
PBS	Phosphate-buffered saline
PDK1	3-phosphoinositide dependent protein kinase-1
PEA-15	15 kDa phosphoprotein enriched in astrocytes
PIP	Phosphatidylinositol phosphate
PIP2	Phosphatidylinositol bisphosphate
PIP3	Phosphatidylinositol triphosphate
PIP3K1	Phosphatidylinositol-4-phosphate 5-kinase
PMSF	Phenylmethanesulfonylfluoride
PTB	Phosphotyrosine binding domain
Rac	Ras-related C3 botulinum toxin substrate 1
Raf	Rapidly accelerated fibrosarcoma
RAP	Ras related protein
Ras	Rat sarcoma

Rho	Ras homolog
RIAM	Rap1-GTP-interacting adaptor molecule
Rock	Rho-associated protein kinase
rpS6	40S ribosomal subunit protein S6
RSK	90 kDa ribosomal S6 kinase
SDS-PAGE	Sodium dodecyl sulfate polyacrylamide gel electrophoresis
Ser	Serine
SH	Src Homology domain
sh	Short hairpin RNA
SOS	Son of sevenless
THD	Talin head domain
Thr	Threonine
TLN	Talin
TPBS	Tween phosphate-buffered saline
Tyr	Tyrosine

## LIST OF PUBLICATIONS

- I. RSK2 activity mediates glioblastoma invasiveness and is a potential target for new therapeutics. Sulzmaier, F.J., and **Young-Robbins, S.S.**, Jiang, P., Geerts', D., Prechtel, A., Matter, M.L., Santosh, K., & Ramos, J.W. *Oncotarget* (revision).
- II. PEA-15 is an endosomal and microtubule-binding phosphoprotein that regulates  $\alpha 5 \beta 1$  integrin recycling. Caliva, M.J., and **Young-Robbins, S.S.**, Valmiki, M.J., Opoku-Ansah, J., Vaidyanathan, H., Matter, M.L., Grimes, M.L., & Ramos, J.W. *JCB*. (revision).
- III. RSK2 suppresses integrin activation and fibronectin matrix assembly and promotes cell migration. Gawecka, J.E., and **Young-Robbins, S.S.**, Caliva, M.J., Sulzmaier, F.J., Heikkilä, M.M., Matter, M.L. & Ramos, J.W. *J. Biol.Chem.* 287(52): 43424-43437 (2012).
- IV. Bit-1 mediates integrin-dependent cell survival through activation of the NF $\kappa$ B pathway. Griffiths, G.S., Grundl, M., Leychenko, A., Reiter, S., **Young-Robbins, S.S.**, Sulzmaier, F.J., Caliva, M.J., Ramos, J.W. & Matter. M.L. *J. Biol. Chem.* 286(16): 14713-23 (2011).

# CHAPTER 1

## INTRODUCTION

## 1.1 INTEGRINS

### HISTORY

Integrins represent the largest family of cell adhesion receptors that mediate cell-extracellular matrix (ECM) and cell-cell adhesion. Integrins regulate critical cellular processes such proliferation, cell growth, differentiation, and migration by providing a functional link between the extracellular environment and the cytoskeleton. The discovery of integrins was driven in large part by research into the growth differences between normal and transformed cells. In 1973, R.O. Hynes observed that the ECM protein fibronectin was present on the surface of a normal cell to a much greater extent than of transformed cells<sup>1, 2</sup>; and that surface association of fibronectin correlated with an increase cell adhesion and spreading in normal cells, whereas transformed cells were loosely adherent and were displayed rounded morphology. Furthermore, when purified fibronectin was exogenously added to the media, the transformed cells became more adherent and the normal cell morphology restored<sup>3, 4</sup>.

The identification of integrins as the fibronectin cell surface receptor relied on two distinct research strategies. The first utilized affinity chromatography with peptide fragments of fibronectin that could bind proteins, such as fibrin, that mediate cell adhesion. This approach identified the minimal binding sequence in fibronectin as the tetrapeptide, RGDS<sup>5</sup>. The second strategy relied on a screen for monoclonal antibodies that interfered with adhesion of myoblast to matrix-coated surfaces. This resulted in the isolation of two antibodies, CSAT and JG22, which recognize antigens that lined up with both fibronectin and actin<sup>2, 6, 7</sup>, thus supporting the hypothesis that the ECM and cytoskeleton were linked. By

1986, the receptor had been cloned and sequenced from the CSAT complex and was given the name “integrin” for its function as an integral membrane protein linking the extracellular matrix to the cytoskeleton<sup>8</sup>.

## STRUCTURE

Integrins are Type I heterodimeric receptors that consist of two non-covalently bound  $\alpha$  and  $\beta$  subunits (fig 1.1). There are eighteen  $\alpha$  and eight  $\beta$  mammalian subunits that combine to form 24 distinct integrins that bind extracellular proteins differentially<sup>9</sup>; although most integrins recognize several ECM proteins, some are highly specific such as  $\alpha_5\beta_1$ , which only recognizes fibronectin (table 1.1). Each heterodimer consists of a large extracellular domain that binds to ligands, a single-pass transmembrane domain, and a short cytoplasmic domain. The cytoplasmic domains or tails form links with the cytoskeleton through cytoplasmic adaptor proteins<sup>9</sup>. The tails of the  $\beta$  subunit are highly homologous and contain NPxY motifs that bind proteins containing PTB (phosphotyrosine binding) domains. There are conserved GFFKR and HDR(RIK)E sequences in the membrane proximal regions of the  $\alpha$  and  $\beta$  tails, respectively, that form a putative salt bridge between the arginine (R) of the  $\alpha$  subunit and the aspartic acid (D) of the  $\beta$  unit<sup>10, 11</sup>. Although unconfirmed by structural data, the salt bridge is thought to have a regulatory role in integrin activation. The  $\alpha$  subunit tails are highly divergent and with the exception of paxillin, little is known about proteins that interact with them.

Integrins exist in three distinct conformational states that correspond to differences in affinity for ligand<sup>9</sup>. On the cell surface integrins are typically expressed in a bent-closed

state. The salt bridge is thought to maintain this inactive low-affinity state<sup>12, 13</sup>. Upon activation by intracellular cues, integrins extend their extracellular domains to attain the extended-closed or intermediate affinity state. In this state, the salt bridge is intact and integrins bind their ligand to a limited degree. If the relative concentrations of extracellular ligands and intracellular signaling cues are sustained the salt bridge will be disrupted and the integrin transmembrane domains will part to attain the open-extended high-affinity state.

#### REGULATION OF INTEGRIN ACTIVATION

In addition to their role as adhesion receptors, integrins transduce signal bi-directionally across the plasma membrane. Upon binding to the ECM, integrins undergo conformational changes that lead to the “outside-in” transduction of external signals. When bound to multivalent ligands, integrins cluster at the plasma membrane where their cytoplasmic tails serve as platforms for the recruitment of adaptor and signaling proteins to form focal complexes. Focal complexes are transient and either disassemble or mature into focal adhesions (FA). FAs link the actin cytoskeleton to the ECM and mediate cellular responses to external signals such as proliferation and migration.

Inside-out signaling pathways regulate integrin affinity for its ligand (fig 1.2). The signals originate from cell surface receptors or cytoplasmic proteins that activate signaling cascades that lead to the activation or inactivation of integrins. The RAS superfamily of small GTPases modulate integrin activation differentially depending upon the RAS isoform and cell

type involved<sup>14</sup>. For example, R-RAS in fibroblast activates integrins<sup>15</sup>, whereas H-RAS is implicated in the inactivation of integrins.

The cytoplasmic adaptor protein, talin, is an important regulator of the activation of integrins and the formation of the integrin-cytoskeleton linkage. Currently, there are two models that describe the activation of talin to bind  $\beta$ -integrin tails: activation by phospholipid phosphatidylinositol 4,5-bisphosphate (PIP<sub>2</sub>) or activation by Rap1<sup>16,17</sup>. Rap1 GTPase is a positive regulator of integrin activation via its effector Rap1-GTP-interacting adaptor molecule (RIAM). Overexpression of RIAM induces integrin activation and cell adhesion; conversely, knockdown of RIAM displaces Rap1-GTP from plasma membrane and abrogates Rap1-induced adhesion.<sup>17, 18</sup> Calcium-induced loading of GTP by Rap1 induces formation of an “integrin activating complex” of RIAM and talin, which then targets talin to the integrin and where it is subsequently activated<sup>17,19</sup>.

Phospholipid phosphatidylinositol 4,5-bisphosphate is highly enriched in the plasma membrane and interacts with many focal adhesions proteins, including talin<sup>20</sup>. The binding of talin to  $\beta$ -integrin tails is regulated through its interaction with PIP<sub>2</sub>. PIP<sub>2</sub> binds to talin's head domain (THD), which releases an autoinhibitory interaction between the integrin-binding site within the head domain and talin's rod domain<sup>21,22</sup>. The subdomains of the THD electrostatically interact with PIP<sub>2</sub> in the plasma membrane and orient talin for optimal binding to the  $\beta$ -integrin tail<sup>23</sup>.

Kindlin potentiates the activation of integrins by talin. There are three isoforms of kindlin (1-3) in humans and all cooperate with talin<sup>24</sup>. The mechanism by which kindlin exerts its positive effects on talin-mediated activation is not known. Kindlin binding to integrin tails is necessary for the activation of the integrins, but not sufficient<sup>25</sup>. Calderwood

*et al.* suggest four modes in which kindlin may act as a co-activator of integrins; 1) kindlin binding to integrins tails may orientate talin for optimal binding to the tails; 2) kindlin may serve as adaptor protein that induces integrin clustering to increase avidity of integrin adhesion; 3) kindlin recruits other activators to cooperate with talin; and lastly, 4) kindlin may displace inhibitors of integrin activation<sup>25</sup>.

Adaptor proteins that inhibit integrin activation negatively modulate talin-integrin tail interactions. Integrin inactivators bind to the  $\alpha$ -tails or bind NPxY motifs on the  $\beta$ -tails<sup>26-28</sup>. Talin binds to the membrane-proximal NPxY motif in the integrin tails<sup>25, 28-30</sup>. Tyrosine phosphorylation within this motif by SRC decreases talin's binding affinity and promotes binding of scaffolding protein DOK1 (docking protein 1)<sup>25, 26, 30</sup>. Another protein that binds  $\beta$ -integrin tails via its PTB domain is ICAP1. Unlike DOK1, ICAP1 binds to the membrane-distal NPxY motif and suppresses kindlin-integrin interactions to prevent activation by talin<sup>25, 26, 28, 30</sup>. KRIT1 complexes with ICAP1 to terminate its inhibitory effect. FilaminA, a large actin cross-linking protein, simultaneously bind both membrane-proximal and membrane-distal NPxY motifs on the  $\beta$ -integrin tail<sup>26, 28, 31</sup>. FilaminA has been shown *in vitro* to displace talin on the  $\beta$ -integrin tails in a dose-dependent manner<sup>31</sup>. Sharpin is the only ubiquitously expressed inactivator that binds to the  $\alpha$ -subunit of the heterodimer<sup>26, 27</sup>. Sharpin engages with inactive integrins and binds to the conserved WKXGFFKR sequence of the  $\alpha$ -tail, suggesting Sharpin has a role in maintaining the salt bridge to keep integrins inactive(fig 1.1)<sup>26, 27</sup>. MDGI (mammary-derived growth inhibitor) binds to the  $\alpha$ -tail specifically in mammary epithelial cells and inhibits  $\beta_1$  integrins<sup>32</sup>.

## INTEGRIN-MEDIATED CELL MIGRATION

Cell migration is an elaborate and highly regulated process that requires dynamic interaction between the cytoskeleton and ECM at the leading and trailing edge of a cell. Migration occurs through an integrated multistep cycle (fig 1.3) of protrusion, adhesion assembly and maturation at the leading, cell body translocation, adhesion disassembly and detachment at the cell's rear<sup>33-35</sup>. The spatial and temporal regulation of adhesion strength is critical during migration and is influenced by the surface expression, surface density, recycling and activation state of integrins. In metastasis any one of or all integrin-related variables is aberrant.

At the leading edge of a migrating cell, integrin clustering leads to the formation and maturation of FA by forming links to actin stress fibers in a process that is regulated by Rho/ROCK GTPases<sup>36, 37</sup>. The linkage exerts force on the focal adhesions that stimulates integrin-mediated signaling which results in the phosphorylation of myosin light chain by myosin light chain kinase (MLCK)<sup>36, 37</sup> and increased contractility. The binding of talin and paxillin to  $\beta$ -integrins tail, recruit focal adhesion kinase (FAK) and its subsequent activation by the Src family of kinases<sup>38</sup>. The FAK/Src complex activates CRK-associated substrate (p130Cas), which then facilitates the activation of RAS-related C3 botulinum toxin substrate 1(RAC) via GEF Dock 1(DOCK1)<sup>38, 39</sup>. RAC1 activation leads to membrane ruffling and the formation of lamellipodia<sup>40</sup>.

Focal adhesion disassembly and turnover are critical to cell migration. However, the molecular events that promote FA disassembly are not well defined and our knowledge fragmented. It well established that microtubules have an essential role in FA disassembly<sup>41-</sup>

<sup>43</sup>. Focal adhesion disassembly is initiated by the extension of microtubules to the FA which subsequently are destabilized by calpain cleavage of FAK, paxillin, and talin<sup>41, 43</sup>. In addition to its role in FA maturation, FAK also participates in FA turnover<sup>41, 44</sup>. FAK recruits the endocytosis regulator dynamin into FA via its interaction with the adaptor protein Grb2 to the integrin and initiates the latter's internalization<sup>45, 46</sup>.

## 1.2 RSK2

### RIBOSOMAL PROTEIN S6 KINASE ALPHA -3

Ribosomal protein S6 kinase alpha-3 (RSK2) is a member of the p90RSK family of serine/threonine kinases whose downstream targets regulate transcription, proliferation, growth, survival, and migration. Erikson and Maller purified RSK from unfertilized *Xenopus laevis* eggs in 1985 and subsequently, identified RSK as the kinase that phosphorylated rpS6 (40S ribosomal subunit protein S6)<sup>47</sup>. Since its discovery, four mammalian isoforms have been identified. The four isoforms, RSK1- RSK4, share 73-80% homology sequence homology and have highly conserved functional motifs<sup>48-52</sup>. Orthologues of RSK are found in *Drosophila melanogaster*, and *Caenorhabditis elegans*, but not in yeast or plants<sup>53</sup>. Members of the p90RSK family of kinases include two structurally related homologues, MSK1 (mitogen-and stress-activated kinase-1) and MSK2 (mitogen-and stress-activated kinase-1)<sup>54-56</sup>.

RSK2 is an effector of the RAF/MEK/ERK mitogen-activated protein kinase pathway (fig 1.5). The cascade lies downstream of the small GTPase RAS that serves as a molecular switch to turn the signaling cascade on and off. RAS GTPase cycles from a guanosine diphosphate

(GDP)-bound inactive state to an active state that it is bound to guanosine triphosphate (GTP). RAS activation occurs upon extracellular mitogen binding to the epidermal growth factor receptor (EGFR), a receptor tyrosine kinases (RTK). Dimerization of the ligand-bound receptor promotes autophosphorylation of its cytoplasmic tyrosine residues forming a docking site for the adaptor protein, GRB2 (Growth factor receptor-bound protein 2). Meanwhile, GRB2 binds to Son of Sevenless (SOS) via its two SH3 domains. The GRB2-SOS complex binds to the phosphotyrosines in the receptor through the SH2 domain of GRB2 leading to activation of SOS. Activated SOS, a guanine nucleotide exchange factor, promotes the exchange of RAS-bound GDP for cytosolic GTP. Active RAS binds RAF (Rapidly Accelerated Fibrosarcoma) releasing RAF autoinhibition. RAF, a serine/threonine kinase, initiates the cascade that activates the tyrosine/threonine kinase MEK (mitogen-activated protein kinase kinase) that then activates the serine/threonine kinase ERK (extracellular signal-regulated kinase). RSK2 is a substrate of ERK<sup>47</sup>.

#### RSK2 STRUCTURE AND THE REGULATION OF RSK2 ACTIVATION

RSK2 is an unusual kinase in that it contains two structurally distinct but functional kinase domains (fig 1.4). The N-terminus kinase domain (NTKD) is homologous to the AGC (protein kinase A, G, and C) family of kinases, which also include AKT (protein kinase B)<sup>54-56</sup>. Whereas, the C-terminus kinase domain (CTKD) is closely related to the CAMK (Ca<sup>2+</sup> / calmodulin-dependent protein kinases) family, whose members include AMPK (AMP-activated protein kinase, MARK (MAP-regulating kinase) and DAPK (death-associated protein kinase)<sup>54-56</sup>. The only known function of the CTKD is to activate the NTKD, which phosphorylates substrates that are both nuclear and cytoplasmic. A conserved regulatory

linker that consists of a helix-turn motif and hydrophobic motif connects the two kinase domains. A D-domain docking site lies in the C-terminal end of RSK2 followed by a type 1 PDZ (post synaptic density protein ; PSD95), Drosophila disc large tumor suppressor (Dlg1), and zonula occludens-1 protein (ZO-1) - binding domain motif<sup>54</sup>. The D-type ERK1/2 docking sequence (L-Xaa<sub>2</sub>-K/R-K/R-Xaa<sub>5</sub>-L) in RSK does not contain the typical sequence found in D-domains, rather it more closely aligns with the KIM (kinase interaction motif) consensus sequence<sup>54</sup>.

The activation of RSK2 is complicated and not fully elucidated. It requires autophosphorylation, the input of several kinases and is spatially regulated<sup>54-56</sup>. All isoforms of RSK contain six residues that become phosphorylated upon mitogen stimulation<sup>57</sup>. Using mutational analysis Darby *et al.* identified that four of the six sites are essential for RSK activation in humans and determined the hierarchy in which they are phosphorylated. In RSK2 those sites are S227, S369, S386, and T577<sup>57</sup>. The current model (fig 1.4) suggests that ERK initiates RSK2 activation by binding to the C-terminal D-domain and subsequent phosphorylation of T577 and possibly T365 and S369<sup>57</sup>. This activating step requires the targeting of ERK to RSK2 by the scaffolding protein PEA-15 (15 kDa phosphoprotein enriched in astrocytes)<sup>58</sup>. Mutants of PEA-15 that cannot bind ERK or RSK2 do not enhance ERK phosphorylation of RSK2. Similarly, RSK2 proteins that bear mutations in the D-domain cannot be activated upon mitogen stimulation nor by docking-binding mutants of ERK<sup>55</sup>. ERK phosphorylation activates the CTKD, which in turn autophosphorylates S386 in the hydrophobic motif of RSK2. Phosphorylation at this site forms a docking site for constitutively active PDK1 (3'-phosphoinositide -dependent kinase-1). RSK2 interaction

with the PDK1-interacting fragment (PIF) of PDK1 increases PDK1 catalytic activity several-fold<sup>56</sup>. Highly activated PDK1 phosphorylates the NTKD at S227 resulting in full activation of RSK2.

In addition to the requirement for posttranslational modification, full activation of RSK requires transient translocation from the cytosol to the plasma membrane. ERK phosphorylation of T577 may facilitate this translocation. To address this question, Blenis *et al.* attached a myristoylation sequence to the NTD of RSK1 and found that membrane-bound RSK1 is constitutively active and promotes autophosphorylation of the hydrophobic motif<sup>59</sup>. Furthermore, activation of myristoylated RSK1 is independent of ERK. Myristoylated RSK1 lacking the D-domain, was activated to a level similar to the wild-type myristoylated RSK<sup>59</sup>. Thus it appears that ERK may have a dual role in activating RSK: phosphorylation and targeting RSK to the membrane<sup>59</sup>.

RSK2 inactivation occurs by both *cis* and *trans* mechanisms. In the basal state, ERK and RSK2 form a complex through the D-domain. Upon mitogen stimulation, activated ERK initiates the activation sequence by phosphorylating T577. Once activated the NTKD autophosphorylates S737 in the D-domain, which disassociates ERK from RSK. The two inactive kinases complex in the cytosol<sup>54</sup>. Protein phosphatase-2C $\delta$  (PP2C $\delta$ ) was identified in a yeast two-hybrid screen as a binding partner of RSK2<sup>60</sup>. Doehn *et al.* found that PP2C $\delta$  interacts with all RSKs isoforms *in vivo* and regulate the dephosphorylation of RSK. The binding of PP2C $\delta$  to RSK is negatively regulated by ERK phosphorylation of PP2C $\delta$  at Thr315 and Thr333<sup>57</sup>.

## RSK2 SUBSTRATES

The substrate specificity of RSK has been determined using synthetic peptide libraries and was found to require the minimum sequence Arg/Lys-Xaa-Arg-Xaa-Xaa-Ser/Thr or Arg-Arg-Xaa-Ser/Thr<sup>61</sup>. Romeo *et al.* identified that RSK preferentially phosphorylated serine rather than threonine by a factor of five-fold, and in agreement with this the majority of RSK substrates are phosphorylated on serine residues<sup>54</sup>. Other serine/threonine kinases of the basophilic class such as AKT, S6k 1/2 and MSKs, have been shown to target this sequence<sup>56</sup>.

The localization of RSK2 in multiple subcellular compartments imparts to RSK the ability to regulate a wide array of cellular processes. Based on the nature of its substrates, RSK2 has roles in transcriptional regulation, cell-cycle regulation, translational regulation, and cell survival (fig 1.5) (table 1.2). RSK2 regulates the intermediate-early gene response and was found to phosphorylate many transcription factors, including serum response factor (SRF), nuclear factor- $\kappa$ B (NF- $\kappa$ B), NFAT, and the transcription initiation factor TIFIA<sup>54-56, 62</sup>. RSK2 has been reported to activate and cAMP response element-binding protein (CREB)<sup>49, 54, 56</sup> and cFOS<sup>49, 54, 56, 63</sup>. Studies conducted in an RSK2-deficient fibroblast cell line derived from patients with the Coffin-Lowry syndrome showed impaired EFG-induced phosphorylation of CREB and induction of cFOS<sup>64, 65</sup>. However, CREB phosphorylation was found to be normal in stimulated platelet-derived growth factor (PDGF) and insulin-like growth factor (IGF-I) fibroblasts derived from RSK2 KO mice suggesting another kinase can phosphorylate CREB depending on cellular content<sup>64, 65</sup>. Sequentially, it was shown that MSKs could phosphorylate CREB *in vitro* with a  $K_m$  much lower than RSK<sup>66, 67</sup>.

Inhibition of RSKs using pan-inhibitor SL-0101 or siRNA against RSK1 and RSK2 was shown to inhibit proliferation in human prostate and breast cancer cell lines that overexpress both isoforms<sup>68, 69</sup>. This data indicates that both RSK1 and RSK2 positively regulates cancer cell proliferation. RSK promote cell cycle progression by phosphorylating transcriptional activator cFOS which upregulates the expression of cyclin D1 during the G1/S transition<sup>70,71</sup>. The oncogenic properties of cFOS in the development of osteosarcoma in mice was found to be dependent on RSK phosphorylation of cFOS on S362<sup>72</sup>. Another protein through which RSK1/2 may regulate G1 progression is the cyclin-dependent kinase (CDK) inhibitor p27<sup>kip1</sup>. RSK phosphorylation of T198 prevents p27<sup>kip1</sup> translocation into the nucleus by promoting its association with 14-3-3<sup>73</sup>.

The RAS/MAPK and AKT/PI3K pathways converge at the point of RSK2 to stimulate translation by increasing the rates of translation initiation and elongation by stimulating ribosome biogenesis. AKT regulates translation by phosphorylating and inactivating the GAP function of tuberous sclerosis complex-1/2 (TSC1/2), a heterodimer of TSC1 and TSC2. TSC1/2 complex negatively regulates the small RAS-like GTPase RHEB<sup>49, 54-56, 74</sup>. Activated RHEB associates with mammalian target of rapamycin complex-1 (mTORC1). Through an unknown mechanism, RHEB promotes mTOR signaling to serine kinase S6K1/2 and translation initiation factor 4EBP1, which leads to translation and cell growth. RSK influences protein synthesis by impinging on the mTOR pathway at multiple steps. RSK2 directly promotes mTORC1 signaling by phosphorylation of raptor and indirectly by regulating the subcellular localization of TSC2 via phosphorylation of S1798<sup>54-56</sup>. Both RSK2 and S6K enhance the rate of translation by phosphorylating the translation factor eIF4B<sup>54-56</sup>.

RSK2 also regulates mRNA translation through mTOR-independent mechanisms. As previously described, RSK phosphorylation of SP6 leads to the translation of mRNAs that encode for proteins that promote growth in *Xenopus* oocytes and various somatic cells. Lastly, RSK-mediated phosphorylation of GSK3  $\beta$  was found to inhibit its kinase activity and thereby release the inhibition on the translation initiation factor eIF2B<sup>54-56</sup>.

RSKs promote cell survival through both transcription and posttranslational mechanisms. RSK phosphorylation of transcriptional activator CREB was shown to upregulate transcription of antiapoptotic *bcl-2*, *bcl-xl*, and *mcl1* genes in primary cortical neurons<sup>75-78</sup>. RSK also directly modulates the activity of BCL family members<sup>49</sup>. RSK2 phosphorylates the proapoptotic mitochondrial protein BAD preventing its ability to inhibit the BCL2 and BCL-XL while enhancing its ability to bind to cytosolic 14-3-3<sup>75-78</sup>. Cytosolic BAD cannot antagonize the pro-survival function of BCL-XL. RSK directly inhibits caspase activity in Hepatic stellate cells by phosphorylation of C/EBP $\beta$  in response to Hepatoxin CC14<sup>79</sup>. Phosphorylation of T217 creates a functional XEXD caspase inhibitory box that binds and inhibits caspase 1 and caspase 8<sup>79</sup>. RSK also blocks the activities of proapoptotic death-associated protein kinase (DAPK). Overexpression of DAPK in HEK293 cell leads to extensive cell death<sup>75</sup>. Phosphorylation by RSK on S289 was found to inhibit DAPK and increase cell survival in response to mitogenic stimulation<sup>75</sup>. RSK promotes survival through activation of the transcription factor NF $\kappa$ B by phosphorylating NF $\kappa$ B inhibitor I $\kappa$ B $\alpha$  on S32 and inducing its degradation<sup>80,81</sup>.

## RSK2 PHENOTYPE AND RSK EXPRESSION

The Coffin-Lowry syndrome (CLS) is a rare X-link disorder characterized by craniofacial and skeletal abnormalities and severe mental retardation with characteristic dysmorphism<sup>82</sup>. Hanauer *et al.* mapped the disease to the locus encoding RSK2. To date, 75 distinct disease associated mutations in *rsk2* have been identified with a vast majority resulting in premature translation termination of RSK2 or complete loss of RSK2 transferase activity<sup>82</sup>. The mental retardation phenotype of the mutations ranges from mild to severe. The association between mental retardation and loss of RSK2 function is consistent with expression levels of *rsk2* in the brain. *rsk2* expression in the adult brain is highest in the neocortex, the hippocampus, and Purkinje cells, regions with high synaptic activity that are essential for cognitive function and learning<sup>49, 54-56</sup>. RSK2 knockout (KO) mice (*rsk2*<sup>-/-</sup>) display impaired learning and cognitive function as well as poor coordination compared to wild-type littermates<sup>55</sup>. RSK2 KO mice also develop a progressive skeletal disease, osteopenia, due to impaired osteoblast function and osteoclast differentiation<sup>83</sup>.

The *rsk4* gene is another RSK isoform located on the X-chromosome. However, there is no evidence linking its aberrant expression to mental retardation. The level of RSK4 transcripts is significantly lower than compared to other RSKs. Northern analysis of adult mouse tissue showed RSK4 expression in brain, heart, cerebellum, and kidney tissue with no detectable levels in the lung, liver, pancreas and adipose tissue<sup>49, 54-56</sup>.

Transcripts of *rsk1-3* have been detected in all human tissue and brain tested<sup>49, 54-56</sup>. However, there are differences in the relative expression of each isoform. RSK1 is expressed predominantly in the kidney, lungs, and pancreas; whereas both RSK2 and RSK3 transcripts

are abundant in skeletal muscle, heart, and pancreas<sup>49, 54-56</sup>. In the brain, elevated levels of RSK1 transcripts have been detected in tissues with high proliferative capacity, whereas RSK3 is predominately expressed in the developing neural and sensory tissues<sup>56</sup>. Although *rsk1*<sup>-/-</sup> and *rsk3*<sup>-/-</sup> as well as the *rsk1*<sup>-/-</sup>, *rsk2*<sup>-/-</sup>, *rsk3*<sup>-/-</sup> triple knockout mice are viable, no phenotypes have been reported<sup>55, 84</sup>.

#### CHEMICAL INHIBITORS OF RSK

There are three classes of RSK inhibitors commonly used to study RSK function; to date, no RSK isoform-specific inhibitor has been identified (fig 1.6). The first inhibitor of RSK, SL-0101, was discovered by Smith *et al.* in a screen of botanical extracts. SL-0101 is an acetylated flavonol glycoside from the tropical plant *Forsteronia refracta*<sup>69</sup>. It is an ATP-competitive inhibitor that targets the NTKD of RSK<sup>69</sup>. The molecule was tested against a panel of 70 kinases and was shown to be relatively selective to RSK1-2 within the nanomolar range<sup>69, 85</sup>. SL-0101 inhibits RSK2 *in vitro* with an IC<sub>50</sub> of 90 nM at an ATP concentration of 10 μM and an EC<sub>50</sub> of 50 μM *in vivo*<sup>49, 54, 85, 86</sup>. The significant reduction in the efficiency of SL-0101 in intact cells may be a concern for specificity at higher levels. SL-0101 inhibited proliferation of MCF-7 breast cancer cell line but did not alter proliferation in the normal breast cell line MCF-10A<sup>49, 54, 86</sup>. SL-0101 may specifically target cells that rely on RSK for growth as the molecule also inhibited proliferation of the human prostate cancer cell line LNCaP and the androgen-independent human prostate cancer cell line PC-3<sup>49, 56</sup>.

The dihydropteridine BI-D1870 synthesized by Sapkota *et al.* is another ATP-competitive inhibitor that targets the NTKD of RSK<sup>87</sup>. BI-D1870 was found to inhibit all

isoforms of RSK *in vitro* with IC<sub>50</sub>'s of 15-30 nM at an ATP concentration of 100 μM<sup>49, 54, 86</sup>. However, at a concentration of 10 μM BI-D1870 showed a two-fold higher potency for RSK1-2 than RSK3-4<sup>49, 86, 87</sup>. This led to the proposition that design of isoform-specific inhibitors should target the structural divergence between the NTKD of the RSKs<sup>49</sup>. In a screen against a large panel of kinases, BI-D1870 inhibited RSK2 activity by 98% at 0.1 μM<sup>86, 87</sup>. The inhibitor was found to inhibit PLK1 (83%) at a concentration that was 3 to 10-fold higher than that of RSK2. BI-D1870 also inhibited the activities of Aurora B, DYRK1a, CDK2-A, Lck, CK1, and GSK3 at concentrations 10 to 100-fold relative to RSK2<sup>49, 86, 87</sup>.

The pyrrolopyrimidine FMK is an irreversible inhibitor of RSK1, RSK2, and RSK4. FMK inhibits RSK2 with an *in vitro* IC<sub>50</sub> of 15 nM and an EC<sub>50</sub> of 200 nM. FMK contains a reactive electrophile in its fluoromethylketone motif that forms a covalent linkage with the thiol group of a cysteine located in the ATP-binding pocket of the CTKD<sup>56, 86, 88</sup>. Using a structural bioinformatics-based approach, Cohen *et al.* discovered the CTKD of RSK is unique among human kinases in that it possesses two ligand filters in the CTKD<sup>86, 88</sup>: a cysteine residue and a threonine gatekeeper in the ATP-binding pocket. The requirement by FMK for both filters is demonstrated by its inability to inhibit RSK3. Unlike the other RSKs, RSK3 possesses a methionine gatekeeper<sup>86, 88</sup>. Furthermore, in human epithelial cell lysates, biotin-labeled FMK was found only to react with RSK1 and RSK2, which were identified using quantitative immunodepletion with specific antibodies<sup>86, 88</sup>.

These inhibitors have significantly contributed to our understanding of RSKs signaling. However, none these inhibitors are isoform specific and therefore cannot be used to study how individual isoforms contribute to human physiology and pathologies. While the

advent of CRISPR/Cas9 gene editing technology allows for loss or gain of function studies from chromosomal editing of individual RSK isoforms, new isoform specific pharmacological inhibitors must be identified to study both heterodimeric and homodimeric RSK protein interactions.

## 1.3 TABLES

Table 1.1 THE INTEGRIN FAMILY OF CELL ADHESION RECEPTORS

Integrin	Subunit kDa $\alpha$ : $\beta$	Chromosome number	Ligand	Cell/tissue distribution
$\alpha_1\beta_1$	200:140	5:10	Collagen, laminin	Smooth muscle, T cell, endothelium, Hepatocyte
$\alpha_2\beta_1$	160:140	5:10	Collagen, laminin	Epithelium, endothelium, leukocytes, platelets
$\alpha_3\beta_1$	150:140	17:10	Collagen, laminin, fibronectin	Epithelium, endothelium
$\alpha_4\beta_1$	150:140	2:10	Fibronectin, V-CAM1	Leukocytes, melanomas
$\alpha_5\beta_1$	155:140	12:10	Fibronectin	Endothelium, platelets, hepatocytes, lymphocytes
$\alpha_6\beta_1$	140:140	2:10	Laminin	Most cells, platelets
$\alpha_7\beta_1$	140:140	NR:10	Laminin	Muscle, melanoma, glioma
$\alpha_8\beta_1$	160:140	NR:10	Basal lamina	Epithelium, brain, endothelium, myeloid
$\alpha_v\beta_1$	150:140	2:10	Fibronectin, vitronectin	Fibroblasts, tumor cells, osteoblasts
$\alpha_L\beta_2$	180:95	16:21	I-CAM	Leukocytes, myeloid cells
$\alpha_M\beta_2$	170:95	16:21	Fibronectin, I-CAM	Neutrophils, lymphocytes, monocytes
$\alpha_X\beta_2$	150:95	16:21	Fibronectin	Granulocytes, monocytes
$\alpha_{IIb}\beta_3$	150:105	17:17	Fibrinogen, fibronectin	Megakaryocytes, platelets, melanoma
$\alpha_v\beta_3$	150:105	2:17	Vitronectin, fibronectin, fibrinogen, osetopontin	Osteoclasts, GBM, endothelium, melanoma
$\alpha_6\beta_4$	150:2400	2:17	Laminin	Neurons, fibroblasts, epithelium
$\alpha_v\beta_5$	105:105	2:NR	Vitronectin, fibronectin	Pancreas, fibroblasts, carcinoma cells
$\alpha_v\beta_6$	150:105	2:NR	Fibronectin	Epithelium, carcinoma cell

Note: NR = not-reported. Adapted from<sup>89</sup>.

TABLE 1.2 RSK SUBSTRATES

Substrate	Phosphorylation site(s)
AS160	RRRHAS <sup>341</sup> APSHV (h) RSRCSS <sup>318</sup> VTGVQ (h) RGRLGS <sup>588</sup> VDSFE (h) RKRTSS <sup>751</sup> TCSNE (h)
ATF1	LARRPS <sup>63</sup> YRKIL (h)
ATF4	PSPGGS <sup>251</sup> RGSPR (m) GSPNRS <sup>245</sup> LPSPG (h)
Bad	RSRHSS <sup>112</sup> YPAGT (h, r)
Bub1	Not determined
c-Fos	AHRKGS <sup>362</sup> SSNEP (r)
C/EBP $\beta$	PSKKPS <sup>105</sup> DYGYV (r) AKAKKT <sup>217</sup> VDKLS (m)
Capacua	PGKRRTQSLSS <sup>173</sup> ALPKE (h)
CCT $\beta$	RVRVDS <sup>260</sup> TAKVA (h)
CMyBP-C	AGTGRRTS <sup>288</sup> DSHEDAG (r)
CREB	LSRRPS <sup>133</sup> YRKIL (h, m)
CRHSP24	RTRTFS <sup>52</sup> ATVRA (h)
DAPK	LSRKAS <sup>289</sup> AVNME (h)
DCL1	VTRTRSLS <sup>322</sup> TCNKRVG (r)
eEF2K	RVRTLS <sup>366</sup> GSRPP (h)
eIF4B	RSRTGS <sup>422</sup> ESSQT (h)
ER81	FRRQLS <sup>191</sup> EPCNS (h, m) YQRQMS <sup>216</sup> EPNIP (h, m)
Erp1	RCRRLS <sup>335</sup> T <sup>336</sup> LRER (x)
ER $\alpha$	RERLAS <sup>167</sup> TNDKG (h, r)
Filamin A	RRRAPS <sup>2152</sup> VANVG (h, r)
GSK3 $\beta$	RPRTTS <sup>9</sup> FAEPG (r)
Hist H3	TKQTARKS <sup>11</sup> TGGKAPR (h)
HSP27	PAYSRALS <sup>78</sup> RQLSSGV (h), AYSRALS <sup>82</sup> RQLSSGV (h)
I $\kappa$ B $\alpha$	LLDDRHDS <sup>32</sup> GLDSM @, RHDSGLDS <sup>36</sup> MKDEDYE (r)
I $\kappa$ B $\beta$	DADEWCDS <sup>19</sup> GLGSLGP (r), WCDSGLGS <sup>23</sup> LGPDAAA (r)
KCNK3	GLMKRRSS <sup>393</sup> V (h)
Kv4.3	YPSTRSPS <sup>535</sup> LSSHSGL (r), LPATRLRS <sup>569</sup> MQELSTI (r)
L1CAM	RSKGGKYS <sup>1154</sup> VKDKEDT
LKB1	KIRRLS <sup>431</sup> ACKQQ (m)
Mad1	RIRMDS <sup>145</sup> IGSTV (h)
MEF2c	LHRNVS <sup>192</sup> PGAPQ (r)
METTL1	RQRAHS <sup>27</sup> NPMAD (h)
MRLC	KRPQRATS <sup>19</sup> NVFAMFD (h)

MITF	SSRRSS <sup>409</sup> MSAEE (h)
Myt1	Serine residues (x)
NDRG2	LSRSRTAS <sup>332</sup> LRSAASV (h), RSRRTLS <sup>350</sup> QSSESGT (h)
NFAT3	Serine residues (h, m)
NFATc4	GRRKRS <sup>676</sup> PTQSF (h, m)
NHE-1	RARIGS <sup>703</sup> DPLAY (h)
nNOS	KVRFNS <sup>847</sup> VSSYS (r)
NOR1	GTTGRLPS <sup>377</sup> KPKSPLQ (m)
Nur77	RGRLPS <sup>354</sup> KPKQP (m)
p27 <sup>kip1</sup>	LRRRQT <sup>198</sup> * (h)
p65	SGDEDGS <sup>536</sup> IADMDFS (h)
PKR	KRTRSKGT <sup>451</sup> LRYMSPE (h)
PLD1	PIPTKRHT <sup>147</sup> FRRQNVK (r)
PPP1R3A	PQPSRRGS <sup>46</sup> DSEDIY (H), SSGTRRVS <sup>65</sup> FADSFGE (H)
RanBP3	RERTSS <sup>58</sup> LTHSE (m)
Raptor	TPRLRS <sup>719</sup> VS <sup>721</sup> S <sup>722</sup> YIGNI (h)
rpS6	KRRRLS <sup>235</sup> S <sup>236</sup> LRAST (h)
SH3P2	AVRTLS <sup>202</sup> NAEDY
SHANK	Not determined
SOS1	RRRPES <sup>1161</sup> APAES (h)
SRF	LKRSL <sup>103</sup> EMEIG (h)
TCP-1	GSRVRVDS <sup>260</sup> TAKVAEI (H)
TH	RFOGRRQS <sup>71</sup> LIEDARK (H)
TIF-1A	LYMQPS <sup>649</sup> PL* (h)
TSC2	RKRLIS <sup>1798</sup> SVEDF (h)
VASP	LARRRKAT <sup>298</sup> QVGEKTP (H)
YB-1	RKYLRS <sup>102</sup> VGDGE (h)

Abbreviations: h, human; m, mouse; r, rat; x, *Xenopus*. Adapted from<sup>49, 52</sup>

## 1.4 FIGURES

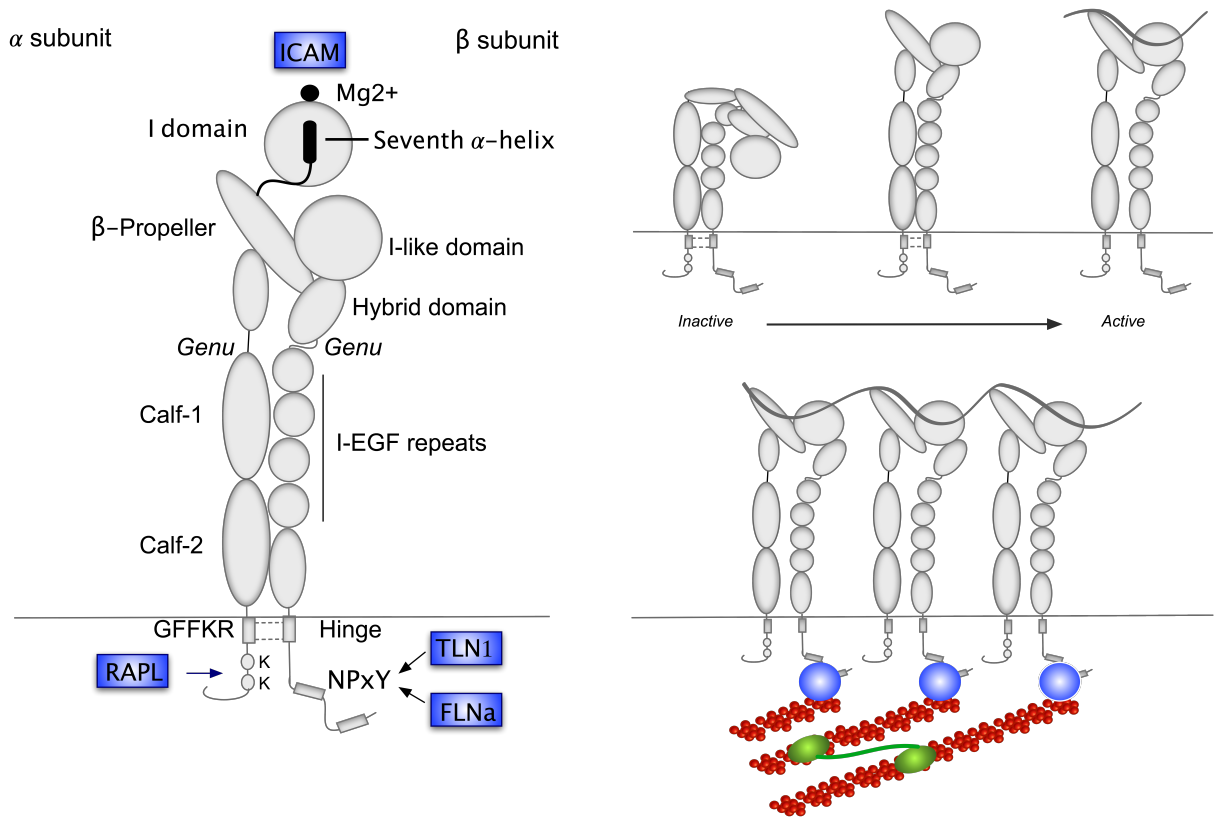


FIGURE 1.1 INTEGRINS ARE HETERODIMERIC CELL ADHESION RECEPTORS

1.1 Left. Integrins are cell adhesion receptors that consist of two noncovalently linked subunits, an  $\alpha$ -subunit, and a  $\beta$ -subunit. They are single pass transmembranes receptors that bind to ligands through their large extracellular domains. The short cytoplasmic domains of integrins recruit cellular molecules to form platforms (blue circles) that regulate both signal transduction and the actin cytoskeleton (red). Right top. The RAS family of GTPases modulate the affinity of integrins for their ligands. On the cell surface, Integrins are expressed in the inactive state. Upon activation, integrins move through an intermediate state to a high-affinity binding state. Right bottom. Once activated, integrins can cluster and increase the avidity of cell adhesion by coupling multiple focal adhesions (blue circle) to the cell substratum. Myosin II (green).

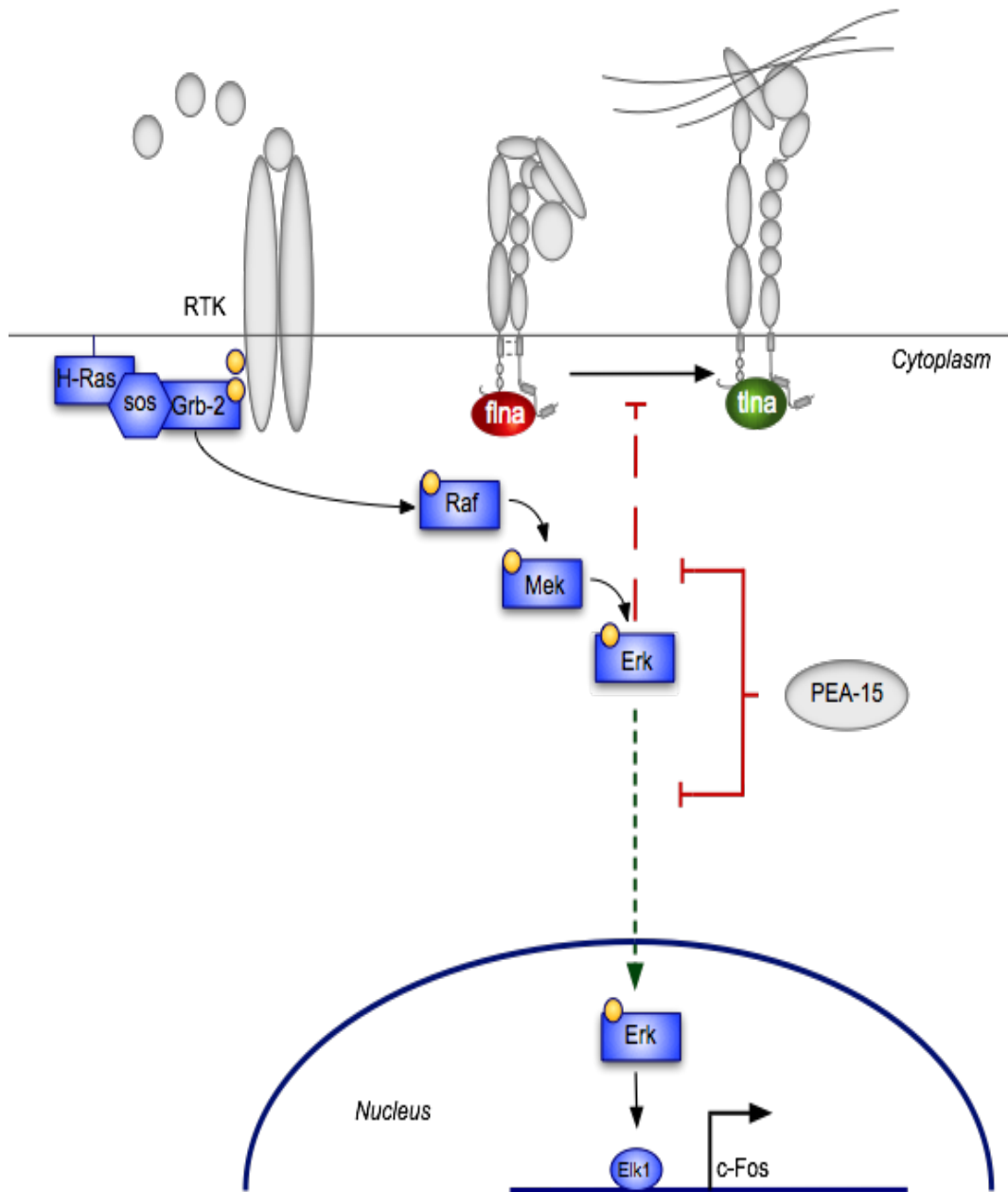


FIGURE 1.2 INTEGRINS ARE ACTIVATED BY INSIDE-OUT SIGNALING

1.2 H-RAS signaling leads to inactivation and suppression of integrin function. However, the mechanism by which H-RAS inhibits integrin activation is poorly understood. Active RAF can inactivate integrins through ERK-dependent and independent mechanisms. Cytosolic adaptor proteins can act as activators or inactivators of integrin. Depicted is the activator talin and inactivator filaminA.

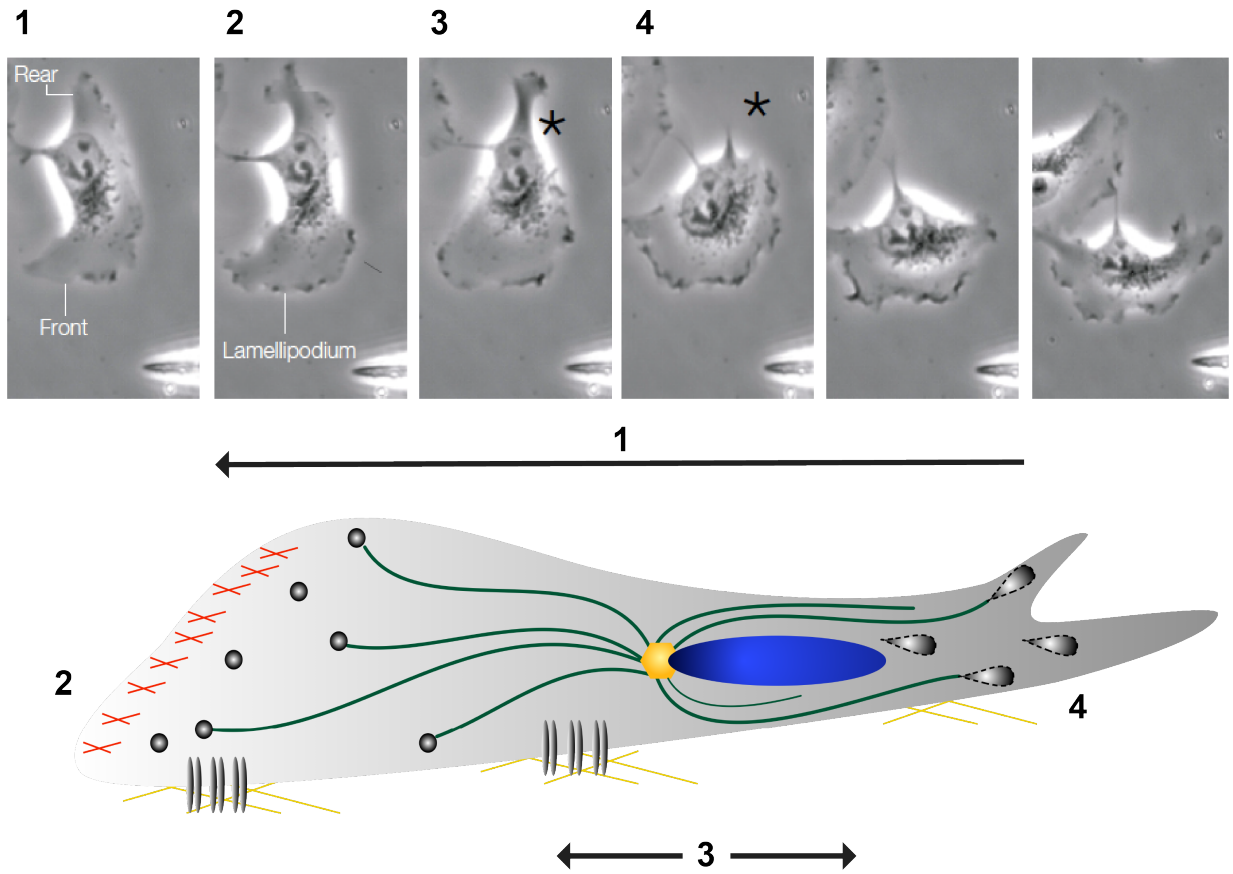


FIGURE 1.3 CELL MIGRATION IS A MULTISTEP CYCLIC PROCESS

1.3 Top. Micrographs representing the stages of cell migration<sup>90</sup>. Depicted is a Hep3 adenocarcinoma cell responding to insulin stimulation. Top and bottom. 1, the cell polarizes in response to extracellular cues. The polarized cell reflects the spatial distribution of intracellular molecules and cytoskeletal changes that are necessary for cell migration<sup>90</sup>. 2, the lamellipodia extends forward at the leading edge where integrins and their adaptor proteins form nascent focal complexes. 3, the cell body contracts through the action of myosin II and propels forward along the cell substratum. 4, mature focal adhesions at the rear edge of the cell either disassemble or are recycled back to the forefront to form new focal complexes.

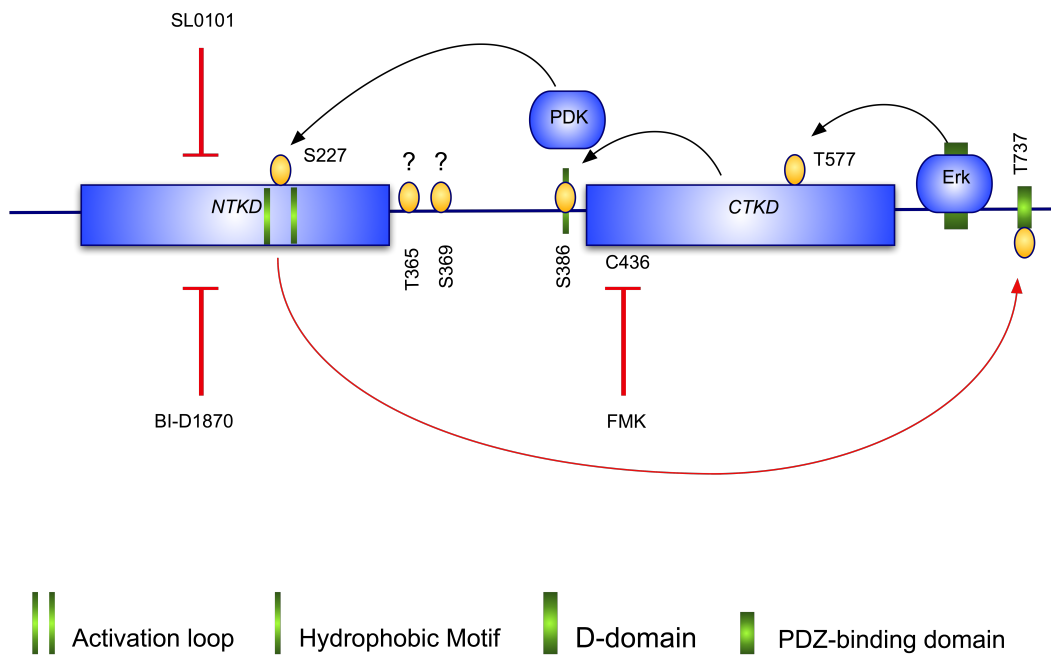


FIGURE 1.4 THE STRUCTURE AND REGULATION OF RSK2 ACTIVATION

1.4 RSK2 is characterized by two functional kinase domains. The NTKD is homologous to members of the AGC family of kinases. The CTKD shares homology with the CaMK family. A regulator linker domain connects to the two kinase domains. Activation of RSK2 is associated with phosphorylation at six sites (yellow ovals). Upon mitogenic stimulation activate RAF signals to its effector kinase MEK that activates ERK. ERK binds to D-domain of RSK2 and phosphorylates the CTKD. The activated CTKD phosphorylates the S386 in the hydrophobic motif that functions as a docking site for PDK1. PDK1 phosphorylates the NTKD, which activates it to phosphorylate substrates. RSK2 can regulate reactivation by autophosphorylation of the C-terminal domain, which prevents ERKS ability to dock in the D-domain. The kinase (s) responsible for the phosphorylation of regulatory residues T365, and S369 has not been identified.

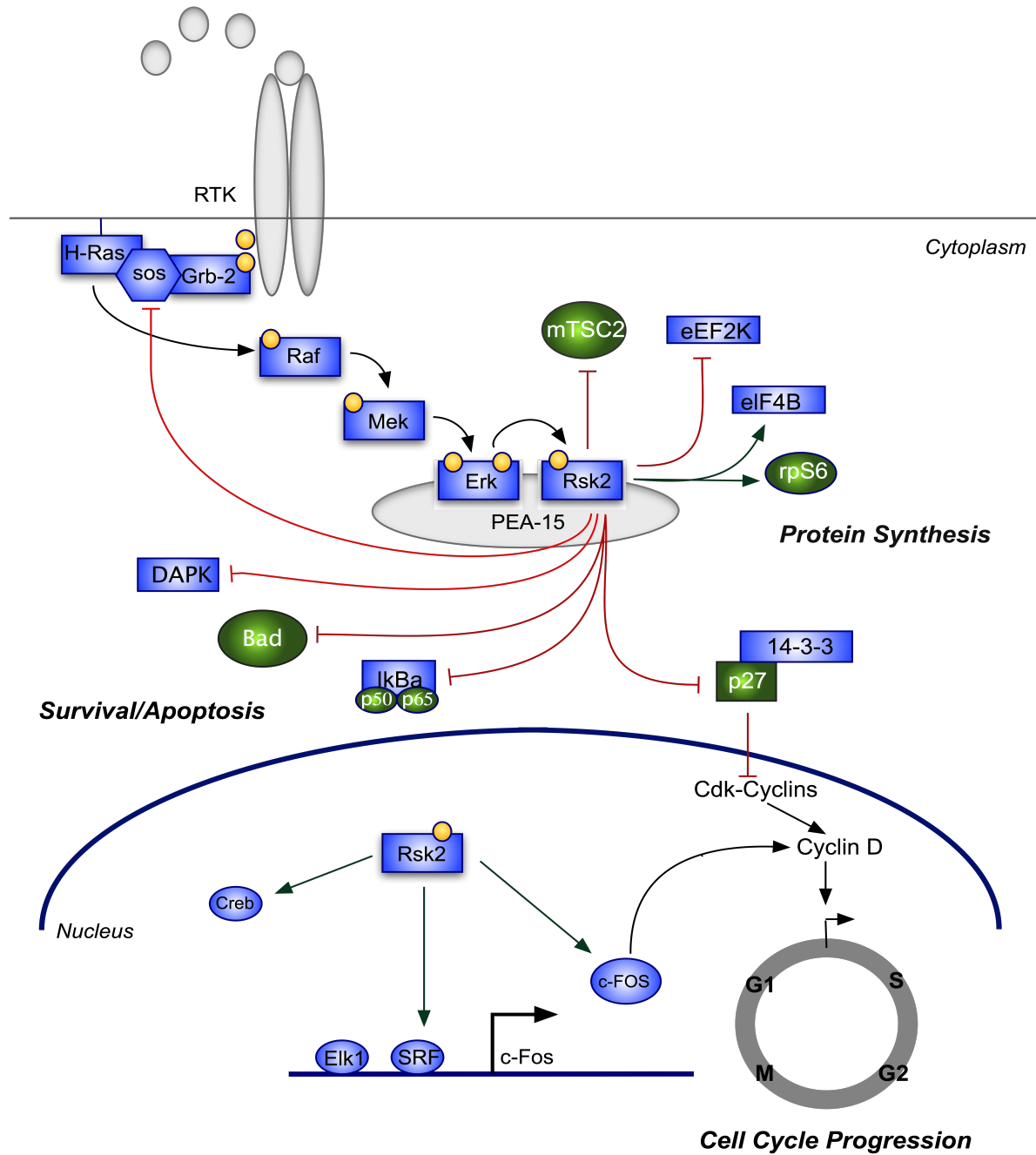
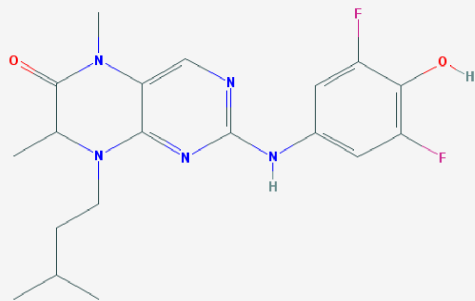
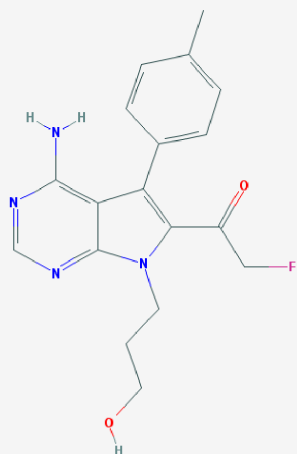


FIGURE 1.5 RSK2 SUBSTRATES ARE BOTH CYTOSOLIC AND NUCLEAR

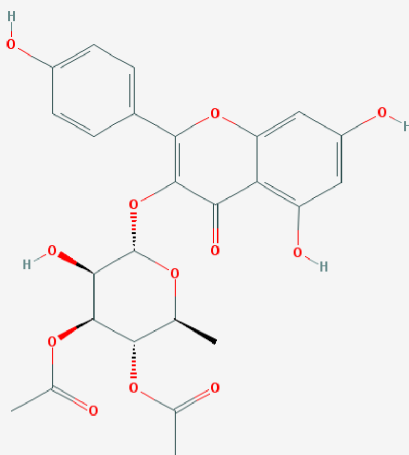
1.5 ERK activation of RSK2 is mediated by the scaffold protein PEA-15. Active RSK2 can translocate to the nucleus where it initiates transcription of genes that regulate proliferation, survival, and differentiation. RSK2 regulates survival, translation, proliferation, and motility by posttranslational modification of cytosolic targets.



BI-D1870



FMK



SL-0101

FIGURE 1.6 CHEMICAL STRUCTURE OF RSK2 INHIBITORS

1.6 Diagram of the chemical structure of RSK2 inhibitors used in this study. The pan-RSK ATP competitive inhibitors are SL-0101 and BI-D1870. The nonreversible inhibitor FMK covalently modifies RSK1, RSK2, and RSK4.

## CHAPTER 2

### RSK2 SUPPRESSES INTEGRIN ACTIVATION AND PROMOTES CELL MIGRATION

The majority of the work in this chapter has been published in

The Journal of Cell Biology 2012 Dec 21;287(52)

Gawecka & Young-Robbins, *et al*<sup>91</sup>

## 2.1 INTRODUCTION

Cell adhesion and migration are essential for a diversity of cellular functions such as embryonic development, tissue regeneration, and the immune defense<sup>26, 92, 93</sup>. Integrins are cell adhesion receptors that link the extracellular matrix to the actin cytoskeleton through adaptor proteins that bind integrin cytoplasmic tails. During cell migration, the ECM-integrin-actin linkage undergoes dynamic modification to allow the cell to invade into the surrounding matrix and propel the cell forward. This includes the formation of nascent integrin focal adhesions at the leading edge and the disassembly of mature focal adhesions at the trailing edge of the cell<sup>94, 95</sup>. The activation state and avidity of the integrins modulate the adhesion strength to the ECM.

The RAS superfamily of small GTPases regulates the activation state of integrins. There are four isoforms of RAS (R-RAS, H-RAS, K-RAS, or N-RAS) that can signal to activate or inactivate integrins depending on the RAS GTPase involved and the cell type. H-RAS suppresses integrin activation via its downstream effector, RAF-1, in a transcription-independent manner<sup>96</sup>. The inactivation of integrins is reverse by the action of mitogen-activated protein kinase (MAPK) phosphatase 1 (MKP1), an extracellular signal-regulated kinase MAPK phosphate<sup>97, 98</sup>. This implicates the RAF/MEK/ERK pathway in the suppression of integrin activation mediated by H-RAS. However, activated ERK does not result in the phosphorylation of integrins in the presence of active H-RAS or RAF, indicating that integrins are not the targeted substrate of ERK<sup>99</sup>; this prompted investigations for unknown effectors of H-RAS signaling to integrins.

The activation state is also regulated by cytosolic adaptor proteins that bind to integrin cytoplasmic tails. These include the activators talin and kindlin as well as inactivators such as filaminA. FilaminA is a 280 kDa cytosolic protein that organizes actin filaments into networks and links them to the plasma membrane by binding to  $\beta$ -integrin tails<sup>100</sup>. The organization of the actin networks regulates the shape of the cell and undergoes dynamic reorganization during cell migration. FilaminA and talin have overlapping binding sites on the  $\beta$ -integrin tails, which implicates filaminA as a negative regulator of integrin activation<sup>31</sup>. In fact, knockdown of filaminA in NIH3T3 cell increased the activation level of  $\beta$ 1 integrins, supporting an inhibitory role for filaminA in integrin activation<sup>31</sup>.

RSK2 is a substrate of ERK and mediates many cellular functions of the RAS/MEK/ERK pathway. Aberrant expression of RSK2 is associated with several human pathologies, for example, genetic mutations in RSK2 are associated with Coffin–Lowry syndrome, a rare X-linked disorder characterized by craniofacial and skeletal abnormalities, mental retardation, short stature, and hypotonia<sup>101</sup>. RSK2 is also a key regulator of skin carcinoma<sup>102</sup> and is over expressed in both breast and prostate tumors and promotes proliferation in these cells<sup>103</sup>. It can also promote cell invasion and metastasis in head and neck cancer and in lung cancer<sup>104, 105</sup>. We investigated if RSK2 could mediate H-RAS suppression of integrin activation.

## 2.2 RESULTS

### RSK2 INHIBITS INTEGRIN ACTIVATION

H-RAS suppression of integrin affinity for the ligand is mediated via its downstream effector kinase RAF1. However, integrins are not a substrate of ERK. We, therefore, investigated the effects of RSK2 on the activation of integrins and observed that in the presence of dominant active RSK2 integrin activation was suppressed to a level similar to that of dominant active H-RAS (fig. 2.1A). Furthermore, we found that H-RAS suppression of integrin activation could be bypassed by coexpression with dominant negative RSK2 (fig 2.1A) or by inhibition of endogenous RSK2 (fig. 2.1B).

Similarly, we investigated whether stable knockdown of RSK2 altered the activation state in HeLa cells. Integrin activation significantly increased with the knock-down of RSK2 expression in the presence of DA-HAS (fig 2.1C), which suggest that RSK2 lies downstream of H-RAS in the suppression pathway. Furthermore, rescue of the inhibition phenotype by transfection of wild-type RSK2 in knock-down cells indicates that suppression is RSK2 dependent (fig 2.1D). We also found that a functional consequence of RSK2 inhibition of integrin activation is a 3-fold reduction in adhesion to fibronectin by DARSK2 (fig. 2.1D).

### RSK2 ENHANCES INTEGRIN-MEDIATED CELL MIGRATION

Cell migration is modulated by integrin adhesion, and we have shown that active RSK2 can inhibit activation of integrin Gawecka & Young-Robbins *et al*<sup>91</sup> found that the overexpression of dominant active RSK2 increased the number of cells migrating through the membrane of a transwell similarly to what was observed for overexpression of dominant

active H-RAS or the RAF-1 mutant, which cannot bind MEK or activate ERK (fig 2.2A). And, they noted that active RSK2 gradually promotes cell migration through the time course of 24 h (fig 2.2B) and at that same time point, there is nearly a two-fold increase in migration (Fig 2.2C). Additionally, when endogenous RSK2 was inhibited with the FMK they observed a significant decrease in migrating cell (fig 2.2D). RSK2 inhibitors, FMK or SL0101, do not affect the viability of the cells (fig 2.2E).

#### RSK2 ASSOCIATES WITH INTEGRIN CYTOPLASMIC TAILS

Integrin cytoplasmic tails serve as platforms for adaptor and signaling proteins in focal adhesions. Gawecka & Young-Robbins *et al*<sup>91</sup> observed that colocalization of RSK2 and talin at the plasma membrane. We, therefore, investigated whether RSK2 associated with the integrins tails. Using bead-bound integrin cytoplasmic tails, we pulled down proteins from CHOK1 cells transfected with dominant active RSK2 or empty vector. We found that RSK2 associated with  $\beta$ -integrin tails, but not the  $\alpha$ IIb-integrin tail (fig 2.3A). We also verified that both filaminA (data not shown) and talin associated with the tails as previously reported<sup>106</sup>. We also observed that RSK2 can bind to the NPxY mutant (Y788A) of the  $\beta_1$ -integrin tail that neither talin nor filaminA can bind and that RSK2 bound to the  $\beta$ -integrin tails independently of talin and possibly filaminA (fig 2.3A). We next investigated if endogenous RSK2 can complex with  $\beta$ -integrin tails and whether RSK2 must be activated for binding. To address this question, we ran lysates from CHOK1 cells stimulated with EGF or treated with MEK inhibitor over bead-bound  $\beta$ -integrin tails. We found that both phosphorylated and unphosphorylated RSK2 complexed with purified integrin tails (fig 2.3B).

## RSK2 PHOSPHORYLATES FILAMINA AND PROMOTES ITS BINDING TO INTEGRIN TAILS

To further investigate how RSK2 modulates integrin activity, we examined whether RSK2 can phosphorylate focal adhesion proteins, and found that RSK2 phosphorylated a band that corresponded to 260-280 kDa (fig 2.4A). Since this size corresponds to the mass of either filaminA (280 kDa) or talin (260 kDa), we tested RSK2 phosphorylation on purified talin or filaminA. We found that RSK2 does not phosphorylate talin, but did phosphorylate filaminA as previously reported (fig 2.4B)<sup>107, 108</sup>. We confirmed the site of phosphorylation to be that which had been said to affect migration, although, no mechanism had been proposed (fig 2.4C). We asked if posttranslational modification might have an effect on filaminA binding to integrin tails and observed that endogenous filaminA only bound to  $\beta_1$ -integrin tails in the presence of active RSK2 (fig 2.4D). If RSK2 activity is required to promote filaminA association to integrin tails, then inhibition of RSK2 activity should impair filaminA binding. We, therefore, treated cells with RSK2 inhibitor SL-0101 and ran the lysates over the bead-bound integrin cytoplasmic tails. We found when that filaminA failed to bind integrin cytoplasmic tails in the presence of RSK2 inhibitor, whereas in control cells filaminA bound to both  $\beta_1$ - and  $\beta_7$ -integrin tails (fig 2.4E). This indicates that RSK2 activity is required for filaminA to bind to integrin tails.

## FILAMINA AND RSK2 COLOCALIZE AT THE PLASMA MEMBRANE

We have demonstrated that RSK2 negatively regulates integrin function. We hypothesized that RSK2 effects on cellular adhesion might be mediated by filaminA inactivation of integrins. In our model (fig 2.5), EFG stimulation of the mitogenic pathway activates RSK2, which transiently translocate to the plasma membrane and targets filaminA.

Phosphorylation of filaminA at S2152 increases its affinity for the  $\beta$ -integrin tails, which triggers the exchange of talin for filaminA at the NPxY motif and deactivates the integrin heterodimer. To test the "exchange" hypothesis, our collaborator, T. Talisman (City of Hope, CA), first investigated the distribution of filaminA at the plasma membrane with photoactivated localization microscopy (PALM). This microscopy method allowed us to follow filaminA molecules at the plasma membrane with increased spatial resolution.

Using pair correlation-PALM (PC-PALM), T. Talisman examined the influence of RSK inhibitor BI-D1870 on the distribution of endogenous filaminA on the cell membrane. She observed clustering of filaminA in the steady state with an auto-correlation of 5 within 50 nm of the plasma membrane (fig 2.6). However, the addition of BI-D1870 leads to a disruption of clusters and reduction of the signal on the membrane. The auto-correlation data averaged 1 indicating the distribution of filaminA was random when RSK2 was inactive.

We hypothesize that RSK2 phosphorylates filaminA upon translocation to the plasma membrane. Therefore, we would expect to see the two proteins colocalized at the membrane. T. Talisman examined the spatial distribution of the filaminA and RSK2 using Direct stochastic optical reconstruction microscopy (dSTORM). To quantitatively assess colocalization between two proteins, she conducted cross-correlation analysis of two-color super-resolution microscopy data. The cross-correlation at 15 indicates significant colocalization between FilaminA and RSK2 at the plasma membrane (fig 2.7).

## RSK2 AND FILAMINA ARE ENRICHED IN THE TRAILING EDGE OF A MIGRATING CELL

Focal adhesion assembly and disassembly in a migrating cell must be spatially and temporally regulated. Focal complexes formed at the forefront of a migrating cell either mature into focal adhesions or disassemble. Whereas, mature focal adhesions at the trailing edge of the cell are disassembled or recycle to back to the leading edge. To examine the spatial distribution of RSK2 during migration we seeded U373MG cell to confluence then treated with RSK inhibitor FMK for 4 hours. The monolayer was scratch with a pipette and stimulated with EGF. 16 h later the cells were fixed and stained for RSK2. RSK2 appears to be throughout the cytosol in cells treated with RSK2 inhibitor, and the cells seem to have lost directionality (2.8A). In contrast, the lamellipodia of cells treated with the vehicle are focused towards the scratch (white dotted line) and RSK2 is enriched both at the leading and trailing edge of the migrating cell (figure 2.8B). We asked if filaminA localized with RSK2 at the leading edge or trailing edge or both during migration. We addressed this question by repeating the assay without inhibitor and stained for filaminA 5 minutes and 30 minutes after EGF stimulation. We found that RSK2 and filaminA colocalize at the plasma membrane 5 minutes' post-EFG stimulation, and both appear to be enriched at the trailing edge of the cell 25 minutes later (figure 2.9).

## UNI RAPR RSK2

To delineate RSK2's role in cell motility, we have made use of technology developed in the laboratory of Klaus Hahn at the University of North Carolina. The Hahn lab engineered a regulatory protein, UniRapR, based on the interaction of the mTOR FKBP domain the cytosolic protein FRB. When the UniRapR domain is inserted into a site allosterically coupled

to the G-loop of the binding pocket, the kinase cannot bind ATP and remains inactive. In the presence of Rapamycin or a non-immunogenic derivative of rapamycin, the domains bind and reactivate the enzyme (figure 2.10). UniRapR allows us for temporal control of the kinase's enzymatic activity. We modeled both kinase domains of RSK2 using PyMOL modeling software (Schrodinger LLC, NY) and identified the positions to insert the UniRapR domain (figure 2.11 A). We found that UniRapR RSK2 (NTKD) could not be reactivated with rapamycin. Therefore, we use this as a kinase-dead (KD) control for UniRapR RSK2 (CTKD). We tested the ability of immunoprecipitated HA-UniRapR RSK2 to phosphorylate SP6 in an in vitro kinase assay. The phosphorylation of the SP6 peptide by UniRapR RSK2 was significantly greater in the presence of rapamycin than with vehicle (figure 2.11B). Whereas, kinase-dead UniRapR RSK levels of phosphorylation were at a level similar to the of the empty vector control even in the presence of rapamycin. We also observed that the degree of phosphorylation of SP6 by UniRapR RSK2 was also significantly greater than the parental construct DA-RSK2. This effect was also noted in the phenotype of cells expressing activated UniRapR RSK2 versus DA-RSK2 (figure 2.12). To test if UniRapR RSK2 could be activated to function in vivo, we performed a transwell migration assay on KO-RSK2 U373MG cells transfected with UniRapR RSK2 using rapamycin as a chemoattractant. Cells treated with rapamycin and expressing UniRapR RSK2 migrated through the membrane of the fibronectin-coated transwell 3-fold over that of cell treated with vehicle or expressing kinase-dead UniRapR RSK2(figure 2.11C).

We have shown enrichment of filaminA and RSK2 in regions of a migrating cell where adhesion disassembly must be tightly regulated for a cell to propel forward. This data suggests that RSK2 inactivation of integrins may promote focal adhesion disassembly. To address this question we followed focal adhesion disassembly using the well-established nocodazole washout assay by Erratty *et al*<sup>109</sup>. Nocodazole disrupts microtubule polymerization. As a result, focal adhesions become stabilized in the presence of the agent. When nocodazole is "washed-out" or removed from the growth media, microtubules polymerize, the adhesions collapse and return several hours later. Consequently, we can observe the process of focal adhesion disassembly separate from adhesion assembly.

We incubated KO-RSK2 U373MG cells transiently transfected with UniRapR RSK2 with nocodazole (10  $\mu$ M) for 4 hours then washed the cells and refreshed the media. Rapamycin was added to the cells 30 minutes before the end of the 4-hour incubation and throughout the assay. The cells were fixed at the indicated time points then stained for tubulin and the focal adhesion marker, vinculin. We found focal adhesions in nocodazole-treated kinase-dead UniRapR RSK2 expressing cells stabilized at the cell periphery and disassembled upon washout (figure 2.13). The adhesions reassembled several hours later to a level similar to that which was observed before nocodazole treatment. However, in cells expressing UniRapR RSK2 rapamycin treatment lead to the disruption of focal adhesions in the presence of nocodazole and the number of focal adhesions that reassembled 2 hours later was significantly less than that observed for kinase-dead UniRapR RSK2 expressing control cells

(figure 2.13). This data infers that RSK2 can promote focal adhesion disassembly in a microtubule-independent manner.

#### RSK2 REGULATES FILAMINA-MEDIATED CELL MIGRATION

FilaminA is a cytoskeletal protein that organizes actin into networks and stress fibers. FilaminA dimerizes forming a V-shaped structure that can induce high angle orthogonal branching of actin and crossing linking at the leading edge of migrating cells. Hence, filaminA function is vital for cell motility. Collectively, our data suggests that RSK2 promotes migration via filaminA inactivation of integrins. To confirm this, we stably transfected filaminA and phosphomutant filaminA (S2152A) into M2 filaminA-depleted cells and examined the effect of DA-RSK2 on filaminA-mediated migration. M2 stably transfected cells were transiently transfected with DA-RSK2 or empty vector then seeded for confluence on a fibronectin-coated coverslip. The monolayer was scratched and the cells allowed to migrate into the scratch for 48 hours. We found that the parental M2 cells were not able to close the scratch in response to active RSK2, nor cells expressing the phosphomutant of filaminA. However, M2 cells expressing both filaminA and DA-RSK2 were able to close the scratch in 48h. Thus posttranslational modification by RSK2 is required for filaminA-mediated migration in M2 cells.

## 2.3 DISCUSSION

We report that RSK2 lies downstream of the oncogene H-RAS in the pathway that suppresses integrin activation, and the functional consequence of inhibition of integrin activity is a reduction in cell adhesion that translates to highly migratory phenotype. Our data indicates that RSK2 is present at integrin tail complexes independent of its activation status and can bind to the NPxY  $\beta$ -integrin mutant in the absence of talin or filaminA. Therefore, upon full activation RSK2 is in a position to phosphorylate filaminA and promote its binding to integrin tails. We have shown that RSK2 phosphorylation of filaminA at S2152 increases its affinity for  $\beta$ -integrin cytoplasmic tails and that inhibition of RSK2 reverses filaminA binding. Furthermore, we verified using high-resolution PALM microscopy that active RSK2 and filaminA colocalize at the plasma membrane.

FilaminA and RSK2 translocated away from protrusions in the lamellipodia towards the rear cytoplasmic region of a migrating cell, intimating that they dynamically regulate cell adhesion during migration. Indeed, we observed that RSK2 could initiate focal adhesion disassembly in a manner not dependent on microtubule polymerization. Interestingly, we noted that filaminA was excluded from the nucleus in migrating cells. FilaminA is highly susceptible to proteolysis by calpain<sup>110</sup>, a calcium-regulated protease which catalyzes proteolysis of substrates involved in cytoskeletal remodeling and signal transduction. calpain cleavage of filaminA yields a 170 kDa fragment and 110 kDa fragment, which can be further cleaved to yield a 90 kDa fragment. The latter can translocate to the nucleus and where it acts as a transcription activator<sup>110, 111</sup>. Phosphorylation of filaminA at S2152 stabilizes the protein rendering it resistant to calpain proteolysis<sup>112, 113</sup>. In addition to RSK2,

this serine can be phosphorylated by other members of AGC family of kinases such as PKA and PKC<sup>110</sup>. Bedolla et al.<sup>114</sup> have shown by immunohistochemistry that in benign prostate and localized prostate cancer filaminA expression was predominantly nuclear, whereas filaminA expression was predominantly cytoplasmic in metastatic prostate cancer. This is in agreement with our observations that in the presence of active RSK2 filaminA is retained in the cytosol and that active RSK2 promotes filaminA-mediated migration. We conclude that RSK2 regulates integrin activation by posttranslational modification of filaminA which initiates changes in cell adhesion that drive a more motile and metastatic phenotype.

## 2.4 MATERIALS AND METHODS

### ANTIBODIES, INHIBITORS, AND PLASMIDS

The antibodies described in this study are from the following sources: RSK2 (Santa Cruz #sc-1430), p-RSK2 S386 (Biosource #A8545), ERK (Santa Cruz #93), p-ERK (Cell Signaling #4370), FilaminA (Cell Signaling #4762) (Abcam #ab51217), pS2152-FilaminA (Cell Signaling #4761), Tubulin (Santa Cruz #sc-5286), Talin (Sigma #T3287), Talin-Head domain (Santa Cruz #15336), HA-probe (Santa Cruz #sc-805) and Vinculin (Cell Signaling #4650). The RSK inhibitors used are FMK (courtesy of J. Taunton, UCSF) and SL0101-1 (Tocris #2250). The following cDNA constructs were also used where described: c-RAFBXB-T481A (courtesy of M. White, UT Southwestern), DA H-RAS (H-RASG12V) (courtesy of C. Der, UNC-Chapel Hill), HA-RSK2, DA-RSK2 (RSK2-Y707A) and DN-RSK2 (K100A)(courtesy of T. Sturgill, UVA), integrin cytoplasmic tails (courtesy of M. Ginsberg, UCSD), HA-talin (courtesy of D. Calderwood, Yale University), Myc-filaminA and Myc-filaminA (S2152A) (courtesy of J. Blenis, Weill Cornell Medical College), and UniRapR Src (YF) (courtesy of K. Hahn, UNC School of Medicine).

### UNIRAPR RSK2 CONSTRUCTION

#### *Gibson Assembly*

Primers for Gibson Assembly fragments were designed according to the manufacture's (New England Biolabs, MA) recommendation (Appendix I). The Gibson Assembly was performed with three fragments. Fragment 1 consisted of pKH3 cDNA at the 5' end and RSK2 at the 3' end. UniRapR was inserted as fragment 2 with 5' flanking cDNA downstream of Ser 89 or Ala

443 for UniRapR RSK2 NTKD and UniRapR RSK2 CTKD, respectively; and 3' flanking cDNA upstream of Ser 91 and Thr 444 for UniRapR RSK2 NTKD and UniRapR RSK2 CTKD, respectively. A linker region coding Gly-Pro-Gly was inserted both 5' and 3' of UniRapR cDNA. Fragment 3 consisted of RSK2 cDNA at the 5' end and pKH3 cDNA at the 3' end. The fragments were annealed into the pKH3 *Bam*HI linearized plasmid at a molar ratio of 3:1 using the NEB Gibson Assembly Master Mix at 50°C for one hr.

#### *Mega Primer PCR*

Mega Primer PCR was performed as previously described<sup>115</sup>. The megaprimer was generated from UniRapR Src (YA) incorporating 30 bps of RSK2 cDNA 5' and 3' as described above. The megaprimer was recombined into the parental plasmid (DA-RSK2) with Phusion Polymerase (New England Biolabs, MA) an annealing reaction at 72°C for 16 minutes with a 30 second denaturing step at 98°C between the 25 cycles.

#### CELL CULTURE AND TRANSFECTIONS

HeLa, CHOK1 and U373MG cells were purchased from the American Type Culture Collection (ATCC, Manassas, VA). HeLa CHOK1 and U373MG cell lines were cultured in DMEM containing L-glutamine (HyClone, Thermo Scientific, Fair Lane, NJ) supplemented with 10% fetal bovine serum, non-essential amino acids and antibiotics. Standard transient transfections for all cell lines were conducted using Genejuice (EMD Millipore), Lipofectamine 2000 or Lipofectamine (Life Technologies, Carlsbad, CA) according to manufacturer's directions.

## IMMUNOBLOTTING

Cells were lysed with ice cold M2 lysis buffer (20 mM Tris-HCl (pH 7.6), 250 mM NaCl, 0.5 % NP-40, 5 mM EDTA, 3 mM EGTA (ethylene glycol-bis(b-aminoethylester)-N,N,N9,N9-tetraacetic acid), 20 mM sodium phosphate, 20 mM sodium pyrophosphate, 3 mM  $\beta$ -glycerophosphate, 1 mM sodium orthovanadate, 1 mM phenylmethylsulfonyl fluoride) containing complete protease inhibitor cocktail (11836153001, Roche, Indianapolis, IN). Cell lysates were cleared by centrifugation. Protein concentration was measured using the BCA assay kit (Pierce, Rockford, IL). Equal protein concentrations of cell lysates were resolved on SDS PAGE. After electrophoresis, proteins were transferred to PVDF (Millipore Corp., Bedford, MA) and immunoblotted. Membranes were blocked for 1 h with blocking buffer (5% BSA in 0.1% TPBS) and then incubated with appropriate antibodies. Membranes were washed and incubated secondary antibodies conjugated to infrared fluorochromes and visualized via the Odyssey Infrared Imaging System (LI-COR Bioscience).

## GENERATION OF M2 MELANOMA CELL LINES

The pCDNA3.1 recombinant plasmids bearing myc-filaminA and myc-filaminA (S2152A) were linearized with restriction enzyme *Ssp* I to facilitate the integration of the cDNA into the genome of the M2 melanoma cell lines. The linear plasmids were transfected with Lipofectamine. 48 after transfection the cells were split to 25% confluence and put under antibiotic selection (Geneticin 500 ug/ml). The cells were feed fresh selective media every 3 to 4 days until antibiotic foci could be detected. The colonies were diluted into 96-well plated and expanded. The cells were then lysed and immunoblotted for filaminA.

## IMMUNOSTAINING AND MICROSCOPY

Cells transfected with Genejuice with the indicated cDNAs. After 24 h, cells were seeded onto fibronectin-coated glass coverslips. 48 h posttransfection, the cells were fixed with 4% paraformaldehyde, permeabilized and blocked. The cells were then stained with the indicated antibodies. Actin was detected using a rhodamine phalloidin dye (Life Technologies). Confocal imaging was performed on a Leica TCS SP5 with 63X Oil Objective (Leica, Solms Germany).

## NOCODAZOLE WASHOUT ASSAY

KO RSK2 U373MG cells seeded onto fibronectin-coated glass coverslips were with transfected with Genejuice and cDNA coding UniRapR RSK2 (Y707A) or kinase-dead (KD) UniRapR RSK2 (Y707A). After 36 h, the growth media was replaced with serum starved media. The cells were treated with nocodazole (10  $\mu$ M) at 48 h posttransfection and allowed to incubate for an additional four h. Rapamycin (500 nM) was added to the nocodazole-treated cells 30 minutes before the end of the four h incubation. The cells were fixed at the indicated time points and stained for tubulin and focal adhesion marker vinculin.

## MIGRATIONS ASSAYS

### *Transwell Migration Assay*

Cells were transfected with Genejuice transfection reagent and indicated cDNAs, then seeded ( $1 \times 10^9$  cells) into fibronectin-coated (10  $\mu$ g/ml) Transwell plates in media supplemented with rapamycin (500 nM). After the cells migrated for the indicated time points they were trypsinized from the bottom of the transwell and stained with Calcein-AM vital dye. The

amount of cells that migrated through the transwell was determined by spectroscopic measurement at 520 nm.

### *Scratch Assay*

M2 and stably expressing filaminA and filaminA (S2152A) M2 cells were grown in 6-well culture plates and transfected with the DA-RSK2 or empty vector constructs using Genejuice transfection reagent. The cells were allowed to grow to confluence then scratched with a 200  $\mu$ L pipette tip. The cells were then washed with serum free media and replaced with media containing 1% serum. Cells were allowed to migrate into the scratch for 48 h. Images of the scratch were acquired immediately after scratching ( $t=0$ ) and at 48 hours. The average closure of the scratch by GFP-expressing migrating cells was measured using ImageJ software (National Institutes of Health, Bethesda, MD), and expressed as relative migration normalized to the  $t_0$  distance.

### INTEGRIN PULL-DOWN ASSAYS

Recombinant, His-tagged human integrin cytoplasmic tail model proteins were produced and purified as previously described. Binding assays using recombinant integrin cytoplasmic tails bound to His-bind resin (Novagen) were performed as previously described. Briefly, CHOK1 cells were transfected with the indicated DNA using Lipofectamine2000 (Invitrogen), and the cells were harvested 48 h later and lysed with XTT lysis buffer. Cell lysates were incubated with integrin tails bound to beads for 24 h, washed, resuspended in SDS sample buffer, heated for 5 min at 95°C, and analyzed for binding by SDS-PAGE. The lysate lanes in the immunoblotting images represent 2.5% or 5% input of total lysate protein

amount mixed with the integrin tails and serves as a reference for relative protein amounts used in the assay.

#### INTEGRIN ACTIVATION ASSAY

The activation state of endogenous  $\beta_1$  integrin in response to transient transfection of the indicated cDNAs was assessed by three-color FACS assays as previously describe. Briefly, 48h after transfection cells were harvested and analyzed for transfection efficiency (GFP) and the binding of integrin  $\alpha_5\beta_1$  binding to FN-(9.11) fusion protein. For each transfection, harvested cells were divided into three tubes. The three preparations were used to assay for binding to ligand alone, binding in the presence of integrin inhibitor (10 mM EDTA), or carried out in the presence of integrin activator (10 mM  $MnCl_2$ ). Activated integrins bound to FN-(9.11) were detected with secondary antibodies conjugated to fluorochromes as indicated (Invitrogen, cat#S868). All incubations and washes were carried out using 1X tyrode buffer (10 mM HEPES, 10 g of NaCl, 1.015 g of  $NaHCO_3$ , 0.195 g KCl, 1 mg/ml dextrose, 1 mg/ml bovine serum albumin, 1 mM  $CaCl_2$ , 1 mM  $MgCl_2$ , pH 7.4). Propidium iodine (1 ng/ $\mu g$ ) was added to each sample for the last 5 min. Samples were washed 1X before analysis. Gating was set such that only living (propidium iodine negative) cells expressing GFP were examined for FN-(9.11) binding. Integrin activation was quantified as an activation index (AI) as previously defined.  $AI=100*(F-F_0)/(F_m-F_0)$ , where F represents the geometric mean fluorescence (GMF) of ligand binding alone,  $F_0$  is the GMF of ligand binding in the presence of inhibitor, and  $F_m$  is the GMF of ligand binding in the presence of activator. Flow cytometry data analysis was done with BD CellQuest Pro FACS analysis software.

#### IN VITRO KINASE ASSAYS

*In vitro* kinase assays were performed as follows. Briefly, 10 µg of substrate was incubated with 100 ng of active RSK2 (SignalChem), and 1.25 nmol of ATP in 1X kinase buffer (Cell Signaling) or 0.8 µCi/µ [γ-<sup>32</sup>P] ATP (PerkinElmer) with 1.25 nmol ATP in 3X kinase buffer. The kinase reactions were carried out at 30 C for 30 minutes; then, terminated by addition of SDS sample buffer. Kinase substrates were prepared as follows: HA-Talin (Santa Cruz HA[Y-11]) was immunoprecipitated from lysates prepared from CHOK1 cells that had been serum starved (0.5% FBS) for 24 hours. The complexes were precipitated by incubation with A/G agarose beads (Santa Cruz), collected and washed with RIPA buffer. Wild-type and mutant FilaminA were purified as glutathione *S*-transferase (GST) fusion proteins from *Escherichia coli* (BL21[DES]) as previously described.

#### ADP-GLO KINASE ASSAY

Hela cells were transfected with Genejuice transfection reagent and cDNA coding HA-tagged DA-RSK2, UniRapR RSK2, Kinase-dead (KD) UniRapR RSK, or empty vector. After 48 h, cells were lysed and RSK2 immunoprecipitated with an antibody specific to human influenza hemagglutinin. The immunoprecipitated proteins were examined for their ability to phosphorylate SP6 in a ADP-Glo Kinase Assay (Promega Cat #H000). The *in vitro* luminescence kinase reaction were performed according to the manufacturer's directions. Briefly, 10 µg of SP6 (RRRLSSLR) peptide was incubated with 100 ng of immunoprecipitated RSK2, and 1.25 nmol of ATP in the presence of or rapamycin (500 nM) or vehicle. The kinase reactions were carried out at 37 C for 15 minutes; then, terminated and remaining ATP

depleted by the addition of ATP-Glo reagent for 40 minutes at room temperature. The remaining ADP was converted to ATP, which is detected via a luciferase/luciferin reaction by addition of Kinase Detection Reagent for 30 minutes at room temperature. The amount of luminescence generated in the reaction was quantified using the PerkinElmer EnVision Multilabel Reader.

## 2.5 FIGURES

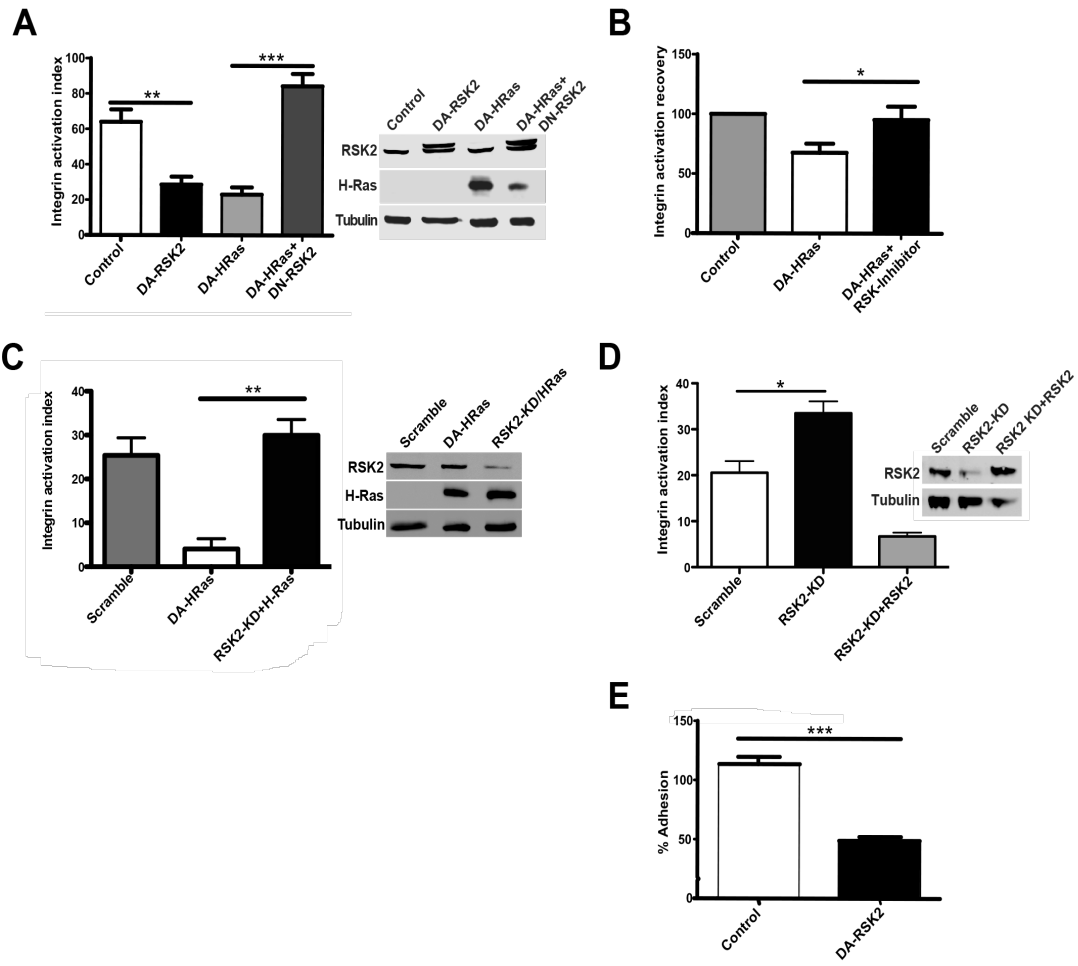


FIGURE 2.1 RSK2 INHIBITS INTEGRIN ACTIVATION AND IMPAIRS CELL ADHESION

2.1 (A) (B) CHOK1 cells expressing chimeric  $\alpha\text{IIb}\beta_3$  were transiently transfected with empty vector (control) or DA-RSK2 (RSK2-Y707A), activated DA-H-RAS (H-RASG12V), or activated DA-H-RAS in combination with DN-RSK2 (H-RASG12V and RSK2-K100A) (A). (B) CHOK1 cells were transiently transfected with empty vector (control) or activated DA-H-RAS (H-RASG12V) and treated for 24 h with carrier or RSK2 inhibitor, FMK (20  $\mu\text{M}$ ). (C) (D) HeLa cells with stable knockdown of RSK2 were transiently transfected with HA-RSK2 or with activated DA-H-RAS (H-RASG12V) additionally, HeLa cells stably expressing scrambled shRNA were also transiently transfected with activated DA-H-RAS (H-RASG12V). Integrin activation was measured by incubating the cells with the ligand-mimetic antibody PAC1 or FN-(9.11) ligand and analyzed by flow cytometry. The percentage of activation is shown. Integrin activation recovery was normalized versus control cells. E, CHOK1 cells were transiently transfected with control vector or DA-RSK2 (RSK2-Y707A). 48 h after transfection, the cells were subjected to a cell adhesion assay to fibronectin. Adherent cells were quantified at 1 h using UV-VIS spectrophotometer. The numbers of cells have been normalized to 100% input - a maximal number of cells that could adhere.

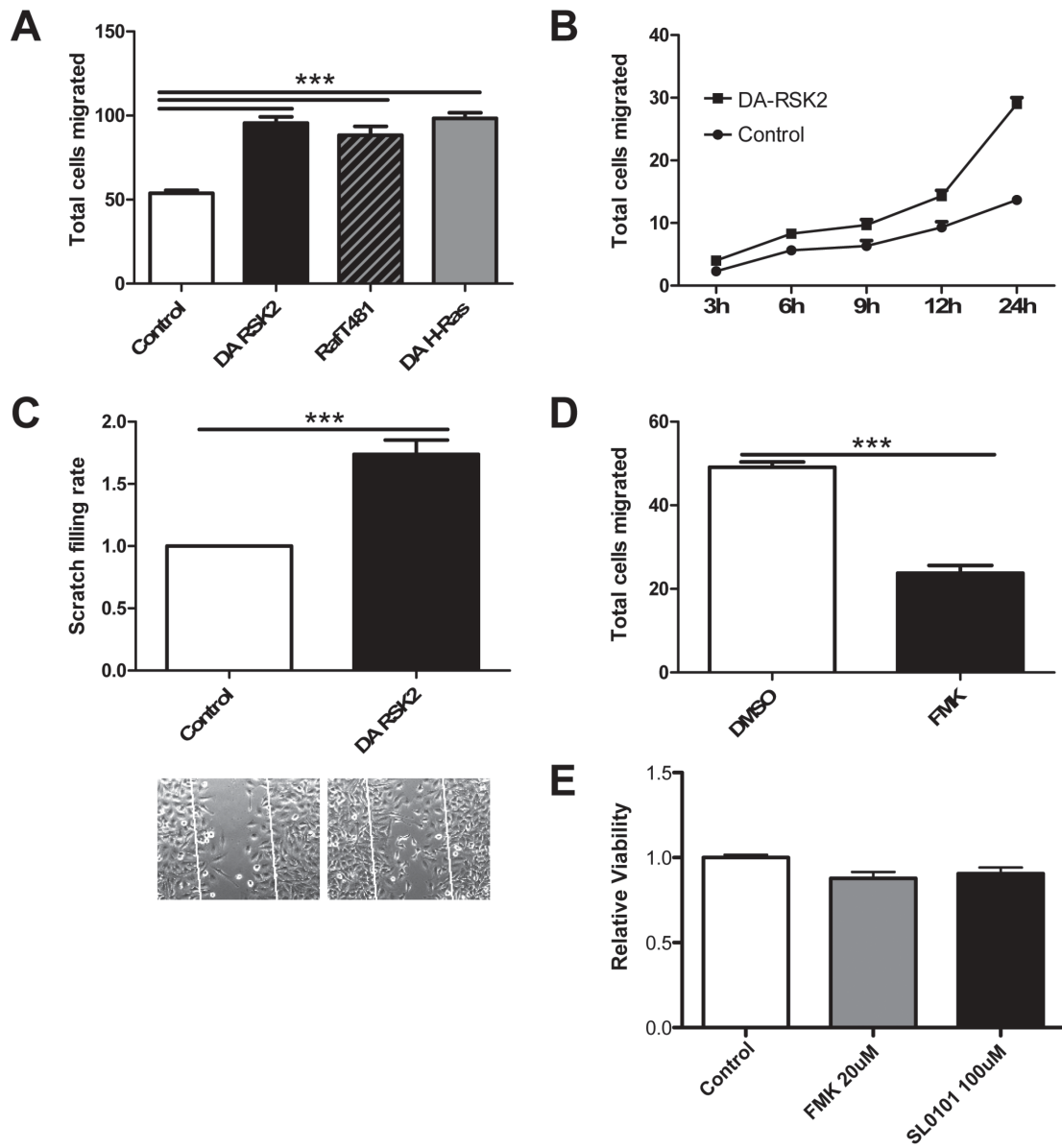


FIGURE 2.2 RSK2 enhances cell migration on fibronectin

2.2 (A) HeLa cells were transfected with indicated plasmids in combination with a vector expressing  $\beta$ -galactosidase. The cells were plated in the upper chamber of a fibronectin-coated Transwell plate. After 6 h, the total number of transfected cells that had migrated through to the bottom of the membrane was counted in random fields using a blinded analysis. (B) (C) HeLa cells were transiently transfected with DA-RSK2 or empty vector. 24 h later, the cell monolayer was scratched. B, the total number of cells that migrated into the scratch area was counted at various time points. (C) relative scratch filling rate was calculated at 24 h. The inset shows a representative image of scratch after 24 h of recovery time. (D) HeLa cells were treated with either the RSK2 inhibitor FMK or Me<sub>2</sub>SO as a carrier control, and the cell monolayer was scratched. The total number of cells that migrated into the scratch area was counted at 24 h. (E) HeLa cell viability in these assays upon exposure to FMK or SL0101-1 was determined by XTT assay. Shown is the relative viability corrected to a treatment with the carrier control (n=3). (Gawecka and Young-Robbins *et al.*)<sup>91</sup>.

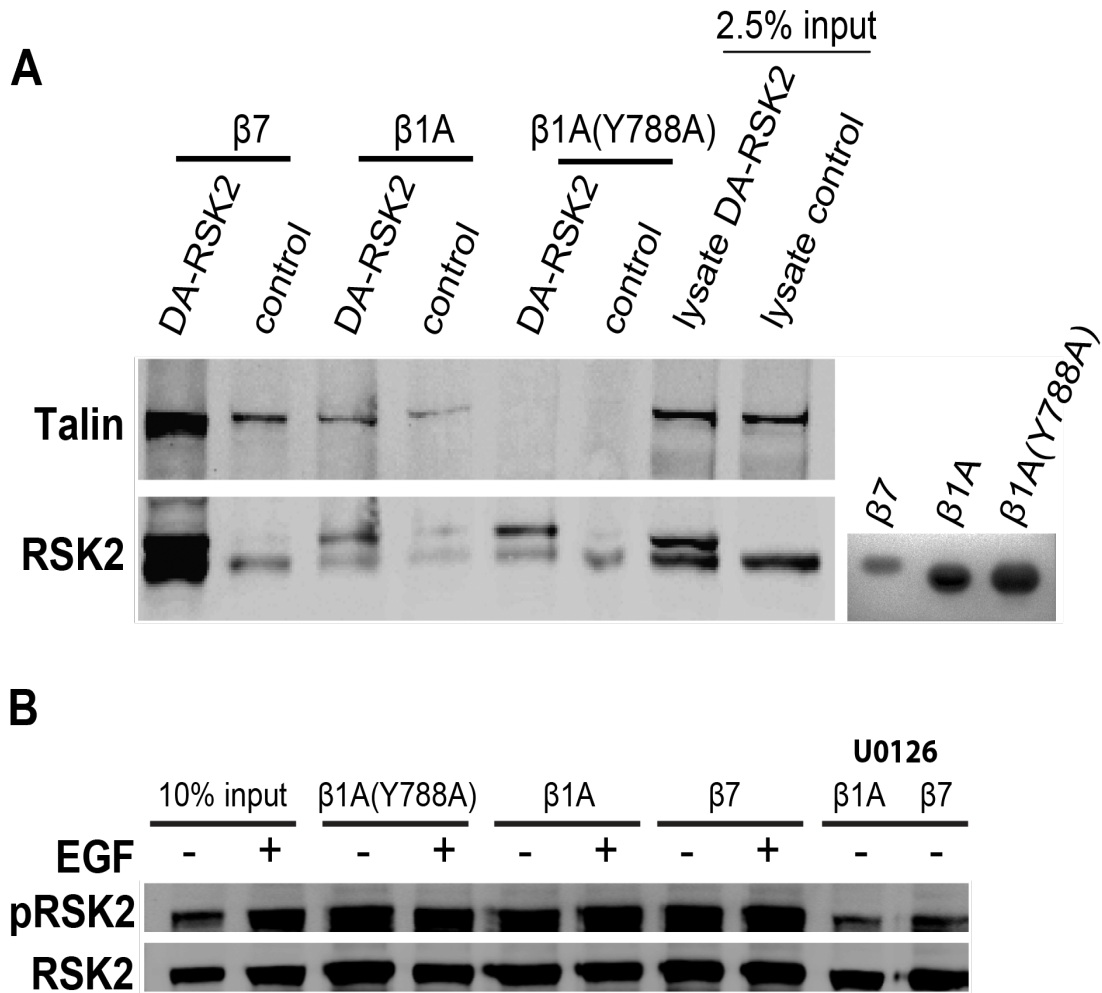


FIGURE 2.3 RSK2 ASSOCIATES WITH INTEGRIN TAIL COMPLEXES

2.3 (A) CHOK1 cells were transfected with DA-RSK2 (RSK2-Y707A) or empty vector (Control). 48 h posttransfection, the cells were lysed and incubated with bead-bound purified integrin cytoplasmic domains. (A) bound RSK2 and talin were detected by immunoblotting as indicated. RSK2 transfection efficiency was verified by immunoblotting of whole cell lysates. A, bead-bound purified integrin cytoplasmic tail expression was verified by Coomassie staining. (B) serum-starved CHOK1 cells were stimulated with EGF (50  $\mu$ g/ml), MEK inhibitor (U0126, 10 $\mu$ M), or with vehicle alone (Me<sub>2</sub>SO). The cells were lysed and incubated with bead-bound purified integrin cytoplasmic tails. B, bound RSK2 and pRSK2 (S386) were analyzed by immunoblotting.

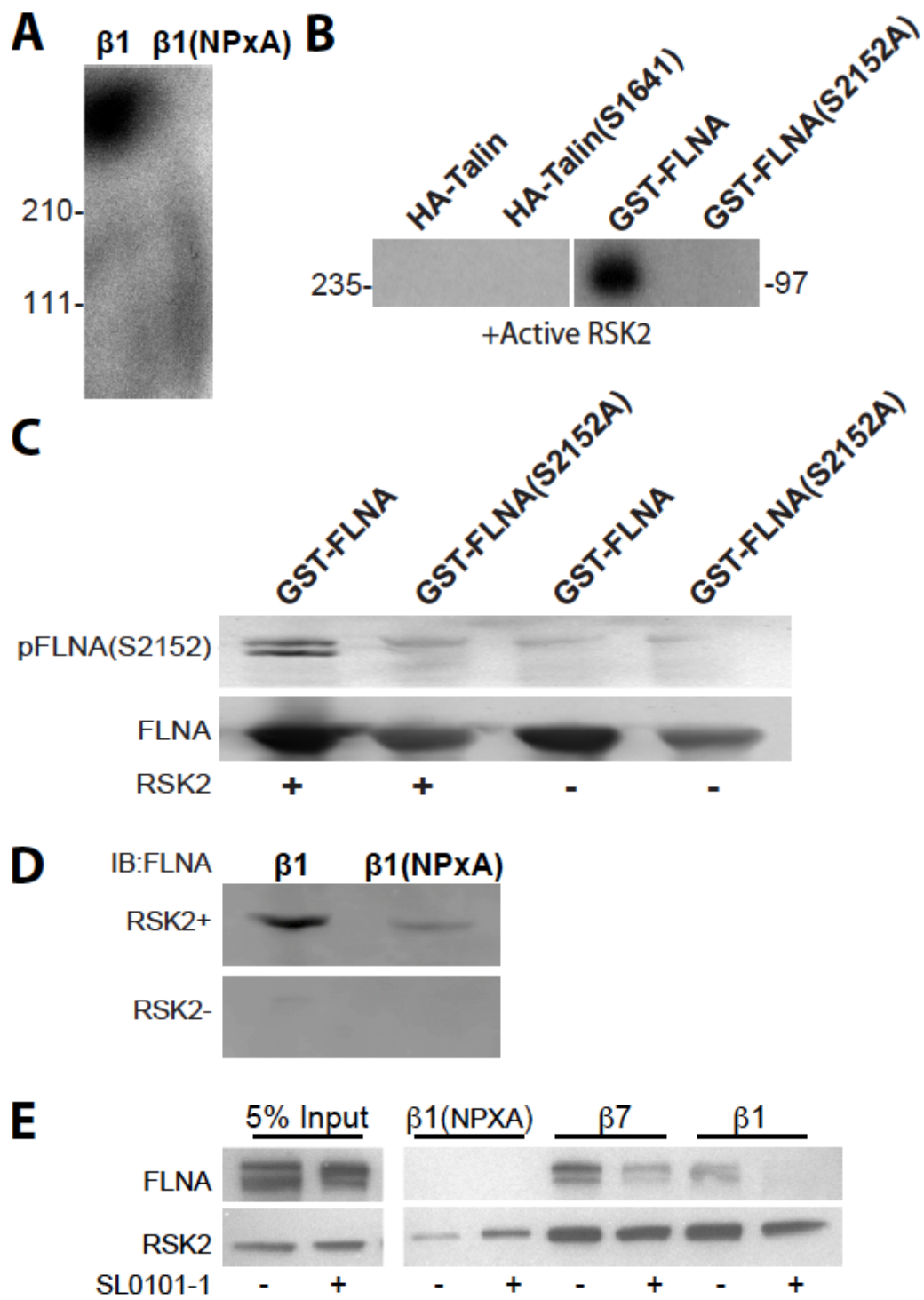


FIGURE 2.4 RSK2 MODULATES FILAMINA BINDING TO INTEGRIN TAILS

2.4 (A) integrin tail complexes were prepared by incubating serum-starved CHOK1 cell lysates with integrin cytoplasmic domains bound to beads. The beads were washed and incubated with purified active RSK2 in a kinase buffer with [ $\gamma^{32}\text{P}$ ]ATP. The autoradiograph is shown. (B) RSK2 phosphorylation of talin and filaminA was assayed in the same manner using [ $\gamma^{32}\text{P}$ ]ATP. HA-talin was immunoprecipitated from lysates prepared from serum-starved CHOK1 cells that were transiently transfected with HA-talin or HA-talin (S1641A). Recombinant GST-filaminA and phosphomutant GST-filaminA (S2152A) were also examined. (C) RSK2 phosphorylation of recombinant GST-filaminA and phosphomutant GST-filaminA (S2152A) was further tested by immunoblotting with an antibody specific for S2152 phosphorylated filaminA. The bottom panel represents a Coomassie stain of purified glutathione-agarose-bound filaminA proteins. (D) lysates from serum-starved CHOK1 cells were incubated with purified RSK2 or control in kinase buffer. FilaminA binding to the tails was determined by immunoblot. (E) CHOK1 cells were incubated with RSK2 inhibitor (100  $\mu\text{M}$ ) or control carrier ethanol for 30 min. Lysates from these cells were then incubated with integrin cytoplasmic tail proteins to determine filaminA binding to integrin  $\beta_7$ ,  $\beta_1$ , and  $\beta_1$  (NPxA) mutants. Input of 5% served as a control for the presence of filaminA and RSK2.

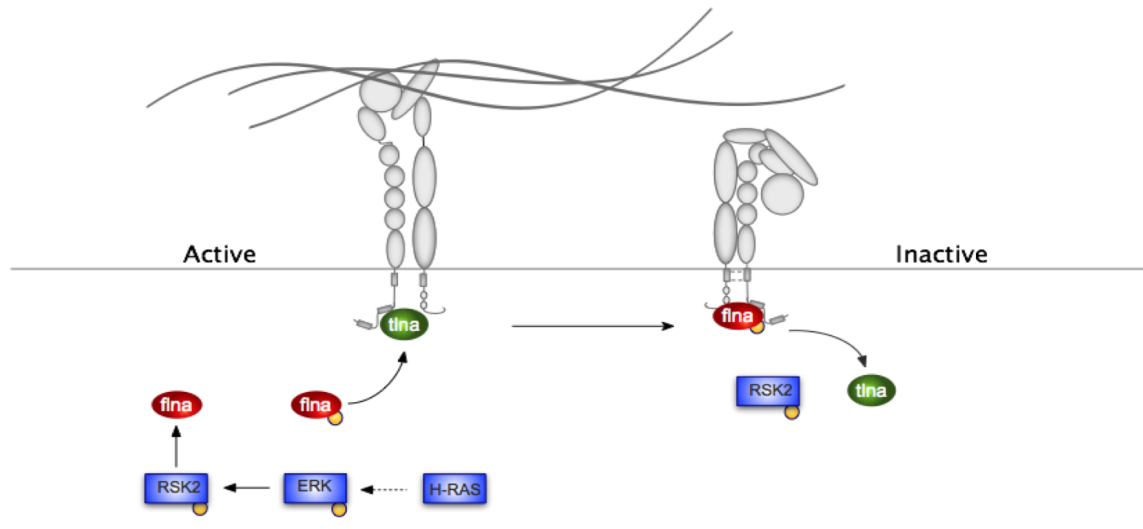


FIGURE 2.5 MODEL OF RSK2 MEDIATED TLN/FLNA EXCHANGE ON INTEGRIN TAIL

2.5 Diagram depicting growth factor receptor signaling activates RSK2. Active RSK2 phosphorylates filaminA at S2152 promoting filaminA binding to integrins. This stimulates the talin/filaminA exchange at the integrin and subsequent integrin inactivation.

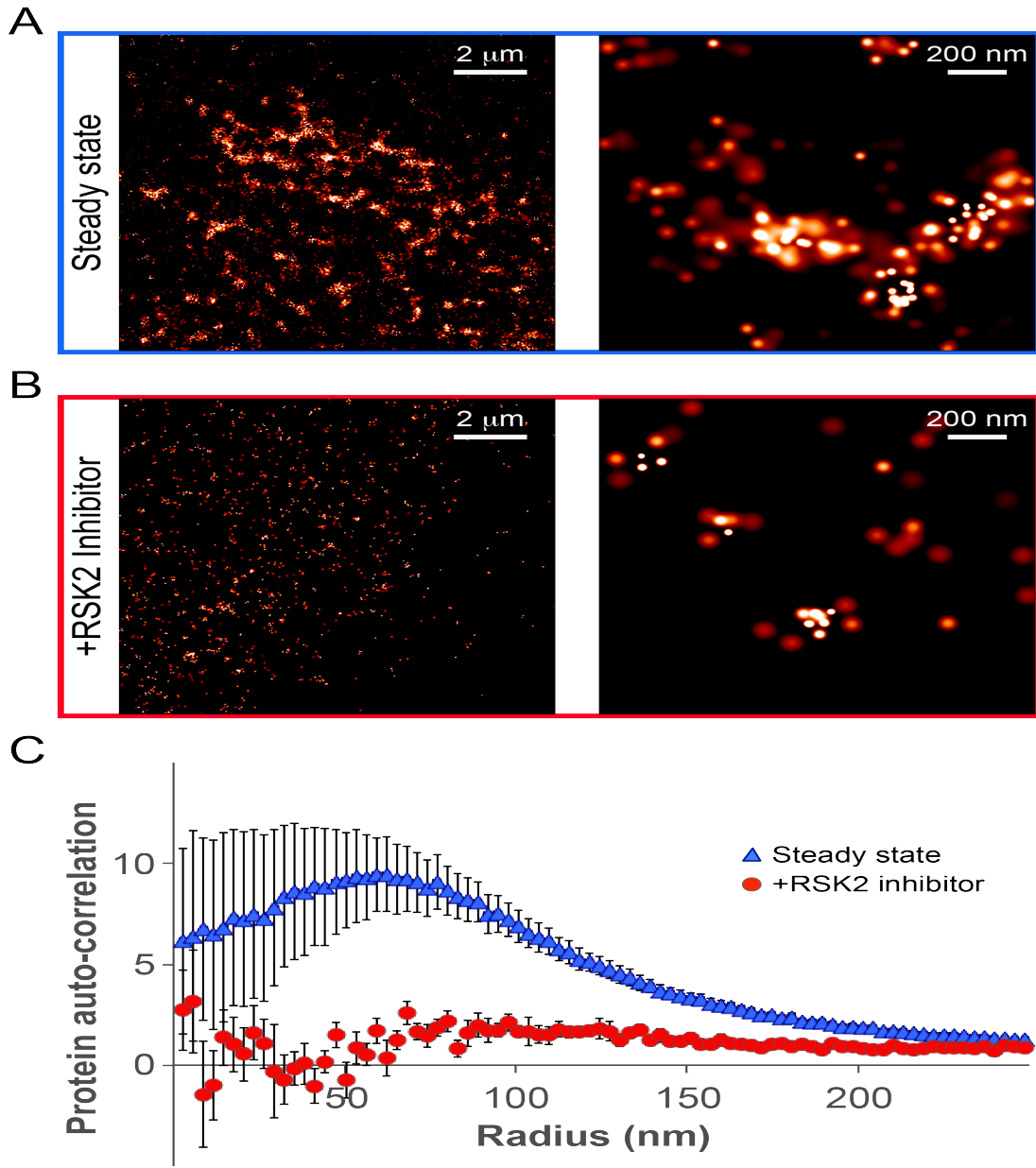


FIGURE 2.6 RSK INHIBITOR IMPAIRS FLNA DISTRIBUTION AT THE PLASMA MEMBRANE

2.6 (A) PALM image showing the distribution of endogenous filaminA in steady state (2  $\mu\text{m}$ ) and magnification of that image (200 nm). (B) Image of filaminA distribution following 24 hour treatment with RSK inhibitor BI-D1870 (10  $\mu\text{M}$ ). High resolution images were generated by analyzing the dataset using maximum blinking time of 25.6 s for Cage 552 dye and group radius of  $2.5 \sigma$ . (C) average protein autocorrection curves in untreated cells (blue triangles, N=9) and after 24 hours' incubation with RSK inhibitor (red circles, N=6); inhibition of RSK results in random distribution of filaminA. (Dr. T. Talisman, City of Hope)

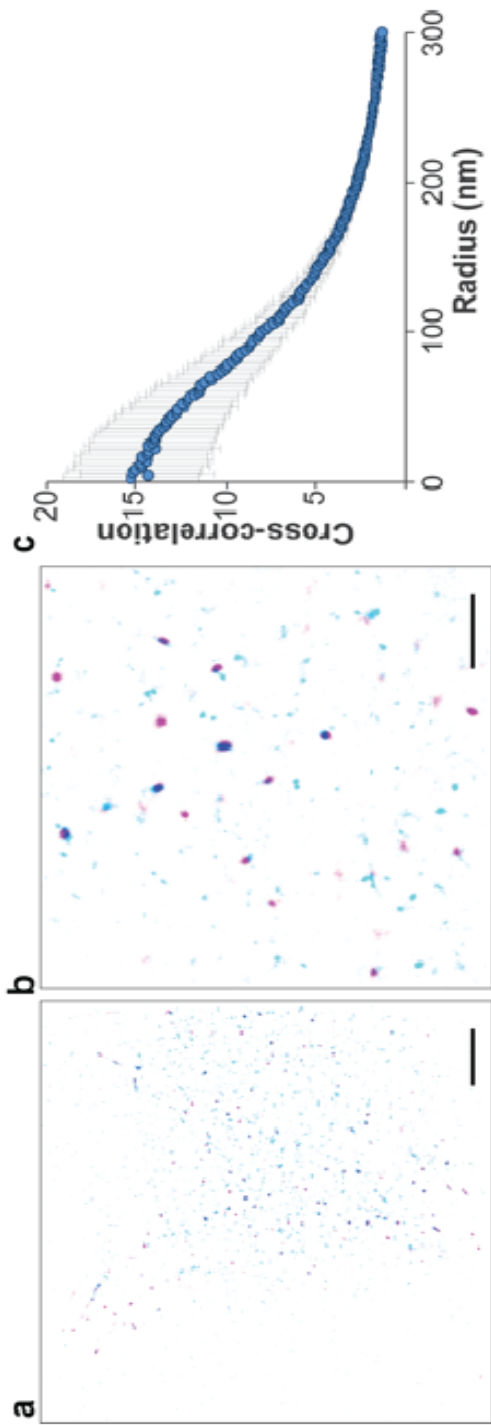


FIGURE 2.7 FILMINA AND RSK2 COLOCALIZIE AT THE PLASMA MEMBRANE

2.7 Distribution of filaminA (magenta, detected with Atto 488) and RSK2 (cyan, detected with Alexa 647) in U373MG cells. Direct stochastic optical reconstruction microscopy (dSTORM)<sup>116</sup> was used to reveal nano-scale distribution of proteins. Affinity tagging with specific primary antibodies and fluorescently labeled secondary antibodies was performed to detect proteins. (A) Whole cell; scale bar, 5  $\mu\text{m}$ , and (B) Enlarged region; scale bar, 2  $\mu\text{m}$ . Overlap is evident in dark blue. Normalized Gaussians are shown; colors are inverted for clarity. (C) To quantitatively assess co-localization between two proteins, we conducted cross-correlation analysis of two-color super-resolution microscopy data, similarly as reported before. Cross-correlation curves show co-localization between filaminA and RSK2 (N=25). No long-range correlations were observed. Standard error bars are shown; area size, 80.28  $\mu\text{m}^2$ . (Dr. T. Talisman, City of Hope)

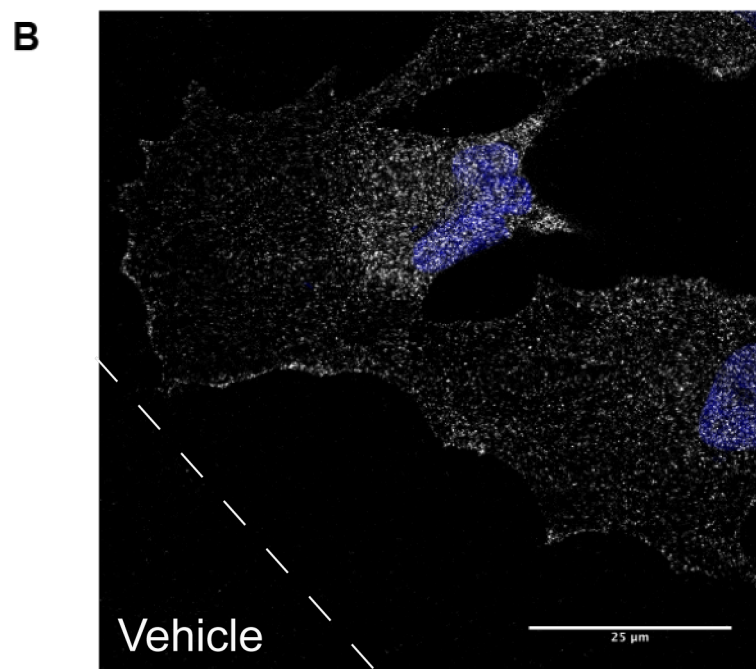
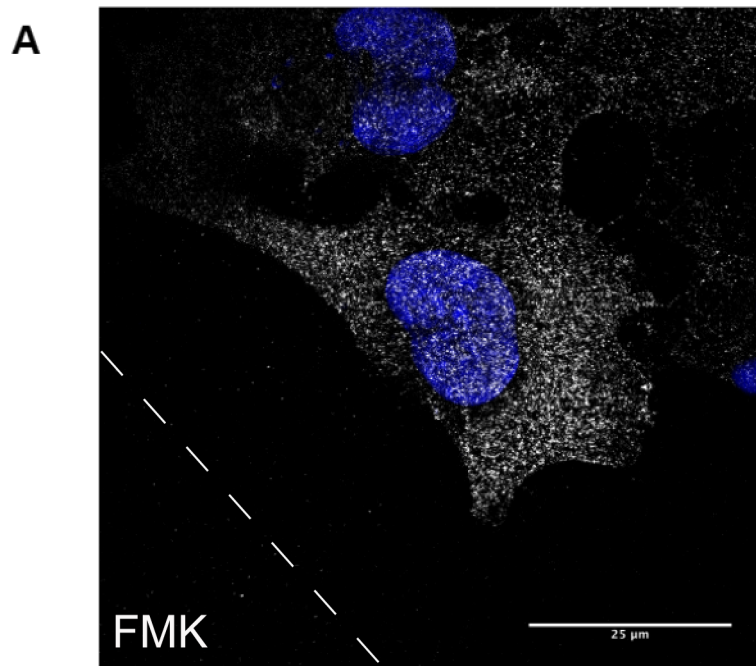


FIGURE 2.8 THE LOCALIZTON OF RSK2 IN A MIGRATING CELL.

2.8 Glioblastoma U373MG cells were treated with FMK inhibitor (20  $\mu$ M) (A) or vehicle (DMSO) for 4 hours then scratched to stimulate migration. After 16 hours, cells were fixed and stained for RSK2 (white). Immunostaining was visualized using TCS SP5 confocal microscope. The scale bars represent 25  $\mu$ m. Dotted line represents the scratch.

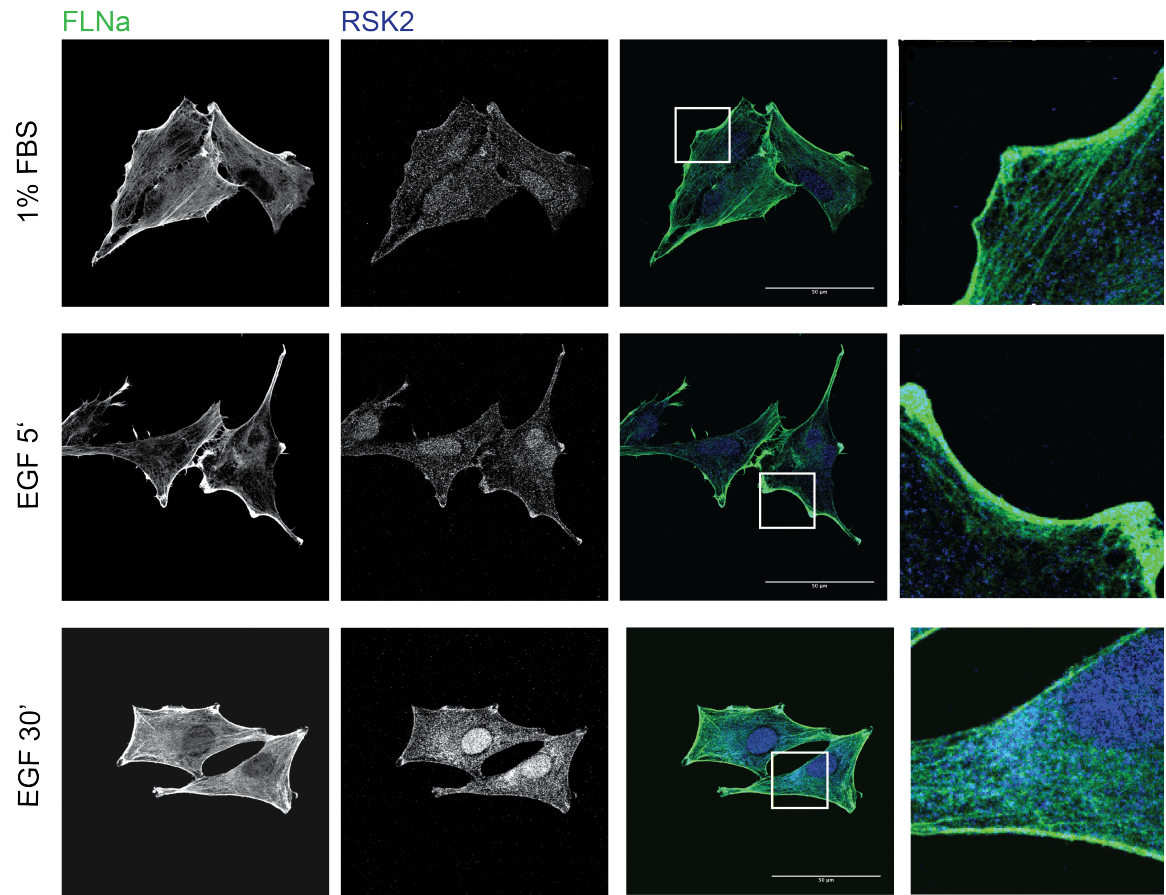


FIGURE 2.9 RSK2 AND FLNA COLOCALIZE AT THE TRAILING EDGE OF A MIGRATING CELL

2.9 Glioblastoma U373MG cells were serum starved for 18 hours then stimulated with EFG (100 ng/ml) for 5 minutes and 30 minutes. The cells were fixed at indicated time points and stained for RSK2 (blue) and filaminA (green). Immunostaining was visualized using TCS SP5 confocal microscope. The scale bars represent 50  $\mu$ m.

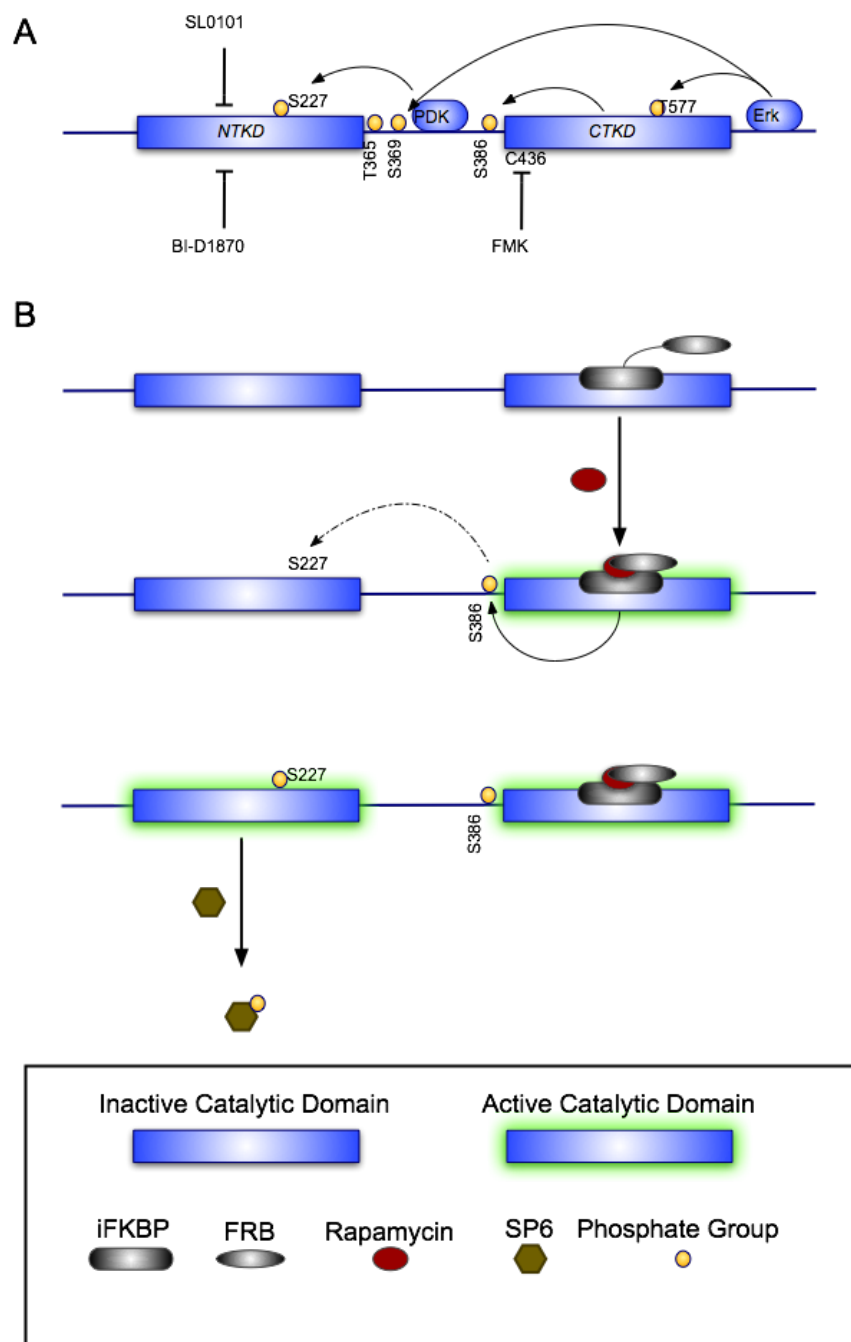
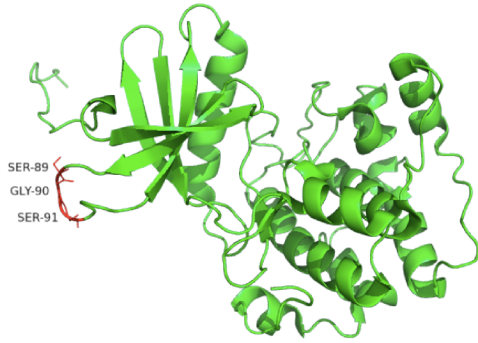


FIGURE 2.10 UNIRAPR RSK2

2.10 (A) RSK2 structure and the key regulatory sites required for full activation of the kinase. (B) A diagram depicting the insertion of UniRapR into a site allosterically coupled to the g-loop of the binding pocket of the CTKD. UniRapR is a single chain regulatory protein based on the interaction of the mTOR FKBP domain and the cytosolic protein FRB. When inserted into the allosteric site, UniRapR disrupts the ability of the CTKD to bind ATP. In the presence of Rapamycin or a non-immunogenic derivative of rapamycin, the two domains bind and reactivate the enzyme.

**A**

NTKD (pdb id: 4NW5). uniRapR insertion site is shown in red



CTKD (pdb id: 4JG6). uniRapR insertion site is shown in red

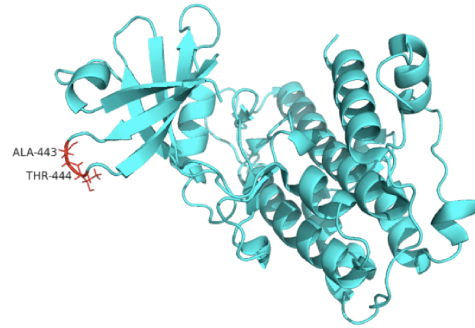
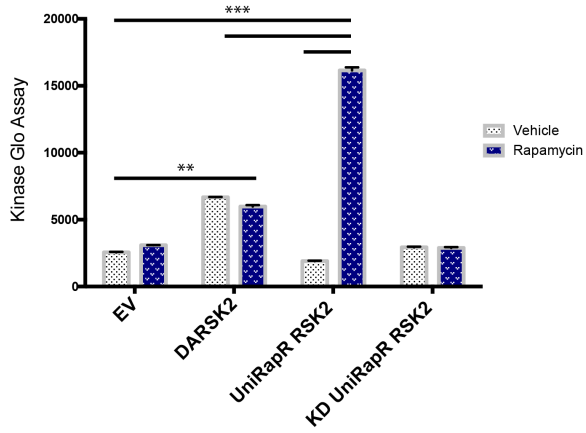
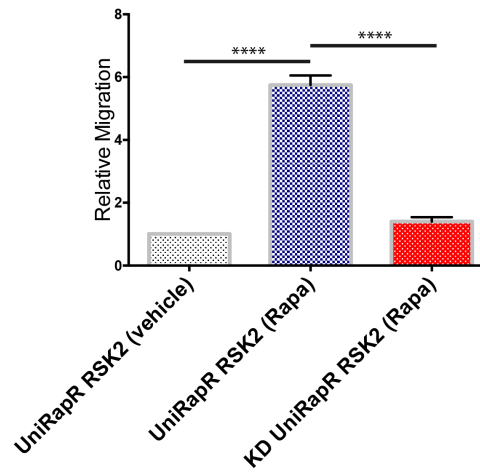
**B****C**

FIGURE 2.11 UNIRAPR RSK2 PHOSPHORYLATES SP6 AND PROMOTES MIGRATION

2.11 (A)(B) PyMol images of the NTKD and CTKD insertion sites, respectively, of the UniRapR domain into the allosteric site. B, HeLa cells were transiently transfected with HA-tagged constructs of DA-RSK2, UniRapR RSK2, Kinase-dead (KD) UniRapR RSK, or empty vector. After 48 h, cells were lysed and RSK2 immunoprecipitated with an antibody specific to human influenza hemagglutinin. The immunoprecipitated proteins were examined for their ability to phosphorylate SP6 in a Kinase-Glo Assay (Promega). (C) HeLa cells were transfected with UniRapR RSK2, KD-UniRapR RSK2 or empty vector. 24 hours posttransfection the cells were seeded into a fibronectin-coated transwell plate in serum starve media supplemented with 500 nM rapamycin, then allowed to migrate for 18 hours. The cells that migrated through the transwell membrane were stained with the vital dye Calcein-AM and the relative migration determined by spectroscopic measurement at 520 nm.

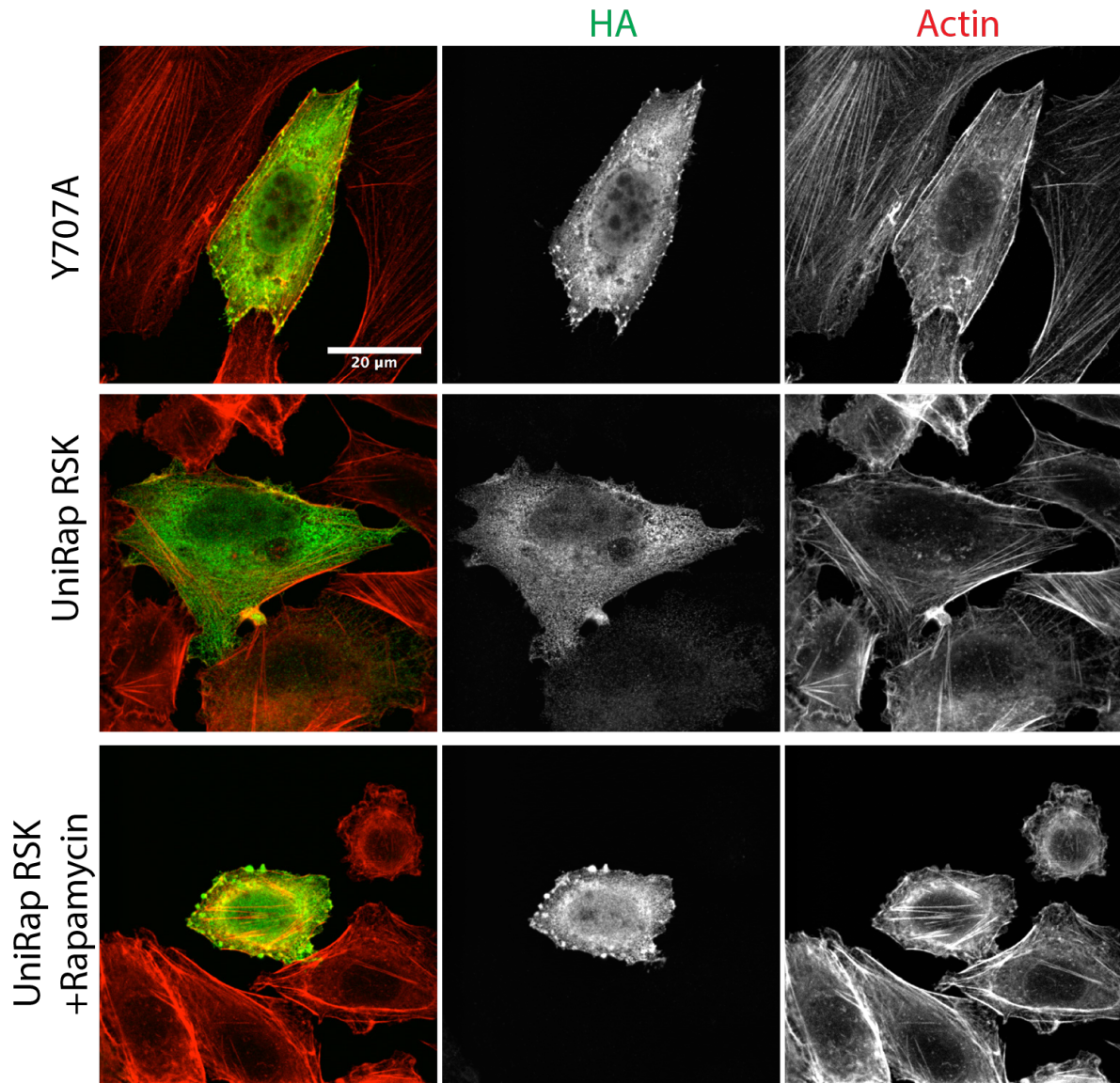


FIGURE 2.12 IMMUNOFLUORESCENT MICROGRAPH OF UNIRAPR RSK2

2.12 KO RSK2 glioblastoma U373MG cells were transiently transfected with UniRapR RSK2 or DA-RSK2. 36 h posttransfection, cells were serum starved for 18 hours before treating with rapamycin (500 nM) or vehicle. The cells were fixed and stained for HA (DA-RSK2/UniRapR RSK2) and actin. Immunostaining was visualized using TCS SP5 confocal microscope. The scale bar represent 20  $\mu$ m.

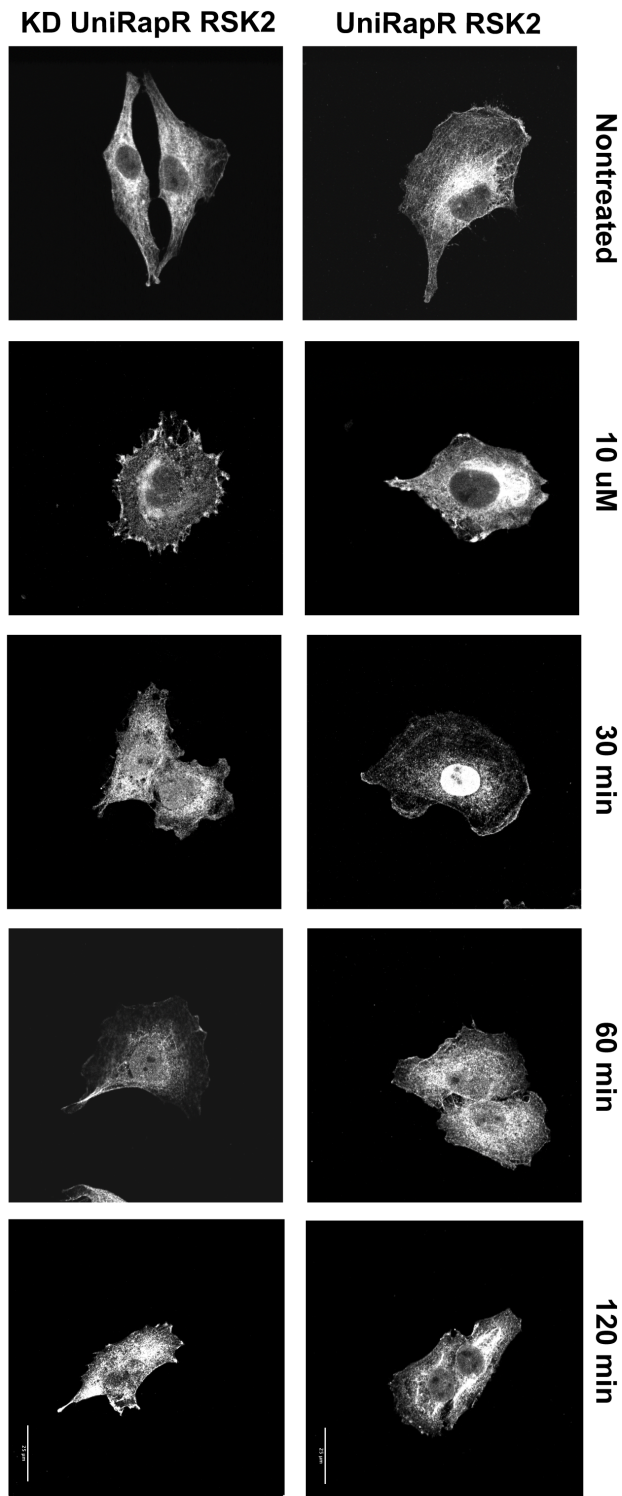


FIGURE 2.13 RSK2 STIMULATES FOCAL ADHESION DISASSEMBLY

2.13 KO RSK2 glioblastoma U373MG cells were transiently transfected with UniRapR RSK2 or a kinase-dead UniRapR RSK2. After 48 hours, the cells were treated with microtubule disrupting agent, nocodazole, for 4 hours in serum starved media. Rapamycin (500 nM) was added to the incubating cells 30 minutes before the end of the nocodazole incubation. The cells were fixed at the indicated time points then stained for both tubulin and vinculin as a marker for focal adhesions.

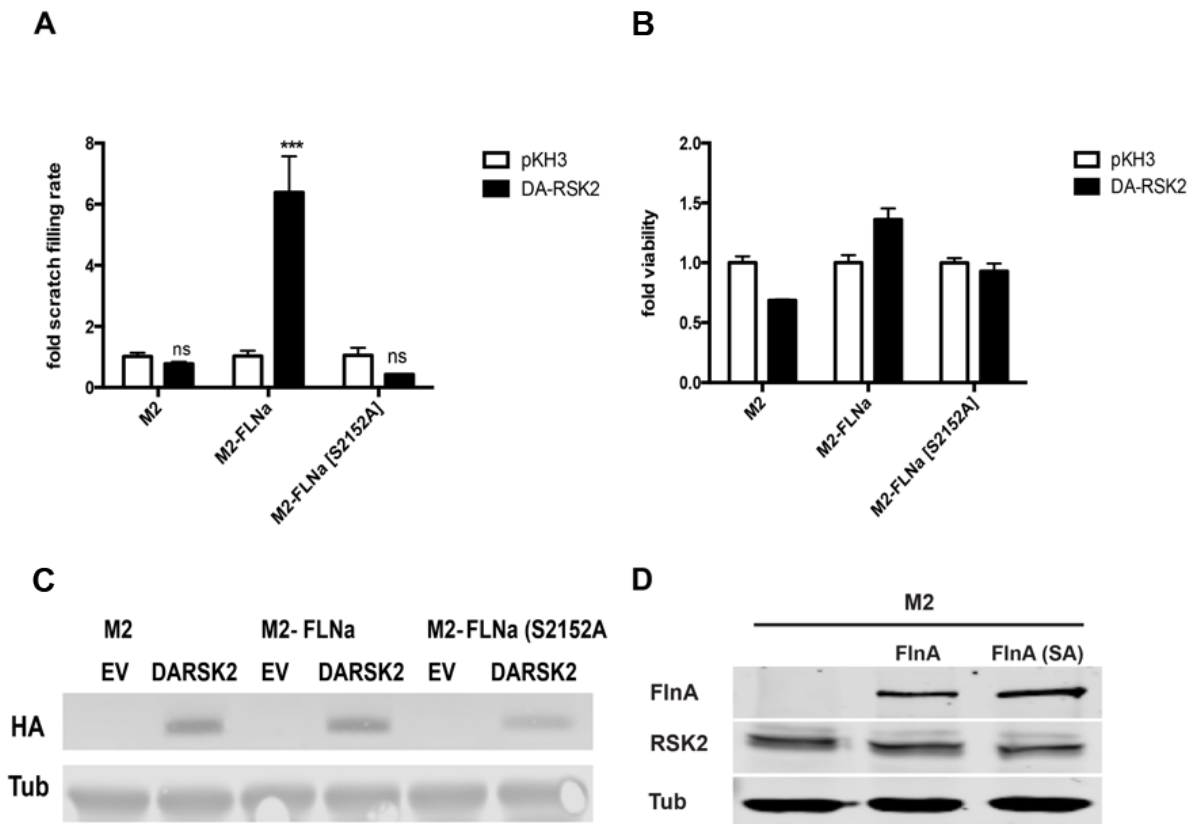


FIGURE 2.14 RSK2 REGULATES FLNA-MEDIATED MIGRATION

2.14 (A) M2 filaminA-deficient melanoma cell line was stably transfected with myc-filaminA or phosphomutant myc-filaminA (S2152A). The M2 cells lines were transiently transfected with HA-tagged DA-RSK2 or empty vector. The transfected cells were grown to confluence on a fibronectin-coated plate then scratched and allowed to migrate for 48 hours. The relative migration of the cells was accessed by measuring the average closure of the scratch width relative to  $t_0$  using ImageJ software. (B) the cells remain viable throughout the assay. (C) the expression of DA-RSK2 was verified by immunoblotting for human influenza hemagglutinin. (D) The expression of myc-filaminA, myc-filaminA (S2152A), and RSK2 in M2 stably transfected melanoma cell line.

## CHAPTER 3

### RSK2 ACTIVITY MEDIATES GLIOBLASTOMA INVASIVENESS AND IS A POTENTIAL TARGET FOR NEW THERAPEUTICS.

The majority of the work in this chapter has been submitted for publication in

Oncotarget

Sulzmaier and Young-Robbins *et al.*

### 3.1 INTRODUCTION

Glioblastoma multiforme (GBM) is the most common malignant primary brain tumor diagnosed in the United States<sup>117, 118</sup>. GBM is a histologically heterogeneous and aggressive tumor that arises from glial cells and their progenitors<sup>119, 120</sup>. GBM cells are highly motile and invade the healthy brain tissue establishing micro-tumors distances away from the primary site. This make complete surgical resection of GBM challenging and contribute to the high recurrence and low survival rates (5.1%) in GBM patients<sup>118 121, 122</sup>. Furthermore, invasive GBM cells are less sensitive to the current standard therapies including radiation and chemotherapy with DNA alkylating agents such as temozolomide<sup>123, 124</sup>. GBM cells spread within the brain by migrating in a mesenchymal fashion along the ECM of myelinated fiber tracts and blood vessels<sup>125, 126</sup>. This migration is mediated by dynamic interactions between the cancer cell and its surrounding ECM through transmembrane cell adhesion receptors like integrins<sup>127-129</sup>. The infiltrative nature of GBM enhances its potential for migration and studies have shown that  $\beta_1$ -integrins facilitate this invasion into normal brain tissue, particularly,  $\alpha_3\beta_1$  integrins<sup>130-133</sup>. In a brain xenograft model, rat C6 cells overexpressing of  $\beta_1$  -integrins were shown to be more invasive than the control parental cell line<sup>131</sup> and treating glioma-derived cell lines with neutralizing antibodies against  $\beta_1$ -integrins attenuates GBM immigration<sup>129, 133, 134</sup>

The RAS oncogene is constitutively active in many glioblastomas due to mutation or amplification of their upstream growth factors. H-RAS negative regulates integrin signaling through its downstream target RSK2<sup>135-137</sup>. RSK2 is a Ser/Thr kinase that activates

transcription and proliferation and regulates apoptosis<sup>54, 56, 138</sup>. RSK2 inhibitors have revealed additional roles for RSK2 in controlling proliferation of prostate and breast cancer cells<sup>139 69, 140</sup> and differentiation of muscle cells<sup>141</sup>. Recent work has shown that RSK2 are required for invasion and metastasis of many cancers<sup>52, 142, 143</sup>. RSK2 directly phosphorylates filaminA. FilaminA is a scaffolding protein that forms an elongated homodimer crosslinking F-actin and thereby affecting invasion<sup>144-147</sup>. Activation of RSK2 by ERK promotes filaminA phosphorylation and enhances its binding to integrin tail complexes thereby modulating focal adhesion activity<sup>137</sup>. FilaminA binds to the integrin cytoplasmic tail at an NPxY motif that also interacts with integrin activator talin<sup>148</sup>. As a result, filaminA and talin may compete for integrin-binding<sup>31</sup>. Finally, filaminA association with the integrin cytoplasmic tails maintains the integrin in the inactive state. RSK2 acts as mediator of cell migration and invasion, thereby driving tumor aggressiveness. Since GBM is characterized by a high degree of invasiveness, we investigated if RSK2 signaling is involved in the progression of this malignancy.

## 3.2 RESULTS

### RSK2 ACTIVITY IS REQUIRED FOR GBM CELL MIGRATION AND INVASION

We have found that RSK2 promotes migration in Hela and CHOK1 cells<sup>137</sup>. Therefore, we predicted that RSK2 activity is required for GBM motility. We examined the effects of RSK inhibition on *in vitro* migration. Treatment of GBM U373MG cells with RSK inhibitors FMK or BI-D1870 attenuated migration in a transwell migration assay along with a haptotactic-chemotactic gradient (figure 3.1). RSK activity was also found to be required for GBM cell lines U87MG and U373MG to invade three-dimensional matrices as inhibition by BI-D1870 resulted in nearly a 2-fold reduction in invasion (figure 1 C, D). All isoforms of RSKs are expressed in the GBM cell lines tested. (figure 3.1 A). To determine if RSK2 specifically was required for GBM invasion, we tested the ability of RSK2 KD U373MG cell to invade 3D-matrices. We found that U373 cells were dependent on RSK2 for invasion (data not shown). These findings confirm the requirement of RSK2 kinase activity for GBM tumor invasion.

### RSK2 MODULATES CELLULAR ADHESION AND IS REQUIRED FOR MIGRATION INTO MOUSE BRAIN SLICES

We previously demonstrated that RSK2 regulates integrin activation and impairs adhesion in Hela cells, we hypothesized that RSK2 might control integrin activity in GBM cells, that too could result in changes in cellular adhesion. We, therefore, determined if RSK activity had a direct impact on GBM adhesion, as an explanation for the observed differences in cell migration and invasion. We found that cells treated with the RSK inhibitor BI-D1870 were significantly more adherent to FN-(9.11), the recombinant cell-binding domain of fibronectin (figure 3.2A). Loss of RSK2 activity affected cell adhesion as early as 10 min after

plating the cells. Conversely, transient transfection of a dominant active mutant of RSK2 (RSK-Y707A) impaired cell attachment, resulting in reduced overall adhesion at multiple time-points (Figure 3.2B).

GBM invasion into brain tissue requires cells to associate with a complex microenvironment that is not entirely replicated using 2D or 3D matrices. Moreover, the current RSK inhibitors are quickly degraded *in vivo* and are not suitable for testing *in situ* in mouse xenograft models. We, therefore, examined the effect of RSK inhibition with BI-D1870 or RSK knock-out using CRISPR/Cas9 deletion on the ability of U373MG tumor spheroids to invade into mouse brain slices. These slices are 200  $\mu\text{m}$  thick and are cultured in media to maintain an environment more relevant to *in vivo* invading GBM tumor cells. We found significantly reduced invasion when RSK activity was attenuated or abolished (Figure 3.2 C and D). These results infer that RSK2 activity is a potent regulator of integrin-dependent cell adhesion and GBM cell migration and invasion.

#### RSK2 ACTIVITY DRIVES PATIENT-DERIVED GBM CELL MIGRATION AND INVASION

In a high-resolution genomic survey, Li *et al.* discovered that established GBM-derived cell lines and primary tumors have significant differences in both genomic alterations and gene expression, and concluded that GBM cell lines might not be an accurate representation of primary gliomas<sup>149</sup>. Therefore, we investigated if RSKs are required for migration and invasion in fresh GBM patient-derived cells. We found that RSK2 is expressed in all patient samples and appears activated in many of the patients (figure 3.3A). We speculated that increased RSK2 expression may contribute to GBM progression and promote tumor recurrence. We tested the effects of RSK2 gene knockout or chemical inhibition on the

migratory capabilities of the patient-derived primary GBM cell line SK748. This cell line was maintained as suspended tumor neurospheres, an *in vitro* culture technique in which cell lines better retain characteristics consistent with fresh patient cells<sup>150, 151</sup>. Scratch migration assays on SK748 showed that both RSK2 knock-out and chemical inhibition (with BI-D1870) decreased cell migration (figure 3.3C). Similarly, RSK2 gene knock-down with shRNA or chemical inhibition significantly blocked GBM SK748 invasion in transwell assays with epidermal growth factor (EGF) and fibroblast growth factor (FGF) as chemoattractants (figure 3.3D). Neither RSK2 gene knock-down nor chemical inhibition affected cell viability or proliferation in these assays, as confirmed through microscopic analysis (figure 3.4B). RSK2 kinase activity is therefore required for primary patient-derived GBM migration and invasion.

#### RSK INHIBITION ENHANCES THE EFFECTIVENESS OF STANDARD GBM THERAPY

Targeting invasion in GBM has been shown to enhance the effectiveness of the current standard of therapy temozolomide combined with irradiation<sup>121</sup>. We investigated whether RSK2 function interference would improve the effectiveness of temozolomide and irradiation therapy using GBM neurospheres derived from a patient with temozolomide resistance (GBM8) *in vitro*. We found that GBM8 cells were resistant to temozolomide and irradiation, with cell viabilities greater than 50% at 100  $\mu$ M drug compound or 4 Gy irradiation treatment (figure 3.4A). Combined treatments did not increase cell death. We observed that knockdown of RSK2 expression sensitized the patient cells to temozolomide, especially at higher concentrations (10  $\mu$ M and 100  $\mu$ M; figure 3.4A). RSK2 knockdown significantly decreased the viability of GBM8 cells treated with 10  $\mu$ M BI-D1870, whereas we

observed little change in control cells containing non-targeting shRNA (Fig. 3.4B). This is likely the result of either suboptimal effects of RSK2 gene knockdown or compensation by RSK isoforms. Importantly, although low concentrations of either temozolomide or BI-D1870 alone had little effect on cell proliferation, combinations showed an additive anti-tumor effect (1  $\mu$ M temozolomide with 1  $\mu$ M BI-D1870; Fig. 3.4c, d). Therefore, the combination of RSK inhibition with temozolomide may be a promising new therapeutic approach in GBM treatment.

RSK2 EXPRESSION IS ELEVATED IN HUMAN GLIOMA TISSUE, CORRELATES WITH HIGH TUMOR GRADE, AND IS PROGNOSTIC FOR POOR PATIENT OUTCOME

We have shown a role for RSK2 in cell migration, invasion, and therapy resistance in established GBM cell line and in fresh patient-derived cells *in vitro*. To verify that our results apply to human patients, we performed RSK2 mRNA expression analyses in extensive human glioma datasets in the public domain. Comparing the brain samples in the “Human Body Map” which consist of the three largest, best annotated public glioma datasets, we find that RSK2 mRNA expression is significantly lower in normal brain tissue than in human glioma samples (figure 3.5), in concordance with a tumor-promoting role for RSK2 in glioma. We also find that RSK2 mRNA expression is highest in aggressive, metastatic, grade 4 tumors than in lower grade (2 and 3) tumors (figure 3.6), suggesting that RSK2 tumor expression is correlated to *in vivo* metastasis. Lastly, using Kaplan-Meier analysis<sup>152, 153</sup>, we were able to determine that the survival of glioma patients with low tumor RSK2 expression is significantly better than that of glioma patients that have high RSK tumor expression. This result was found for the three largest patient cohorts in the public domain (Fig. 3.7),

suggesting this correlation is robust. We concluded that in complete agreement with our *in vitro* studies, high RSK2 expression *in vivo* is linked to metastasis and poor survival rate.

### 3.3 DISCUSSION

Glioblastoma multiforme represent the most aggressive and lethal form of cancer and can affect any age group <sup>121</sup>. The World Health Organization (WHO) classifies astrocytomas on the basis of histologic features into four prognostic grades: grade 1 (pilocytic astrocytoma), grade II (diffuse astrocytoma), grade III (anaplastic astrocytoma), and grade IV (glioblastoma). Grade III and IV tumors are considered malignant gliomas (Wen et al.). In grade IV glioma, GBM, infiltration of primary tumor cells into normal tissue and dissemination throughout the brain is a fundamental but unmet challenge to successful treatment <sup>154</sup>. GBM patients respond poorly to the standard regimen of radiotherapy and chemotherapy that follow tumor resection. The median survival is about 16 months <sup>154</sup>. It is therefore imperative to identify novel approaches to specifically attack GBM invasion.

We previously showed that RSK2 modulates cell adhesion and integrin activity and thereby regulates cell motility (Gawecka). It does so by phosphorylating filaminA, and promoting its association with the integrin cytoplasmic tails. We now find that RSK2 alters adhesion and migration in GBM cells. We observed that RSK co-localizes with filaminA (see chapter 2) and that active RSK disturbs the initial adhesion of GBM cells to ECM. This likely contributes to the increased motility in these cells. RSK can also affect changes in the actin cytoskeleton (data not shown). We now find that these functions of RSK are active in GBM and that RSK inhibition limits GBM invasion.

RSK inhibitors generally affect all isoforms of RSK. However, not all RSKs regulate cell motility in the same way. While RSK2 often promotes migration of cancer cells (Kang 2010),

RSK1 has been shown to negatively regulate cell motility (Lara 2011). The observed effects in GBM cells therefore might be due to a broad inhibition of all RSK isoforms and their cellular functions. Therefore, we knocked down the RSK2 gene in the GBM U373MG cell line, and found that RSK2 can regulate invasion in these cells and in the temozolomide resistant primary patient-derived GBM cells. Further testing of RSK2 gene knock-down and the BI-D1870 inhibitor confirmed the ability to block migration in patient-derived GBM cell lines. Additionally, Kaplan-Meier analysis showed that high tumor RSK2 expression was prognostic for poor outcome, suggesting that RSK2 inhibitors like BI-D1870 may provide an interesting lead in targeting invasion in GBM treatment.

The current standard of treatment for GBM is temozolomide combined with radiotherapy. We therefore tested whether combining RSK inhibition with temozolomide and radiotherapy had an additive effect. We found that RSK inhibition alone could reduce primary patient-derived GBM neurosphere survival and the combination of temozolomide with RSK inhibition was significantly more effective than either treatment alone. No additional effect of radiotherapy was noted for these cells. Currently there are no RSK inhibitors suitable for *in vivo* studies, due to the fact the *in vivo* degradation kinetics are too unfavorable. Therefore, there is a pressing need to identify additional inhibitors that can maintain activity *in situ* for pre-clinical testing of RSK inhibitors.

Taken together, our study describes a novel function for RSK2 in the regulation of GBM cell motility. RSK2 inhibition, and thereby metastasis reduction in GBM is a promising approach for an addition to current standard therapies.

### 3.4 MATERIALS AND METHODS

#### HUMAN CELL LINES AND REAGENTS

Human glioblastoma (GBM) cell line U87MG was obtained from the NCI-Tumor Repository (Frederick, MD). U373MG was a gift from Dr. Santosh Kesari (John Wayne Cancer Center Institute at Providence Saint John's Health Center, CA). Cells were cultured in DMEM supplement with 10 % fetal bovine serum (HyClone, VWR, Radnor, PA), 1% non-essential amino acids and 1% penicillin/streptomycin (Cellgro, Manassas, VA). Cells were incubated in a humidified atmosphere containing 5% CO<sub>2</sub> at 37 °C. Antibodies specific for RSK1[D6D5], RSK2 [D21B2], RSK3(#9343), phospho p90RSK (Ser386) [D3H11], phospho p90RSK (T573)(#9346) were from Cell Signaling. Antibodies for RSK4 [EP1982Y], phosphor p90RSK (S227) [EPR2847Y] were from Sigma-Aldrich. The tubulin antibody [B7] was from Santa Cruz Biotechnologies. The RSK specific inhibitor SL0101 was purchased from Tocris Bioscience (Ellisville, MO), FMK was a gift from J. Taunton (University of California, San Francisco, CA) and BI-D1870 was obtained from BioVision Inc. (Milpitas, CA). Temozolomide (Temodar, S1237) was obtained from Selleckchem (Houston, TX).

#### BRAIN SLICE INVASION ASSAY

Mouse brain slices were cultured as previously described. Whole brain slices of 300 µm thickness were placed on the membrane of six-well plate culture insert (PICM 030 5, Millipore) and washed once with PBS supplemented with magnesium (1 mM) and calcium (1 mM). The brain slices were cultured in 1 ml Eagle's MEM (111, Corning, Corning, NY), 25 mM HEPES, 25% HBSS, 25 % heat-inactivated horse serum, 6.5 mg/ml D-glucose, 100 U/ml

penicillin, 100 µg/ml streptomycin, and 2.5 µg/ml amphotericin B). Thereafter, half of the medium was refreshed every three days. After the second change, the amount of culture medium was reduced to 800 µl to keep the brain slices exposed to air. GBM cell lines (U373MG, U373MG (KO-RSK2), U373MG (NT-RSK2)) were labeled with the PKH67 fluorescent linker (Sigma-Aldrich Cat. MINI67) according to the manufacturer's instructions. The tumor spheroids were formed by seeding  $1 \times 10^7$  labeled cells into a 60 mm ultra-low attachment dish (3261, Corning) containing 5 ml of D-MEM (10-013-CV, Corning) containing 10% FBS, 1X MEM nonessential amino acids (25025CL, Corning), 100 U/ml penicillin, 100 µg/ml streptomycin) and grown for several days. The day before implantation of the tumor spheroids, brain slices for inhibitor experiments were treated with 10 µM of RSK2 inhibitor BI-D1870 or vehicle. After 7 days, the viability of the brain slice was verified by the presence of the cortical lamination and hippocampal structure, then the insert was transferred to a well of a glass-bottom 6-well plate (P06G-1.5-20-F.S, MatTek, Ashland, MA). One small spheroid of approximately 200 µm was transferred to each brain slice as close to the corpus callosum as possible. The co-cultures were maintained for an additional 72 hours. The tumor cell invasion was followed using a confocal microscope (TCS SP5, Leica, Solms Germany).) and a stage-top incubator with digital gas mixer (TokaiHit WSKM/GM8000, Fujinomiya-shi Shizuoka-ken, Japan). The basal plane (0 µm) was determined 4 hours post implantation and serial sections every 20 µm downward from the basal plane to the bottom of the slice were imaged at the indicated time points. Propidium iodine staining of the brain slices at the end of the assay confirmed that the brain slice cultures had remained viable. To quantify the invasiveness of the spheroids, the density of the fluorescent signal was measured in each 20 µm section using ImageJ Software (National Institutes of Health, Bethesda, MD).

## 3.5 FIGURES

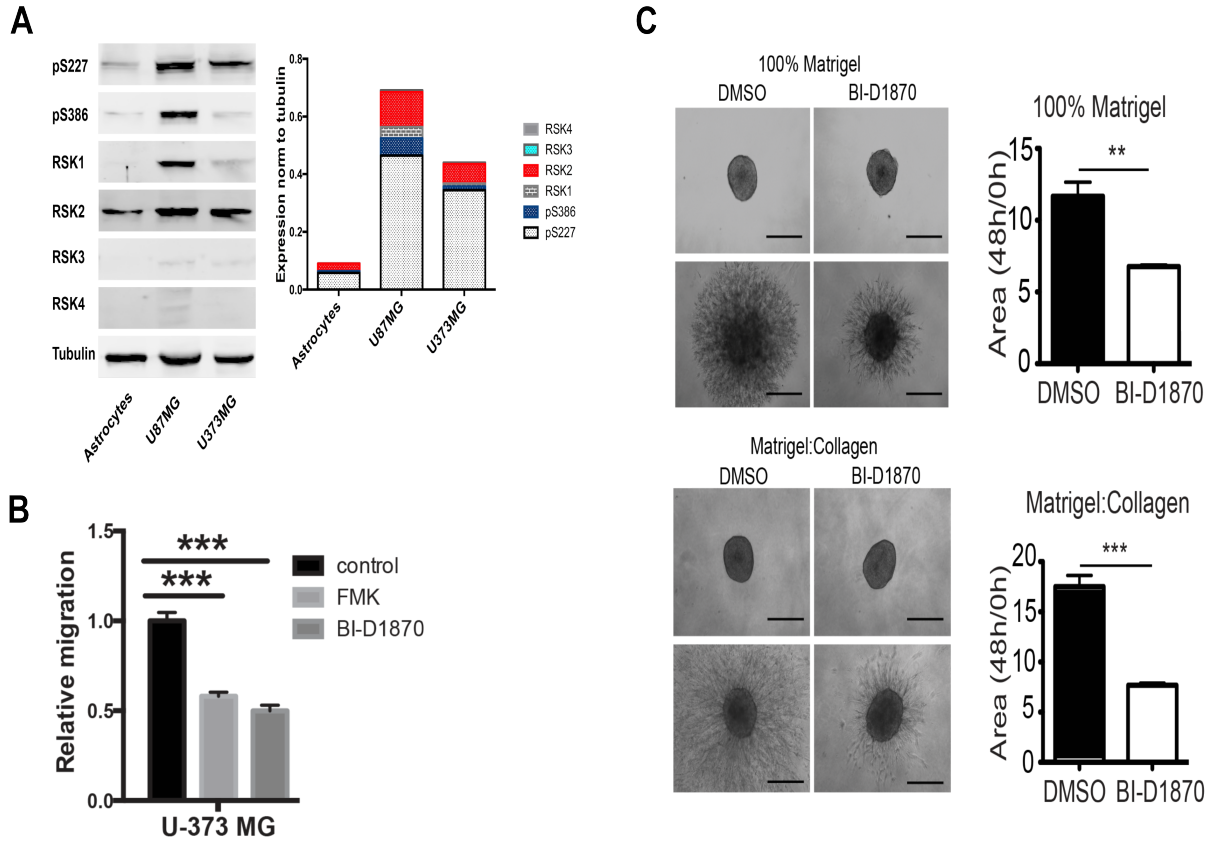


FIGURE 3.1 RSKS ARE REQUIRED FOR GBM MIGRATION AND INVASION

3.1 (A) Immunoblots showing expression of RSK isoforms in astrocytes and glioblastoma cell lines U87MG and U373MG. (B) migration of U373MG cells was determined in the presence of RSK inhibitors (FMK and BID1870) or control DMSO. Relative migration into the scratch was measured at 24 hours. (C)(D) U87MG tumor spheroids were embedded in either 100% Matrigel or a 50% Matrigel/50% collagen mixture and treated with DMSO or 10  $\mu$ M BI-D1870. Images were acquired at 0, 24, and 48 hours after the drug was added. Bar graphs show the quantification of the normalized area of the spheroids as the mean of 3 independent experiments. (B and C Amanda Prechtl).

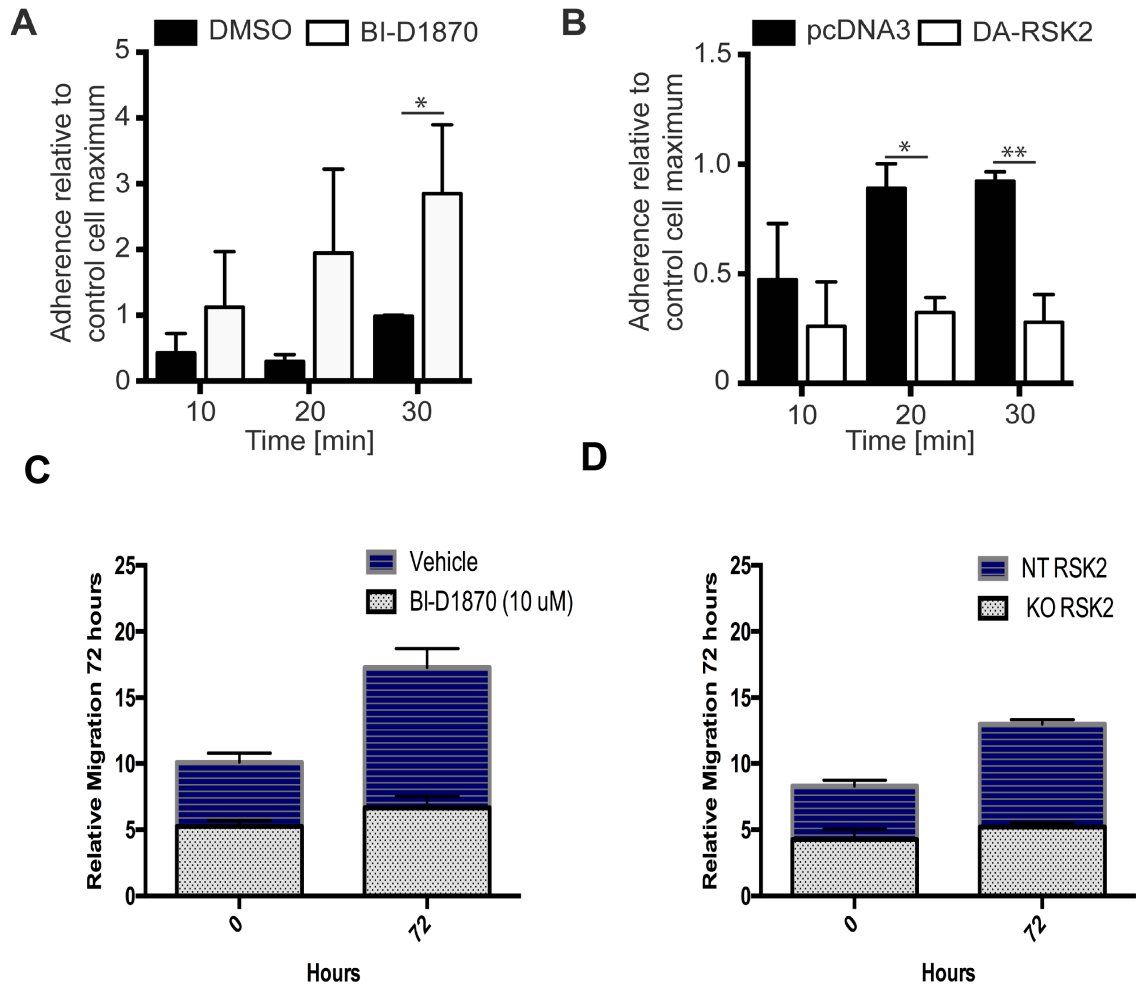


FIGURE 3.2 RSK2 ACTIVITY REDUCES CELL ADHESION TO FIBRONECTIN AND PROMOTES MIGRATION INTO MOUSE BRAIN SLICES

3.2 We examined early adhesion of U87 MG cells on culture plates coated with 3FN-(9-11). Before plating, cells were (a) pre-treated with 10  $\mu$ M BI-D1870 or vehicle (b) transiently transfected with DA-RSK2 or empty vector control. 48 hours after transfection or 15 min after pre-treatment cell adhesion was measured. Bar graphs show the number of cells adherent after the indicated amount of time. The experiment was carried out in 3 independent repeats (A and B, Florian Sulzmaier). We examined the ability of U373 cells treated with BI-D1870 inhibitor (c) or with RSK2 knocked out using CRISPR/Cas9 (d) to migrate into the brain of mice. Whole brain slices of 300  $\mu$ m thickness were placed on the membrane of a six-well plate culture insert. GBM cell lines U373MG, U373MG with RSK2 gene knock-down (KO-RSK2), or U373MG with a non-targeting shRNA (NT-RSK2) were labeled with the PKH67 fluorescent linker. After 7 days, one small spheroid of approximately 200  $\mu$ m was transferred to each brain slice. The co-cultures were maintained for an additional 72 hours. To quantify the invasiveness of the spheroids, the density of the fluorescent signal was measured in each 20  $\mu$ m section using ImageJ Software.

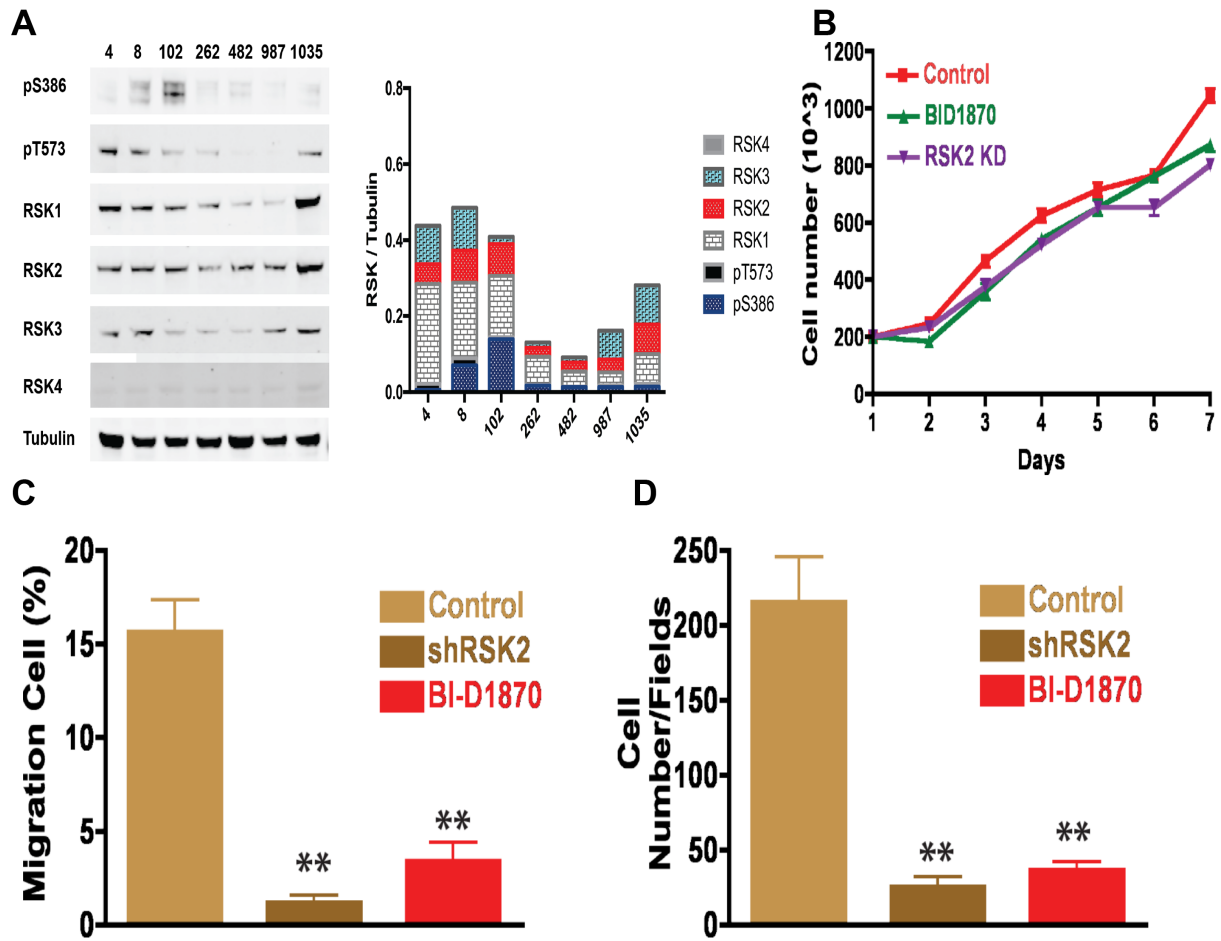


FIGURE 3.3 PATIENT-DERIVED GBM REQUIRE RSK2 FOR INVASION AND MIGRATION

3.3 (A) RSKs are expressed in patient cells and RSKs are active. (B) RSK inhibitors have no effect on proliferation or viability of patient cells in the migration assays. (C) quantification of scratch assay migration experiments and (D) transwell assay. At 24 hours, RSK2 gene knock-down cells and wild-type cells treated with BI-D1870 significantly decreased cell migration in both scratch and transwell assays. (B,C, and D Santosh Kesari, John Wayne Cancer Institute at Providence Saint John's Health Center, CA).

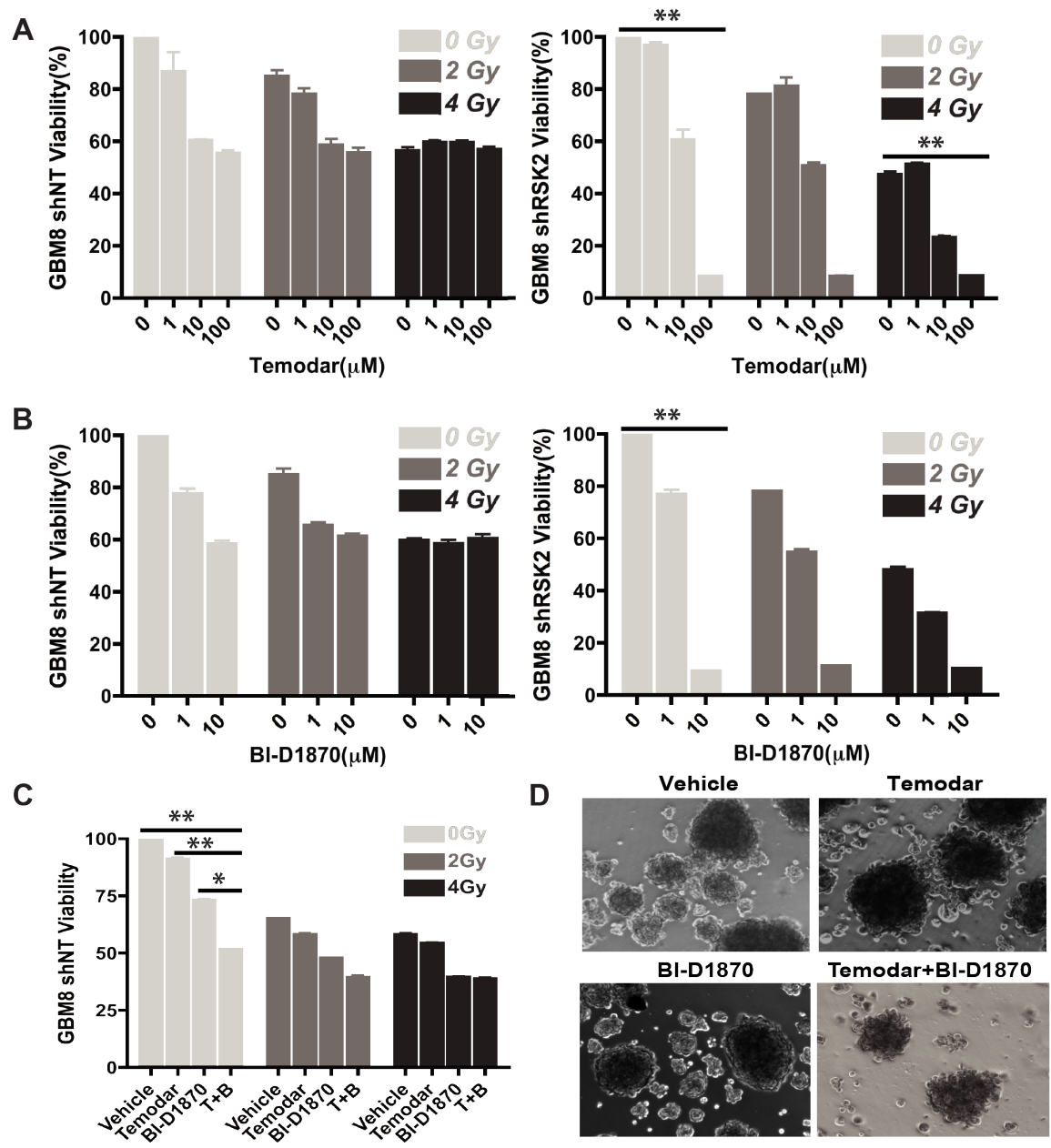


FIGURE 3.4 INHIBITION OF RSK2 SENSITIZES RESISTANT PATIENT-DERIVED GBM TO TEMOZOLOMIDE

3.4 (A) RSK2 gene knock-down sensitized GBM cells to temozolomide and the RSK inhibitor BI-D1870. At high temozolomide concentrations, the cell viability decreased from 57% to 8%. In addition, 10  $\mu$ M RSK inhibitor BI-D1870 decreased cell viability from 58% to 9%. RSK2 gene knock-down had no significantly effect on radiation response. (B) RSK Inhibitor BI-D1870 enhanced the anti-tumor effect of temozolomide in RSK2 gene knock-down cells. For resistant wild-type cells, temozolomide/BI-D1870 combination treatment (both at 1  $\mu$ M), decreased cell viability to 51% as compared to single reagent treatment effects of 91% and 72% remaining viability. (C) (D) The combination of temozolomide and BI-D1870 was more effective at killing GBM cells than either alone. (Santosh Kesari, John Wayne Cancer Institute at Providence Saint John's Health Center, CA).

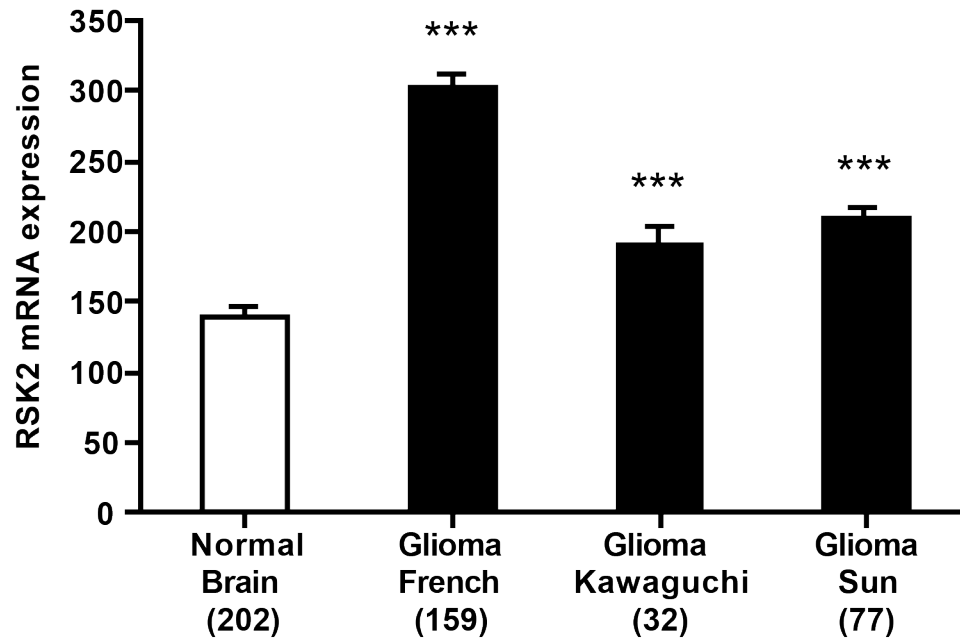


FIGURE 3.5 RSK2 MRNA EXPRESSION IS HIGHER IN HUMAN GLIOMA THAN IN NORMAL BRAIN TISSUE

3.5 Differential RSK2 mRNA expression between the largest collection of normal human brain tissue (from the Roth-504 “Human Body Map”), and the three public human glioma datasets used in further analyses. RSK2 expression is significantly lower in normal brain than in glioma tissue, although glioma mRNA expression can vary between datasets. Y-axis presents RSK2 mRNA expression, X-axis dataset (in bracket the amount of samples in the analysis). For presentation reasons, only GBM (stage 4) samples were used, but the differences remain significant when all dataset samples are analyzed (results not shown). Bars represent average  $\pm$  SEM. (Dirt Geerts, Department of Pediatric Oncology, Erasmus University Medical Center, Netherlands).

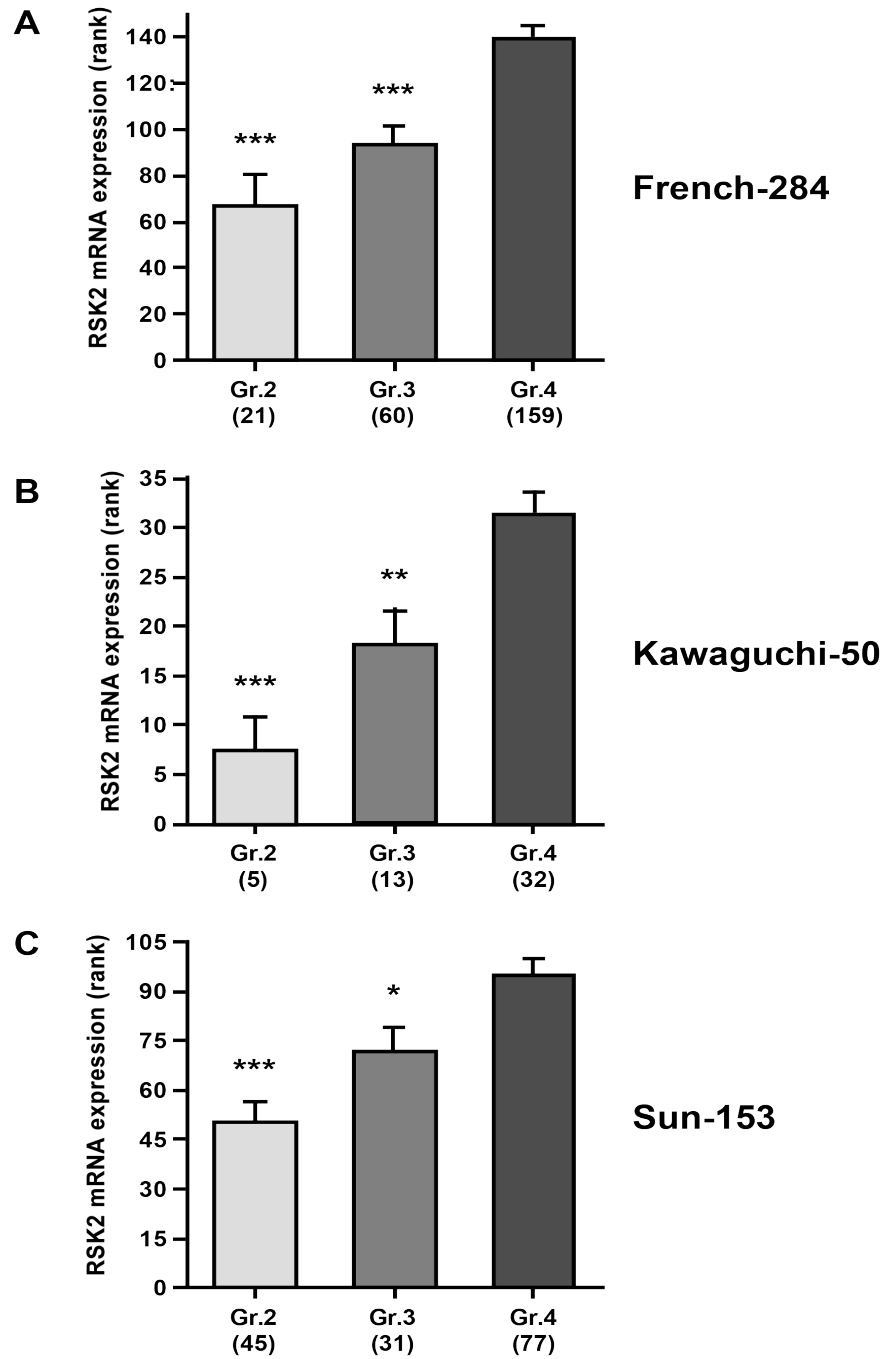


FIGURE 3.6 RSK2 MRNA EXPRESSION CORRELATES WITH HIGH HUMAN GLIOMA TUMOR STAGE

3.6 Correlation of RSK2 tumor mRNA expression with WHO glioma tumor grade (grades 2-4) was analyzed using the Kruskal-Wallis test<sup>152, 153</sup>. The graphs represent the three largest public glioma datasets with full WHO grade annotation: (A) French-284, (B) Kawaguchi-50, (C) Sun-153. Y-axis presents RSK2 tumor mRNA expression (rank-based), X-axis WHO-grade. In all three datasets, RSK2 expression is significantly higher in stage 4 than in stage 2 or 3 tumors. Bars represent average  $\pm$  SEM. (Dirt Geerts, Department of Pediatric Oncology, Erasmus University Medical Center, Netherlands).

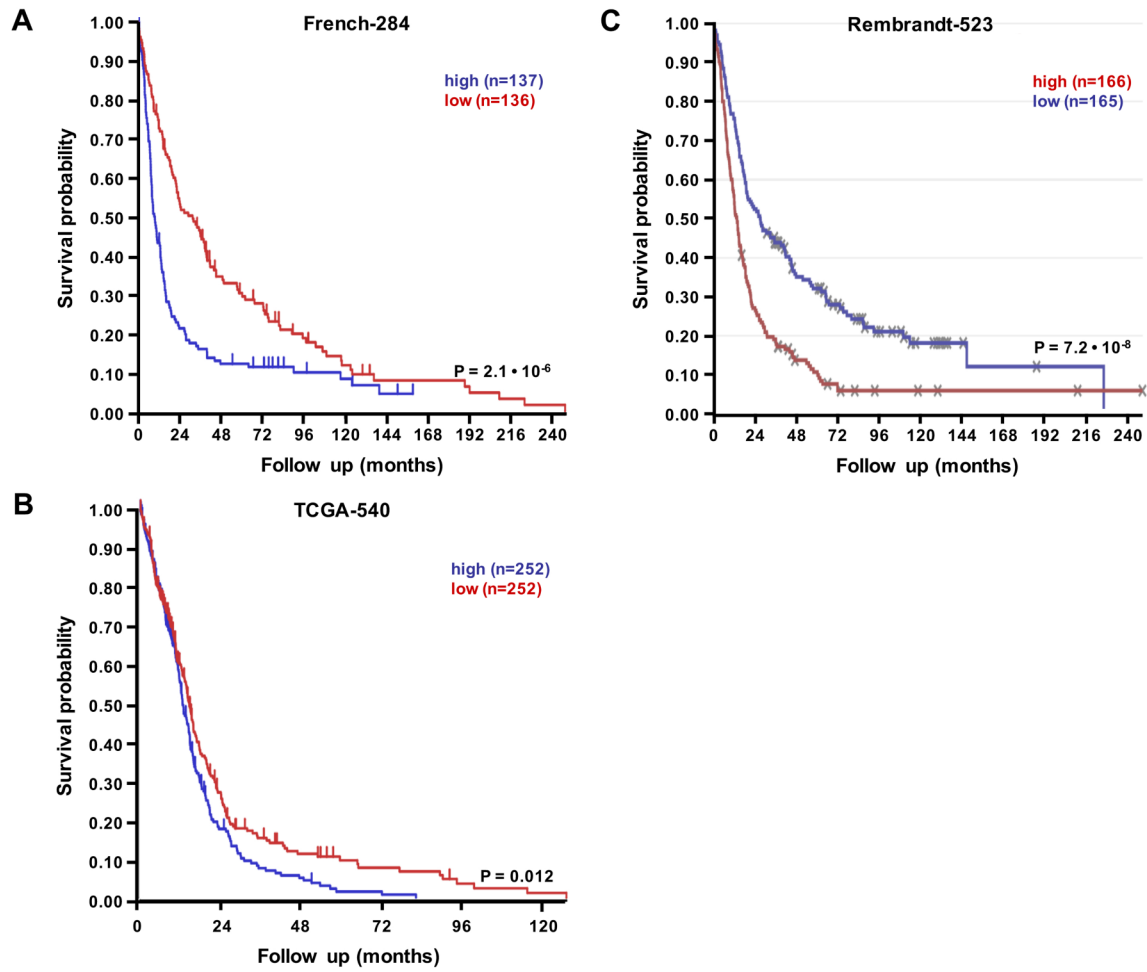


FIGURE 3.7 RSK2 MRNA EXPRESSION IS PROGNOSTIC FOR POOR GLIOMA PATIENT PROGNOSIS

3.7 The prognostic significance of RSK2 tumor mRNA expression in human glioma patients as determined by Kaplan-Meier analysis<sup>152, 153</sup>. The Kaplan-Meier graphs representing the overall survival prognosis of glioma patients based on high or low RSK2 tumor mRNA expression in the three largest public glioma datasets with survival data: (a) French-284, (b) TCGA-540, and (c) REMBRANDT-523 (screenshot from the Betastasis website). No conflicting results were found in other public glioma datasets. The graphs present patient groups separated at median RSK2 tumor mRNA expression. The Y-axis presents survival probability and the X-axis months of follow up. In all three datasets, high RSK2 expression is prognostic for poor outcome. This prognostic significance was also found for average RSK2 expression cut-off. (Dirt Geerts, Department of Pediatric Oncology, Erasmus University Medical Center, Netherlands)

## CHAPTER 4

# PEA-15 IS AN ENDOSOMAL-ASSOCIATED AND MICROTUBULE-BINDING PHOSPHOPROTEIN THAT REGULATES $\alpha_5\beta_1$ INTEGRIN RECYCLING

The majority of the work in this chapter has been submitted for publication in

The Journal of Cell Science.

Maisel Caliva *et al.*

## 4.1 INTRODUCTION

Integrins are transmembrane receptors that integrate adhesion to the extracellular matrix with engagement to the actin cytoskeleton. They are heterodimeric receptors that are essential for a range of physiological and pathological processes that include wound healing, embryogenesis, cancer invasion and metastasis<sup>93</sup>. Integrin affinity for ligands depends on the activation state of the integrin and is regulated by signal transduction proteins such as Rap1 and RSK2, which signal through cytoskeletal proteins such as talin and filaminA, respectively<sup>26, 91, 155</sup>. Endosomal trafficking of integrin further regulates their end function. The endocytosis of integrins promotes focal adhesion disassembly and detachment from the ECM at the rear end of the cell and thereby directs migration. Moreover, aberrant integrin trafficking has been observed in many cancer types<sup>156, 157</sup>. Identification of molecules that control integrin trafficking may, therefore, offer new strategies for the development of integrin-based anti-cancer therapeutics.

Integrin Recycling utilizes the same trafficking mechanisms used by receptor tyrosine kinases<sup>158</sup>. The majority of integrins escape lysosomal degradation through interaction with Sorting Nexin 17 (SNX17) and are diverted by the small GTPase Rab5 into early endosomes<sup>159</sup>. Exchange of Rab5 for Rab11 is required for recycling of integrins back to the plasma membrane. Recycling of integrins also requires cell polarization established by microtubules and small GTPases of the Arf and Rho families<sup>160</sup>. Although cellular adhesions are stable, integrins undergo constitutive recycling. The rate of integrin trafficking can be increased by cell stimulation and is therefore regulated by canonical signaling pathways<sup>161, 162</sup>. For example, phosphorylation of the ArfGAP ACAP1 by AKT is required for  $\alpha 5\beta 1$

recycling in serum-stimulated cells<sup>163</sup>. The enhanced cell migration and invasiveness of many cancer types can be correlated with overexpression or aberrant regulation of many of these proteins<sup>156, 164</sup>.

PEA-15 (Phosphoprotein Enriched in Astrocytes of 15 kDa) is a member of the Death Effector Domain (DED) family and regulates cell adhesion by controlling the activation of integrin (Ramos et al., 1998). PEA-15 interaction with other DED-containing proteins and ERK is regulated by phosphorylation of carboxy-terminal serine residues 104 and 116. In the case of ERK, PEA-15 functions as a scaffold that targets ERK to phosphorylate and activate RSK2<sup>58</sup>. RSK2 phosphorylates filaminA thereby recruiting it to the focal adhesion sites, which leads to suppression of integrin activation and increase migration<sup>137</sup>. PEA-15 has been shown to regulate cell motility in breast cancer, ovarian carcinoma and neuroblastoma<sup>165-167</sup>. We investigated if PEA-15 is required for efficient endosomal recycling of internalized  $\alpha_5\beta_1$  integrin

## 4.2 RESULTS

### PHOSPHORYLATED PEA-15 REGULATES $\alpha_5\beta_1$ INTEGRIN RECYCLING

Constitutive endosomal trafficking of integrins dynamically regulates integrin signaling and cell migration. PEA-15 promotes integrin activation, and given the established role of  $\alpha_5\beta_1$  integrin in cell invasion and drug resistance in glioblastoma (GBM) cells<sup>168-170</sup>, we tested if PEA-15 could influence the endosomal trafficking of  $\alpha_5\beta_1$  integrin in GBM. We examined integrin recycling in PEA-15 knock-down (KD) U87MG GBM cells (Figure 4.1A) and observed a significant decrease in integrin recycling (Figure 4.2B). We detected no difference in integrin surface expression levels and only a slight increase in integrin endocytosis in knockdown cells, perhaps a steady-state result of the decrease in recycling (Figure 4.1C). Integrin recycling was rescued by reconstitution of PEA-15 in the knockdown cell line (Figure 1D). The impairment of integrin recycling in the PEA-15 deficient cells was not due to integrins degrading (4.1E). This suggests that PEA-15 expression is required for efficient recycling of  $\alpha_5\beta_1$  integrin.

Stimulated integrin recycling is driven by phosphorylation of ACAP1 (ArfGAP With Coiled-Coil, Ankyrin Repeat And PH Domains 1) downstream of AKT<sup>163</sup>, which represents a pathway that regulates integrin trafficking independently from other cargoes. AKT phosphorylates PEA-15 at serine residue 116<sup>171</sup>, which has been shown to block the AKT-ERK signaling necessary for differentiation<sup>172</sup>. This indicates that phosphorylation mutants of PEA-15 can be effective tools to analyze AKT-dependent pathways. We therefore tested if phosphorylation at this residue is necessary for PEA-15-mediated integrin recycling. The

S116A mutant of PEA-15 was expressed in knock-down cells, and assayed for integrin recycling. Interestingly, we found that this mutant could not rescue integrin recycling (Figure 4.1D). We also observed a shift in  $\beta_1$  integrin localization in PEA-15 KD cells expressing the S116A mutant. Cells expressing wild type PEA-15 show its colocalization with  $\beta_1$  integrin adhesions. In contrast, cells expressing the S116A mutant exhibited  $\beta_1$  integrin enriched in vesicles (Figure 4.1F).

#### PEA-15 IS REQUIRED FOR CELL MIGRATION IN U87MG CELLS

The recycling of  $\beta_1$  integrins from the trailing edge to the lamellipodia is key to the rate and directionality of cell migration<sup>173</sup>. Therefore, if PEA-15 is required for integrin trafficking, we would predict that knock-down of PEA-15 expression would also impair cell migration. As expected, cells depleted in PEA-15 expression did not migrate into the scratches to the same extent as cells with re-constituted PEA-15 expression. Rescue of PEA-15 in the knock-down cell line fully closed the scratch in the same amount of time as control cells (Figure 4.1A). However, rescue with a double phosphomutant (SSAA) of PEA-15 did not rescue migration, supporting a role for phosphorylated PEA-15 in GBM cell migration in 2D environments. To assess PEA-15 effects in 3D matrices, we embedded PEA-15 KD or scramble control spheroids into a 1:1 mix of Matrigel and collagen, and then allowed for cells to invade into the matrix. We found that PEA-15 KD cells invaded at half the rate compared to scrambled controls, indicating that PEA-15 expression is also necessary for cell invasion in 3D environments (Figure 4.2B). Cells were tested for viability during the assays (data not shown).

The dependence of PEA-15 for cell migration suggests that it is the result of PEA-15 regulation of integrin recycling. We first tested if PEA-15 could traffic with internalized endosomes by incubating HA-PEA-15 overexpressing cells with the GST-FN9.11 ligand. This recombinant ligand consists of repeats of the integrin binding motif in fibronectin. We observed distinct colocalization of PEA-15 with FN.11 in what appears to be a vesicle. We investigated this by co-immunostaining integrins with early endosomal markers in the PEA-15 knock-down cells. If PEA-15 regulates recycling, then we would expect to see a difference in the trafficking route taken by integrins in migrating cells. We observed  $\beta_1$  integrins concentrated at the leading edge and co-localized with both actin and Rab5 early endosomes at vesicles immediately behind the leading edge in scrambled control cells (Figure 4.3A). In contrast,  $\beta_1$  integrin was evenly dispersed throughout the cytoplasm and did not exhibit enrichment at the cell front or co-localization with early endosomes in PEA-15 KD cells (Figure 4.3A). The results suggest that PEA-15 expression is required for normal sorting of integrin to early endosomes, a prerequisite for recycling. This implies that PEA-15 may function as an endosomal adapter protein for integrins. Consistent with this hypothesis, we found that PEA-15 complexed with  $\beta_1$ -integrin cytoplasmic tails (Figure 4.3B). Interestingly, the S116A mutation did not alter PEA-15 binding to the  $\beta_1$  tail. However, both the wild-type PEA-15 and the S116A mutant failed to interact with the  $\beta_1$  cytoplasmic tail when its membrane-proximal NPxY tyrosine is mutated to alanine (NPxA). The tyrosine residue in this motif is essential for talin binding to  $\beta$ -integrins, integrin activation, and integrin trafficking (Margadant et al., 2012).

## PEA-15 DIRECTLY INTERACTS WITH POLYMERIZED MICROTUBULES AND IS REQUIRED FOR MICROTUBULE-DEPENDENT CELL MORPHOLOGY

Endosomes are highly motile and transit on microtubule tracks<sup>160</sup>. Integrin trafficking is therefore influenced by regulators of microtubule dynamics. Microtubule dynamics is fundamental to the establishment of cell polarity, and interestingly, we observed dramatic effects on the actin cytoskeleton in astrocytes cultured from perinatal PEA-15 knock-out (KO) mice compared to wild-type littermate controls (Figure 6A). PEA-15 KO cells exhibited a loss of cell polarity and actin filaments radiated from multiple foci throughout the cytoplasm, suggesting a defect in actin organization. Actin organization was also defective in the U87MG PEA-15 KD cells when adhering to fibronectin (Figure 6A). We observed a decrease in cell protrusions in U87MG PEA-15 KD cells under normal culture conditions, resulting in the assumption of a rounded cell morphology. The data show that PEA-15 is required for polarized cell morphology. This suggests that PEA-15 could function as a regulator of microtubule dynamics. To test this, we depolymerized microtubules in U87MG cells with nocodazole followed by washout to allow microtubule regrowth. Both control and PEA-15 KD cells became rounded after incubation with nocodazole, but only control cells re-established cell protrusions upon nocodazole washout. The effect of PEA-15 on cell morphology is, therefore, dependent on microtubule growth.

## RSK2 ACTIVITY IS REQUIRED FOR PEA-15 MEDIATED RECYCLING OF INTEGRINS

Our data shows that PEA-15 expression is a requirement for efficient recycling of integrin and that recycling is dependent on phosphorylation of PEA-15 at S116. This residue is phosphorylated by AKT and CaMKII. However, RSK2 and AKT share the same consensus

sequence and as a consequence target many of the same substrates. Recently, PEA-15 was identified as a substrate of RSK2 in a phosphoproteomic analysis conducted by Galna *et al.*<sup>174</sup>. To characterize RSK2-dependent phosphoproteome, they devised a comprehensive quantitative MS strategy using pharmacological inhibitors and RNAi. As biological models, they used HEK293 cells treated with the phorbol ester phorbol-12-myristate-13-acetate (PMA) to acutely stimulate RSK activity, as well as A375 melanoma cells, which harbor the B-Raf V600E mutation and therefore have constitutively high RSK activity<sup>174</sup>. We have shown that RSK2 promotes migration in part due to its effects on integrin function. Therefore, we tested if a RSK2-PEA-15 axis mediates integrin recycling. We found that reconstitution of PEA-15 in PEA-15 KD Hela cells in the presence of RSK2 inhibitor FMK could not rescue migration (figure 4.5A). Similar to our observations in U87MG, we detected no difference in integrin surface expression levels when treated with RSK2 inhibitor BI-D1870 and only a slight increase in integrin endocytosis in knockdown cells (figure 4.5B and C).

## 4.5 DISCUSSION

We report that PEA-15 is required for efficient trafficking of integrins in migratory cells. Co-immunostaining and confocal imaging revealed that PEA-15 concentrates on Rab5 containing membranes. Phosphoproteomic approaches applied to isolated endosomes also showed that phosphorylated PEA-15 is highly enriched in endosomes (data not shown). We observed significantly decreased integrin recycling rates in the PEA-15 knock-down cells. This correlates with a slight increase in integrin internalization. Integrin cytoplasmic domains required for integrin activation are also required for efficient recycling. The NPxY motifs on the  $\beta_1$  cytoplasmic tail are essential for integrin activation and subsequent internalization. We show here that PEA-15 can interact with the  $\beta_1$  cytoplasmic tail, and that this interaction is prevented by a tyrosine to alanine mutation at the membrane-proximal NPxY motif. This suggests that PEA-15 binding to the integrin  $\beta_1$  tail may involve interactions with focal adhesion proteins. Thus PEA-15 may distinguish integrins in the early endosome toward the recycling pathway. Taken together this indicates that PEA-15 is a novel endosomal-associated protein and a potential endosomal adapter for integrins.

We found that PEA-15 expression is required for GBM cell motility in 2D scratch assays and 3D invasion assays. This data contrasts with literature concerning the regulation of cell migration by PEA-15 in which PEA-15 expression blocks migration<sup>165-167</sup>. It is plausible that the phosphorylation status of PEA-15 is different in U87MG glioma cells compared to the model cell lines used in other migration studies. U87MG and most GBM cell lines are known to harbor homozygous mutation of PTEN that results in constitutive activation of the PI3K-AKT signaling cascade<sup>175</sup>. Therefore, in the majority of GBM cell lines

endogenous PEA-15 is constitutively phosphorylated at serine residue 116. We report here that PEA-15 mediated integrin recycling requires PEA-15 phosphorylation at serine 116. Our data suggests that GBM cells utilize this pool of phosphorylated PEA-15 to promote integrin recycling that correlates with enhanced migration and invasiveness. This corresponds to the model in which unphosphorylated PEA-15 acts as a tumor suppressor and phosphorylated PEA-15 a tumor promoter<sup>176</sup>. Our data provides a basis to understand how PEA-15 can have opposing effects on migration depending on its phosphorylation status.

Knock-down of PEA-15 in GBM cells blocks the formation of cell protrusions after nocodazole washout. Recycling of endosomes, and therefore cell invasion and migration, requires cell polarity established by a polarized microtubule network. The process of polarization is complex and is regulated by microtubule-associated-proteins (MAPs), Rho family GTPases, and plasma membrane capture proteins that bind to microtubules as they contact the membrane, resulting in a stabilizing feedback loop<sup>177</sup>. We have shown that PEA-15 interacts directly with polymerized tubulin and that phosphorylated PEA-15 co-fractionates with known MAPs in isolated endosomes (data not shown). We, therefore, propose, that PEA-15 is a novel MAP that regulates cell polarity via its interaction with microtubules during the polarization process. If PEA-15 influences microtubule dynamics, this would explain many of the observations reported here. Microtubule contact with the membrane is required for delivery of recycling endosomes and is, therefore, required for both localized Rac activation and integrin recycling<sup>160</sup>. There is also a report of phosphorylated PEA-15 sensitizing ovarian cancer cells to paclitaxel, a drug that kills cells

by disrupting microtubule networks, again suggesting that PEA-15 has a direct role in microtubule dynamics<sup>178</sup>.

Our data shows that phosphorylation of PEA-15 at S116 is a requirement for efficient recycling of integrins. Based on a phosphoproteomic study<sup>174</sup> that identified PEA-15 as a substrate of RSK2 we tested whether an RSK2-PEA-15 axis could mediate integrin recycling of  $\alpha_5\beta_1$  integrins. We found that reconstituted PEA-15 in FMK treated PEA-15 KD HeLa cells failed to rescue integrin recycling. We confirm that the recycling deficient is not due to effect changes in surface expression or internalization of  $\alpha_5\beta_1$ . We have shown that PEA-15 regulates endosomal recycling of integrins and as a consequence promotes migration in GBM cells. PEA-15 has previously been shown to scaffold ERK to RSK2 resulting in full activation RSK2; therefore, we propose that PEA-15 activation of RSK2 lie downstream of RSK2 mediated internalization of inactive integrins. In our model, EGF stimulation of the RAS MAPK pathway leads to the activation of ERK, which is scaffold to RSK2 by PEA-15. Activated RSK2 transiently translocates to the plasma membrane where it phosphorylates filaminA and promoting its association with the  $\beta_1$ -integrin tail. PhosphofilaminA bind to and inactivates the  $\alpha_5\beta_1$  integrin. The inactivated integrin is endocytose in response to cell polarization and is trafficked to the early endosome where it is diverted by RAB11 for recycling back to the plasma membrane (figure 4.6).

## 4.4 MATERIAL AND METHODS

### CELL CULTURE AND REAGENT

U87MG human glioblastoma cells were purchased from the NCI-Tumor Repository, Frederick. HeLa cells were purchased from the American Type Culture Collection (ATCC, Manassas, VA). U87MG, and HeLa cells were grown in DMEM supplemented with 10% fetal bovine serum (Gibco), 1% MEM non-essential amino acids, and penicillin/streptomycin antibiotic. All cell lines were grown in a humidified incubator with a 5% CO<sub>2</sub> atmosphere at 37°C. Cell lines were validated by ATCC STR profiling. All transient transfections were conducted with Genejuice Transfection Reagent (EMD Millipore). Western blot detection of transfected PEA-15 was done with HA tag (sc-7392 and sc-805, Santa Cruz Biotechnology) and PEA-15 microtubule morphology assay with  $\alpha$ -Tubulin (Abcam YOL1/34). Mouse antibodies against  $\alpha$ 5 integrin (#555651, BD Biosciences) were used for capture ELISA of  $\alpha$ 5 $\beta$ 1 integrin in trafficking assays. Rhodamine-phalloidin (actin stain) were obtained from Life Technologies

### MIGRATION ASSAY

NT PEA-15 and PEA-15 KD U87MG cells were grown in 6-well culture plates and transfected with the GFP-PEA-15 constructs using Genejuice transfection reagent. The cells were allowed to grow to confluence then scratched with a 200  $\mu$ L pipette tip. The cells were washed with serum free media and replaced with media containing 1% serum. Cells were allowed to migrate into the scratch for 24 hours. Images of the scratch were acquired immediately after scratching (t=0) and at 24 hours using a Zeiss Axiovert 200M microscope with a 5X objective. The average closure of the scratch by GFP-expressing migrating cells was

measured using ImageJ software (National Institutes of Health, Bethesda, MD), and expressed as relative migration normalized to the  $t_0$  distance.

#### TUMOR SPHEROID INVASION ASSAY

Tumor spheroids were produced using NT PEA-15 and PEA-15 KD U87MG cells as previously described<sup>179</sup> and embedded in a 1:1 Matrigel:collagen mixture. Cells were allowed to invade into the matrix for 48 hours and phase contrast images were acquired at 0, 24, and 48 hours using a 5x objective. To quantify the degree of cell invasion, phase contrast images were processed into binary images with ImageJ. Briefly, raw images were processed with the Find Edges function. An automatic threshold was then applied before measuring the area of particles from 2000 square pixels to infinity. The sum of the areas was then used to represent overall invasion.

#### INTEGRIN TAIL PULLDOWN

Recombinant His-tagged integrin cytoplasmic tails were produced and purified as previously described<sup>179, 180</sup> then immobilized on His-bind resin (Novagen ). HeLa cells were transfected with the indicated constructs and Genejuice. The cells were harvested 48 hours later and lysed in XTT lysis buffer. Cell lysates were then incubated with integrin tails for 24 hours, washed, resuspended in SDS sample buffer, heated for 5 min at 95°C. Precipitated PEA-15 was detected by western blot, and integrin tail expression was detected by coomassie stain.

#### MICROTUBULE REGROWTH ASSAY

U87MG glioblastoma cells are plated to 50% confluence on fibronectin-coated glass coverslips. The cells were serum starved for 30 minutes then treated with nocodazole (10  $\mu$ M) for 4 hours to depolymerize microtubules. Microtubule regrowth was induced by

washing out nocodazole with 2 washes of serum free media. Cells were fixed at time points with ice-cold methanol for 10 minutes at 4°C. Samples were then stained for microtubules and imaged with a Leica TCS SP5 with 63X Oil Objective (Leica, Solms Germany).

#### DEGRADATION ASSAY

Integrin degradation was quantified using an established biotinylation approach<sup>162</sup>. U87MG PEA-15 NT and PEA-15 KD glioblastoma cells are seeded for approximately 50% confluency. The cells were serum starved for 30 minutes in 1% FBS, followed by a wash in ice-cold DPBS and surface biotinylation with Sulfo-NHS-SS-Biotin (0.2 mg/mL) for 20 minutes at 4°C. Cells were washed once then pulsed with pre-warmed 1% serum and incubation for 30 minutes at 37°C. The cells were placed on ice and washed with ice-cold DPBS to stop internalization. Biotin remaining on the surface was removed by incubation with 20 mM MESNA reducing agent for 15 minutes at 4°C; then quenched with 20 mM Iodoacetamide for 10 minutes at 4°C, followed by washes and cell lysis with lysis buffer (25 mM Tris-HCl, pH 7.4, 100 mM NaCl, 2 mM MgCl<sub>2</sub>, 0.5 mM EGTA, 1% Triton X-100, 5% glycerol, protease inhibitor cocktail, 1 mM Na<sub>3</sub>VO<sub>4</sub> and 1 mM PMSF). Lysates were diluted to equal protein concentration and applied to capture ELISA.

#### INTEGRIN RECYCLING ASSAY

To measure integrin recycling, cells are prepared as above for degradation assays. For rescue experiments, HA-tagged constructs were first transfected with Genejuice (Millipore), then re-plated on assay dishes. After surface biotinylation, cells were pulsed at 37°C for 30 minutes followed by surface stripping with MESNA. Internalized integrins are then chased back to the membrane with prewarmed 10% FBS. This was followed by a second round of

MESNA to remove recycled biotin. Cells are then quenched and lysed then applied to capture ELISA. Recycling is calculated as the percent-reduction of post-chase signal from pulse signal.

#### CAPTURE ELISA

Nunc Maxisorp 96-well plates were coated with 50  $\mu$ L of  $\alpha_5$  monoclonal antibodies (#555651, BD Biosciences, San Jose, CA) diluted to 5  $\mu$ g/mL in carbonate/bicarbonate coating buffer (pH 9.2) overnight at 4°C. The plate was washed with PBST (PBS with 0.05% Tween-20) and blocked with 5% BSA in PBST for 1 hour at room temperature. 50  $\mu$ L of lysate (0.2mg/ml) was loaded in triplicate and incubated overnight at 4°C. The plates are then washed and incubated with 50  $\mu$ L HRP-conjugated streptavidin (1:2000) for 1 hour at 4°C followed by generous washing and color development with OPD (1mg/ml supplemented with 30% hydrogen peroxide at 1 $\mu$ l/ml ). The reaction was stopped with 2.5 M sulfuric acid. Absorbance was measured with a plate reader at 490 nm. Recycling is calculated as the percent-reduction of post-chase signal from pulse signal.

## 4.5 FIGURES

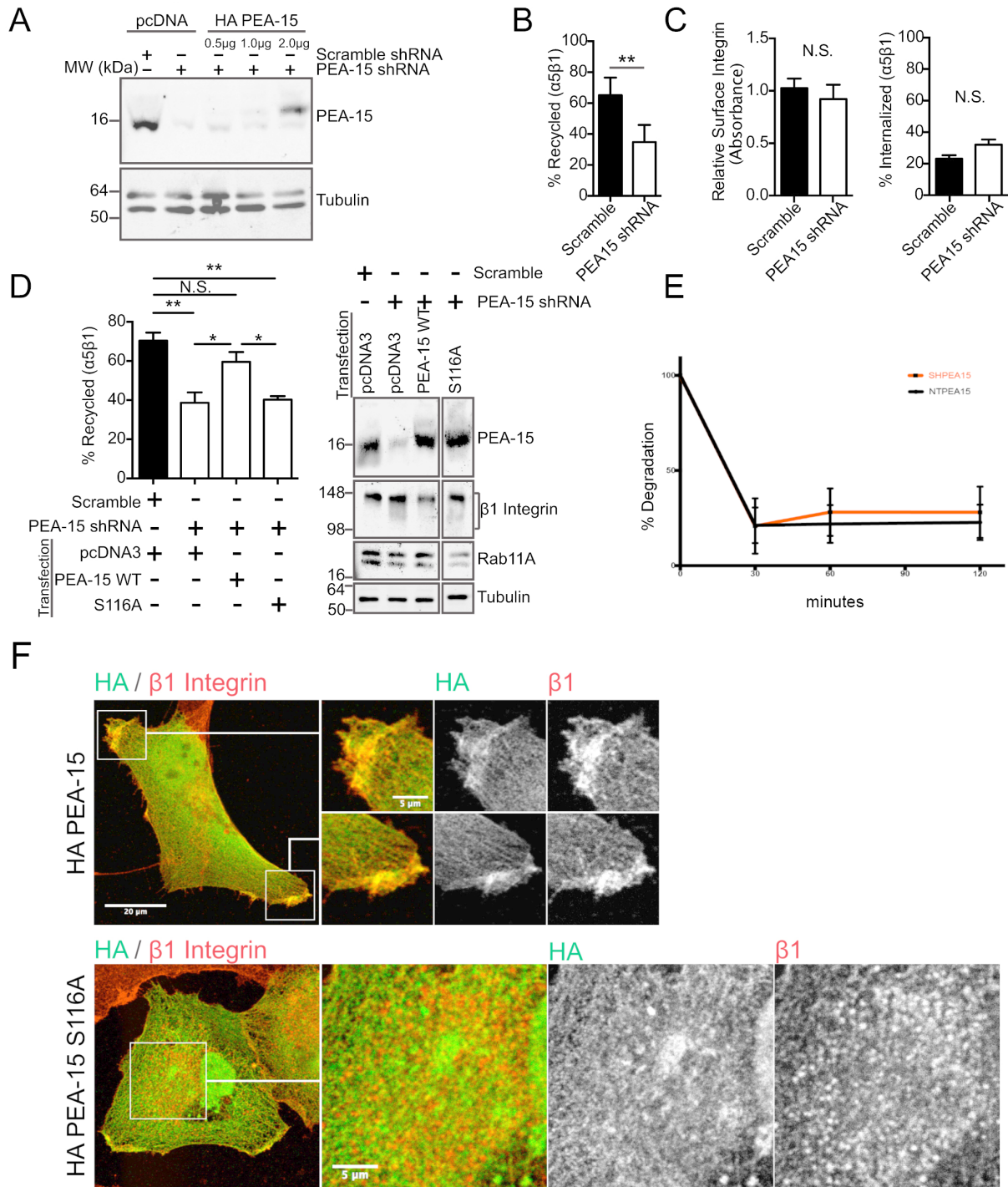


FIGURE 4.1 PHOSPHORYLATED PEA-15 REGULATES  $\alpha 5\beta 1$  INTEGRIN RECYCLING

4.1 A, the PEA-15 KD cell line was produced by lentiviral transduction of a pool of three PEA-15-targeting shRNAs (or scramble sequence) into U87MG cells. The rescue of PEA-15 expression by transfection with increasing amounts of plasmid is shown. B, the surface proteins in the indicated cell lines were labeled with membrane-impermeable sulfo-NHS-SS-biotin. Surface-biotinylated cells were then allowed to internalize integrins with serum starved media for 30 minutes(pulse). The remaining surface biotin was stripped, and internalized biotinylated proteins were chased back to the membrane by stimulation with media containing 10% serum. Recycled surface biotin was removed with a second round of stripping. Strip-resistant (un-recycled) biotinylated  $\alpha_5$  integrin was quantified by capture ELISA using anti- $\alpha_5$  antibodies. Recycling is expressed as a percent-change in signal from pulse controls. Shown is the percentage of internalized integrins recycled by 10 minutes after serum stimulation. C, surface-biotinylated cells were lysed, and the level of surface integrin  $\alpha_5\beta_1$  was quantified by capture ELISA. To measure integrin internalization, surface-biotinylated cells were treated with primaquine. Cells were then put on ice, and residual surface biotin was stripped. Strip-resistant (internalized) biotinylated integrins were quantified by capture ELISA and expressed as a percentage of surface integrin expression. Shown is internalization after 15 minutes with primaquine. D, Integrin recycling was rescued by re-expression of PEA-15 in the KD cells. Expression of the S116A mutant of PEA-15 failed to rescue integrin recycling. Expression of PEA-15,  $\beta_1$  integrin, and Rab11 was confirmed by western blot. (E) Effects of PEA-15 on integrin recycling are due to degradation  $\alpha_5\beta_1$ . F, HA-PEA-15 wild type or S116A mutant was expressed in KD cells. The cells were immunostained for HA tag and  $\beta_1$  integrin. (E, Young)

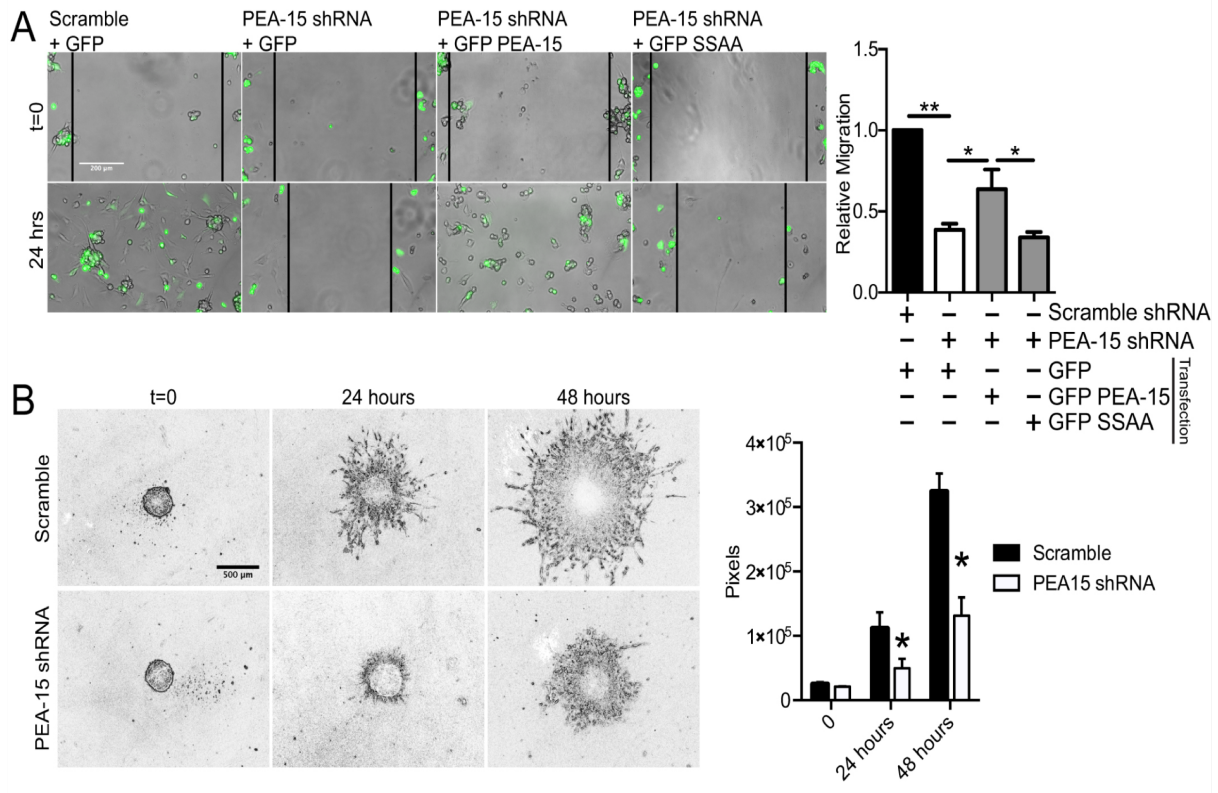


FIGURE 4.2 PEA-15 IS REQUIRED FOR CELL MIGRATION

4.2 A, PEA-15 KD cells were transfected with GFP empty vector or GFP-tagged PEA-15 or the double phosphomutant (SSAA) constructs. The cells were grown to confluence then scratched. Closure due to cell migration of GFP-expressing cells was observed over time. The closure distance was measured using ImageJ analysis software and expressed as relative migration. B, PEA-15 KD and scramble cells were embedded as spheroids in a 1:1 mixture of collagen and Matrigel. Invasion into the 3D matrix was followed over time. The images displayed here are the result of the Find Edges processing function of ImageJ which was performed before quantification of the pixel area taken up by the invading cell mass. (A, B Young)



4.3 (A) HA-tagged PEA-15 was expressed in HeLa cells and plated onto uncoated glass coverslips. The cells were incubated with purified GST-FN.11 which acts as a high affinity ligand for  $\alpha_5\beta_1$  integrins and is subsequently internalized with the integrin. The cells were fixed and stain for HA and GST. (B) Scramble and PEA-15 KD cells were replated on FN-coated glass coverslips and allow to adhere for 30 minutes. Cells were fixed and stained for  $\beta_1$ -integrin, Rab5, and Actin. The Pearson correlation between  $\beta_1$ -integrin and Rab 5 endosomes was measured using ImageJ and the JACoP plugin. (C) Bead-bound purified  $\beta_1$  - integrin cytoplasmic tails were incubated with lysate from HeLa cells expressing HA-tagged wild-type PEA-15 or S116A mutant. NPXA =  $\beta_1$  membrane proximal tyrosine mutated to alanine,  $\alpha$ IIb =  $\alpha$ IIb integrin cytoplasmic tail. HA-PEA-15 was detected in precipitates by western blot. (A, C, Young)

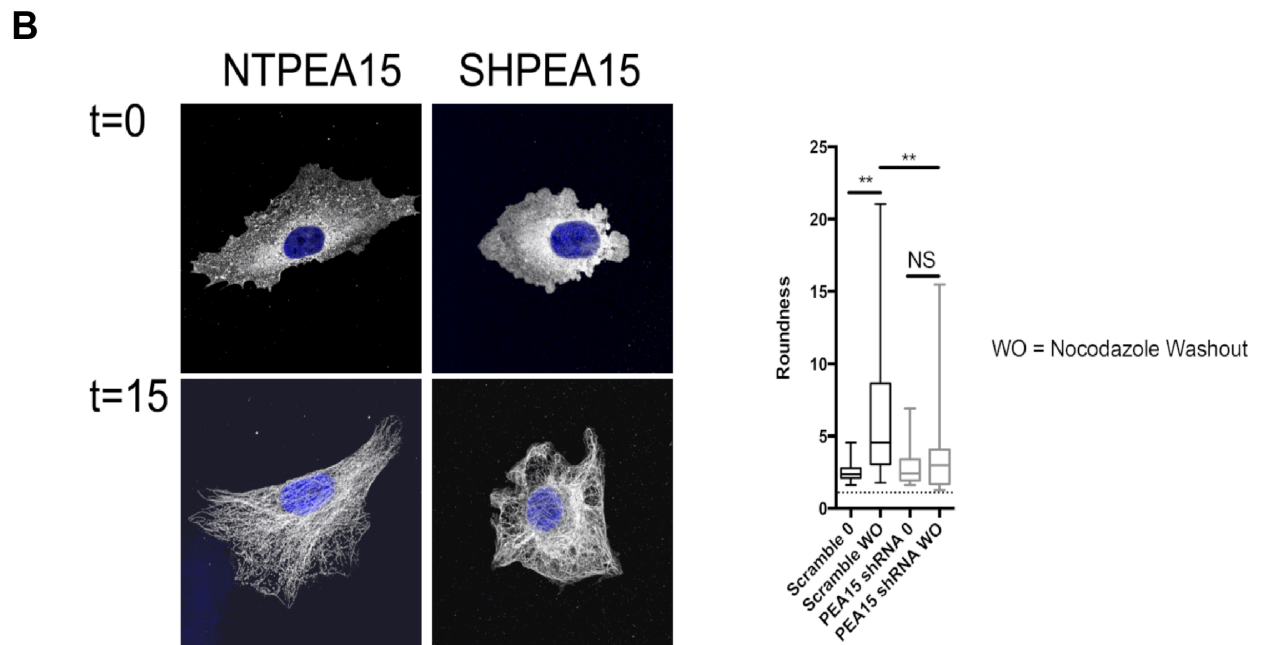
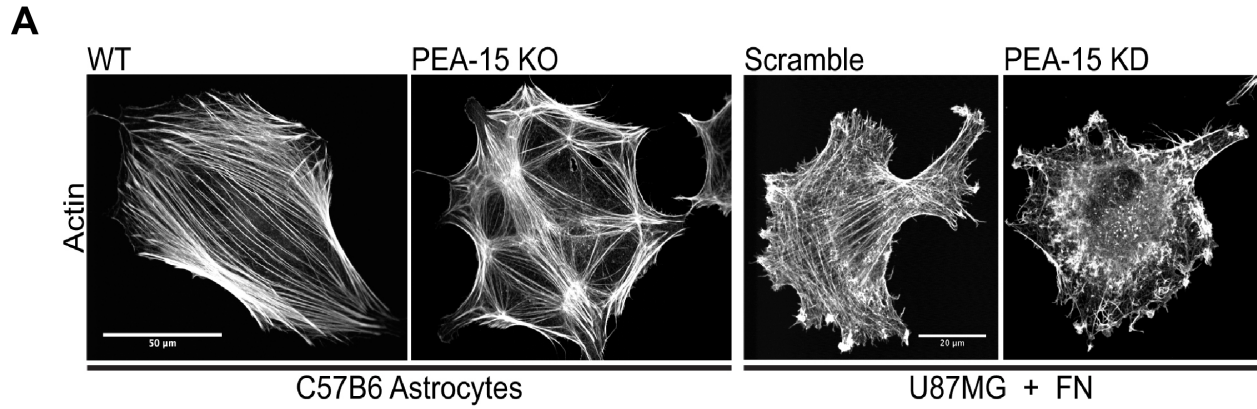


FIGURE 4.4 PEA-15 REGULATES CELL MORPHOLOGY IN A MICROTUBULE DEPENDENT MANNER

4.4 (A) Astrocytes were isolated from perinatal C57 Black 6 mice, fixed and stained for actin. The same was done for the scramble and PEA-15 KD U87MG cells, which were allowed to adhere to FN for 1 hour. (B) Scramble and PEA-15 KD U87MG cells were grown under normal growth conditions, then treated with nocodazole for 4 hours (0-time point). Nocodazole was then washed out, and cells were fixed after 15 minutes. The cells were immunostained for microtubules and was imaged using TCS SP5 confocal microscope. Roundness was measured with ImageJ both after nocodazole treatment and after washout. (B, Young)

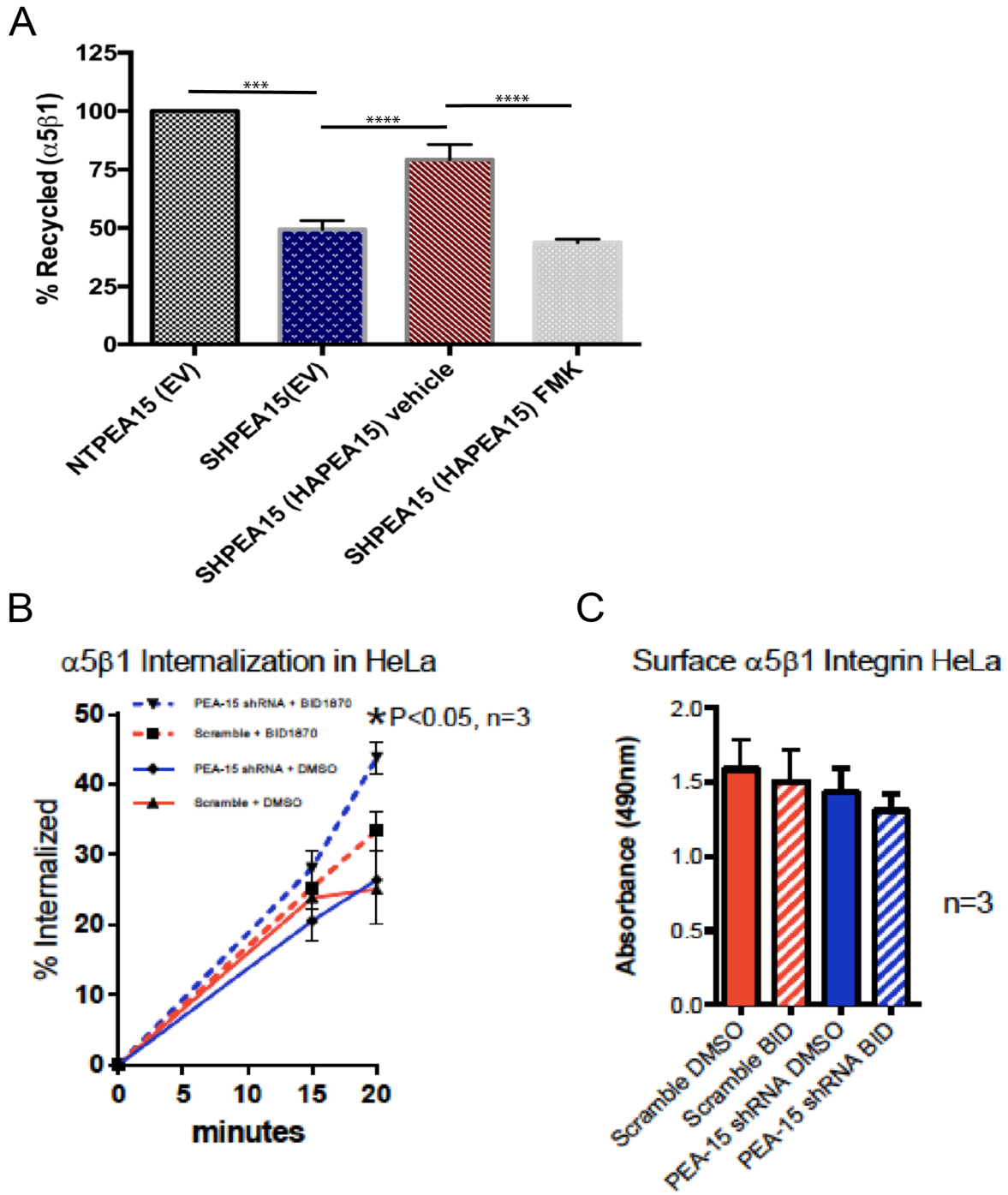


FIGURE 4.5 PEA-15 MEDIATED RECYCLING OF  $\alpha_5\beta_1$  INTEGRINS REQUIRES RSK2 ACTIVITY

4.5 (A) The recycling of the  $\alpha_5\beta_1$  integrins was assessed in PEA-15 scramble and PEA-15 KD HeLa cells. The effects of RSK2 inhibition on the rescue of reconstituted into HA-tagged PEA-15 in knock-down cells was examined by treatment with FMK or vehicle. Surface proteins were labeled with membrane-impermeable sulfo-NHS-SS-biotin, then allowed to internalize with serum starved media for 30 minutes(pulse). The remaining surface biotin was then stripped, and internalized biotinylated proteins were chased back to the membrane by stimulation with media containing 10% serum. Recycled surface biotin was stripped once more, and un-recycled biotinylated  $\alpha_5$  integrin was quantified by capture ELISA using anti- $\alpha_5$  antibodies. Recycling is expressed as a percent change in the signal from pulse controls. Shown is the percentage of internalized integrins recycled by 10 minutes after serum stimulation. (B) To measure integrin internalization, surface-biotinylated cells were treated with primaquine. Cells were placed on ice, and residual surface biotin was stripped. Internalized biotinylated integrins were quantified by capture ELISA and expressed as a percentage of surface integrin expression. Shown is internalization after 15 minutes with primaquine. (C) surface-biotinylated cells were lysed, and the level of surface integrin  $\alpha_5\beta_1$  was quantified by capture ELISA. (A,Young)

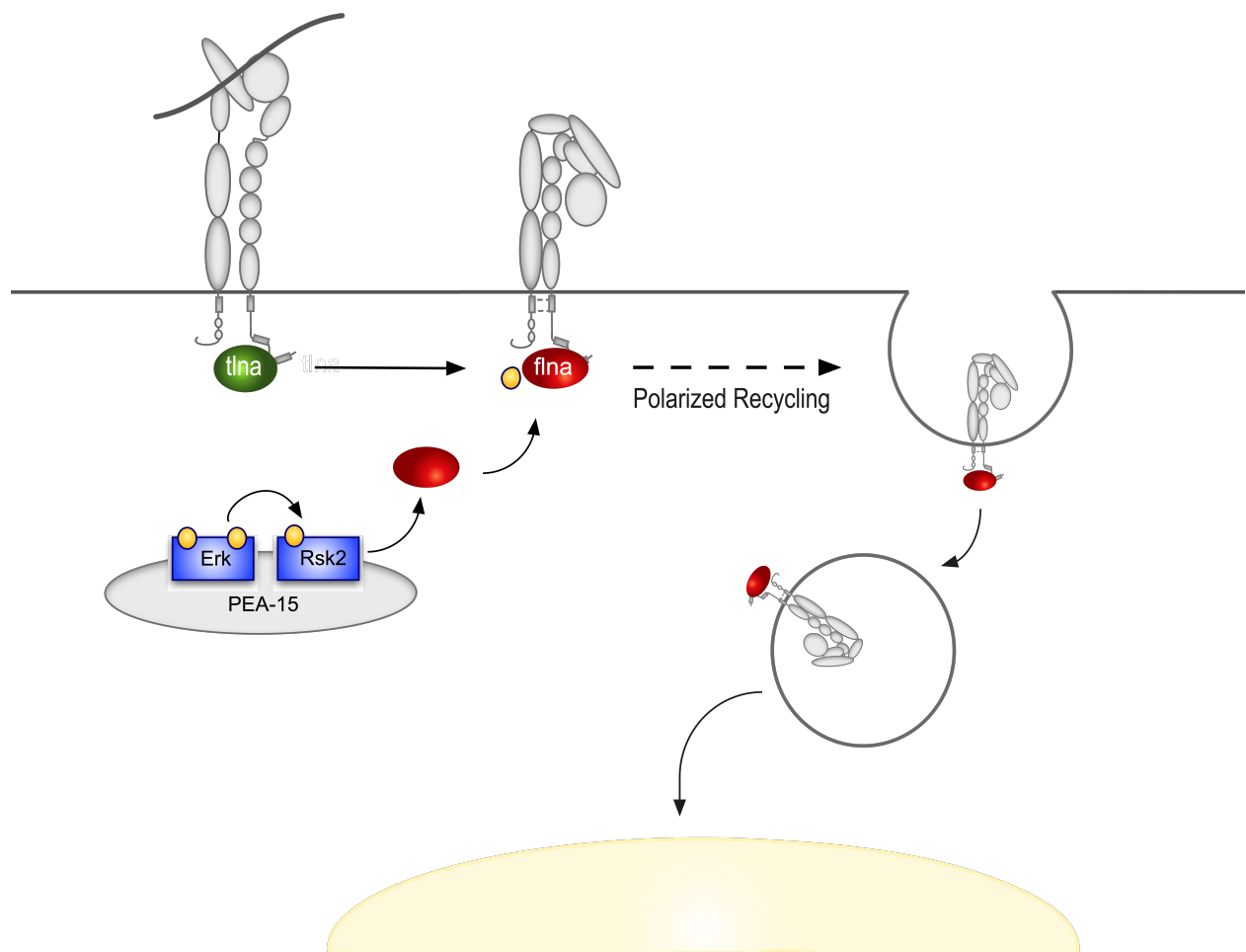


FIGURE 4.6 MODEL OF RSK2-PEA-15 AXIS REGULATING RECYCLING OF  $\alpha_5\beta_1$  INTEGRINS

4.6 Mitogenic stimulation of the RAS MAPK pathway leads to the activation of ERK. PEA-15 scaffolds ERK to RSK2 for the full activation of the latter. RSK2 transiently translocates to the plasma membrane where it phosphorylates filaminA and promotes its association with integrin  $\beta_1$ tail. PhosphofilaminA bind to and inactivates the  $\alpha_5\beta_1$  integrin. The inactivated integrin is endocytose in response to cell polarization and is trafficked to the early endosome. The inactive integrin is the recycled back to the leading edge via Rab 11.

CHAPTER 5  
FUTURE DIRECTION

## 5.1 DISCUSSION

In this study, we have examined RSK2 influence on integrin function in migration and invasion. Integrins modulate migration through spatial and temporal regulated cellular adhesions. We have shown that RSK2 inactivates integrins through posttranslational modification of the large scaffold protein filaminA. FilaminA can be cleaved by calpain to produce a 90 kDa fragment that translocates to the nucleus. Nuclear filaminA is associated with benign and localized prostate cancer, whereas high expression of cytosolic filaminA correlates with metastatic prostate cancer. Phosphorylation by RSK2 blocks calpain cleavage of filaminA and we provide evidence that this results in the redistribution of filaminA to the rear cytosolic region of the cell; where during migration focal adhesions are disassembled or recycled back to the advancing leading edge. We propose that filaminA is phosphorylated by upon RSK2 transient translocation to the plasma membrane and thereafter, filaminA translocates to the trailing edge where it inactivates integrins to drive migration.

We also find that PEA-15 can promote migration through regulation of integrin recycling in an RSK2 dependent manner. Endosomes transport cargo along microtubules tracks. We showed that PEA-15 localizes in endosomes and interacts with microtubules in a manner dependent on its phosphorylation status. Our data indicates that PEA-15 is required for efficient endosomal recycling of  $\alpha 5 \beta 1$  integrins. We found the recycling deficiency of PEA-15 depleted cells could be rescued by reconstitution of wild-type PEA-15, but not a phosphomutant at S116. PEA-15 is known to be phosphorylated by AKT at this residue. However, a recently a phosphoproteomic study revealed that this serine is also phosphorylated by RSK2. We found that reconstituted PEA-15 requires active RSK2 to

rescue recycling. We conclude that PEA-15 is an endosomal protein that forms an axis with RSK2 to mediate integrin recycling.

We report that RSK2 promoted invasion and migration in established glioblastoma cell lines and confirmed that RSK2 could also promote cell motility in freshly derived human GBM cells and into cultured mouse brain slices. We present data that indicates inhibition of RSK2 can sensitize GBM8 temozolomide resistant cells to chemotherapy treatment with temozolomide. In agreement with our in vitro data, using public datasets, we find that RSK2 is expression significantly upregulated in human GBM patients and correlates with advanced tumor stage and poor prognosis.

We have developed a model where activated RSK2 acts upon filaminA to promote recycling of inactivated integrins from trailing edge to the leading edge of a migrating cell (see figure 4.6). However, the assembly and disassembly of focal adhesions during cell migration is tightly regulated, which infers negative regulation. We propose that the lipid kinase, PIPK1 $\gamma$ 90, warrants investigation for a role in the model of RSK2 regulation of integrin adhesions in cell migration.

Phosphatidylinositol 4,5-bisphosphate (PIP<sub>2</sub>) highly enriched in the plasma membrane is an important lipid regulator in many physiological processes. PIP<sub>2</sub> is generated by the phosphorylation of phosphatidylinositol 4-phosphate (PIP) by type I phosphatidylinositol 4-phosphate -5-kinase (PIPK1)<sup>181, 182</sup>. There are three mammalian isoforms of PIPK1, PIPK1 $\alpha$ , PIPK1 $\beta$ , and PIPK1 $\gamma$ , whose subcellular distribution determine their function in physiological events<sup>181, 182</sup>. PIPK1 $\gamma$ , highly expressed in the brain, is comprised of two splice

variants: PIPK1 $\gamma$ 87 and PIPK1 $\gamma$ 90. PIPK1 $\gamma$ 90 has an additional 28 amino acids at its carboxy-terminal end (figure 5.1) that specifically targets its subcellular location to focal adhesions where it interacts with FA proteins; it activates both talin (refer to Introduction 1.1) and vinculin and inhibits filaminA crosslinking of actin<sup>45, 182, 183</sup>.

Src phosphorylates the tyrosine (Y649) in the carboxy-terminal WVYSPL sequence of PIPK1 $\gamma$ 90, which promotes PIPK1 $\gamma$ 90 binding to talin and release of talin autoinhibition (figure 5.2)<sup>45, 183-185</sup>. Unrestricted, talin then interacts with RAIM to form the integrin activation complex which is stabilized at the plasma membrane by electrostatic interaction between the talin head domain and PIP<sub>2</sub><sup>185</sup>. Phosphorylation of the neighboring serine by ERK prevents Src phosphorylation<sup>183</sup>. PIPK1 $\gamma$ 90 has also shown to undergo autophosphorylation, however, the functional consequence of this has not been determined<sup>183</sup>.

We analyzed the protein sequence of PIPK1 $\gamma$ 90 for an RSK2 consensus sequence using the NetPhos 2.0 Prediction software. We found that PIPK1 $\gamma$ 90 contains a serine at residue 555 valued at 0.968 indicating PIPK1 $\gamma$ 90 as a likely target of RSK2 (figure 5.1A). The sequence, RRRTQS<sup>555</sup>, aligns well the consensus sequence of RSK2, R/KXRXXS and the RSK2 phosphorylation sequence of filaminA, RRRAPS

We tested if PIPK1 $\gamma$ 90 could serve as a substrate of RSK2 using purified PIPK1 $\gamma$ 90 in an ATP-depletion *in vitro* kinase assay. PIPK1 $\gamma$ 90 We found that the presence of PIPK1 $\gamma$ 90 alone was able to generate a significant amount of ADP (figure 5.1C), which is indication of autophosphorylation (ref). However, we observed a sizable reduction in autophosphorylation

in the presence of active RSK2. Inhibition of RSK2 activity rescued PIPK1 $\gamma$ 90 autophosphorylation. Thus the data indicates that PIPK1 $\gamma$ 90 is a substrate of RSK2 and that phosphorylation by RSK2 inhibits PIPK1 $\gamma$ 90 autophosphorylation. . We also found that RSK2 and PIPK1 $\gamma$ 90 coprecipitated (figure 5.1B) and colocalized in membrane of membrane protrusions in response to EGF stimulation (figure 5.2).

We propose a new model (figure 5.3) of RSK2 regulation of cellular adhesions in migration incorporating our preliminary findings of RSK2 phosphorylation of PIPK1 $\gamma$ 90 (figure 5.3). In this model, PEA-15 scaffolds ERK to activates RSK2 in response to activated H-RAS. RSK2 translocates to the plasma membrane where it phosphorylates PIPK1 $\gamma$ 90. Inhibition of PIPK1 $\gamma$ 90 reduces the local pool of PIP<sub>2</sub> at the plasma membrane and as a consequence, talin becomes destabilized on the integrin tail and inhibition of filaminA is released. RSK2 phosphorylates filaminA, which binds to the integrin tail displacing talin. The integrin activating complex disassociates and activated ERK phosphorylates PIPK1 $\gamma$ 90 to prevent reactivation of PIPK1 $\gamma$ 90 by Src. The deactivated integrin is endocytosed in response to microtubule induce cell polarity and is sorted to the early endosomes.

In our model we would expect to see a reduction of talin and PIP<sub>2</sub> at the plasma membrane in the presence of active RSK2. This is exactly what *Le et al* observed in when they examine PIPK1 $\gamma$ 90 and talin localization using a phosphomimic of PIPK1 $\gamma$ 90 (S555D). They investigated PIPK1 $\gamma$ 90 as a substrate of AKT. They tested the ability of purified active AKT to phosphorylate GST-PIPK1 $\gamma$ 90 and discovered as we did that phosphorylation of S555 inhibited PIPK1 $\gamma$ 90 autophosphorylation. As mentioned previously RSK2 and AKT often

target the same substrates, therefore it is important when investigating AKT or RSK2 substrates to use appropriate inhibitors to verify the appropriate kinase in the cellular content. Recently PIPK1 $\gamma$ 90 has been shown to have an important role in the recycling of activated integrins. Nadar *et al.* find that FAK and Src colocalize with endocytosed integrins and that the function of FAK in the Rab11 endosomes is to maintain talin association with the integrin in a PIPK1 $\gamma$ 90-dependent manner. Recent studies confirm the importance of PIPK1 $\gamma$ 90 in regulating focal adhesion dynamics. We have demonstrated that RSK2 as a key regulator of integrin activity and propose a novel mechanism by which RSK2 promotes invasion and migration by regulating the local pool of PIP<sub>2</sub> in focal adhesions.

## 5.2 MATERIALS AND METHODS

### IMMUNOPRECIPITATION

Hela transfected with Genejuice and indicated cDNAs. 48 h later cells were lysed and incubated with antibody specific for Human influenza hemagglutinin (HA) or GFP overnight. The immunoprecipitates were isolated from the lysates with A/G agarose beads (Santa Cruz, which were washed twice with lyses buffer, then resuspended in SDS sample buffer, heated for 5 min at 95°C. Immunoprecipitated RSK2 and PIPK1 $\gamma$ 90 was detected by western blot.

### IMMUNOSTAINING AND MICROSCOPY

Cells transfected with Genejuice with the indicated cDNAs. After 24 h, cells were seeded onto fibronectin-coated glass coverslips. 48 h posttransfection, the cells were stimulated with EFG (100ng/ml), fixed with 4% paraformaldehyde, permeabilized and blocked. The cells were then stained with the indicated antibodies. Confocal imaging was performed on a Leica TCS SP5 with 63X Oil Objective (Leica, Solms Germany).

### ADP-GLO KINASE ASSAY

Recombinant GST- PIPK1 $\gamma$ 90 was purified and used as substrate in a ADP-Glo Kinase Assay. The *in vitro* luminescence kinase reaction were performed according to the manufacturer's directions. Briefly, 10  $\mu$ g GST- PIPK1 $\gamma$ 90 or SP6 (RRRLSSLR) peptide was incubated with 100 ng of immunoprecipitated RSK2, and 1.25 nmol of ATP in the presence of BI-D1870 (10  $\mu$ M) or vehicle. The kinase reactions were carried out at 37 C for 15 minutes; then, terminated and remaining ATP depleted by the addition of ATP-Glo reagent for 40 minutes

at room temperature. The remaining ADP was converted to ATP, which is detected via a luciferase/luciferin reaction by addition of Kinase Detection Reagent for 30 minutes at room temperature. The amount of luminescence generated in the reaction was quantified using the PerkinElmer EnVison Multilabel Reader.

## 5.3 FIGURES

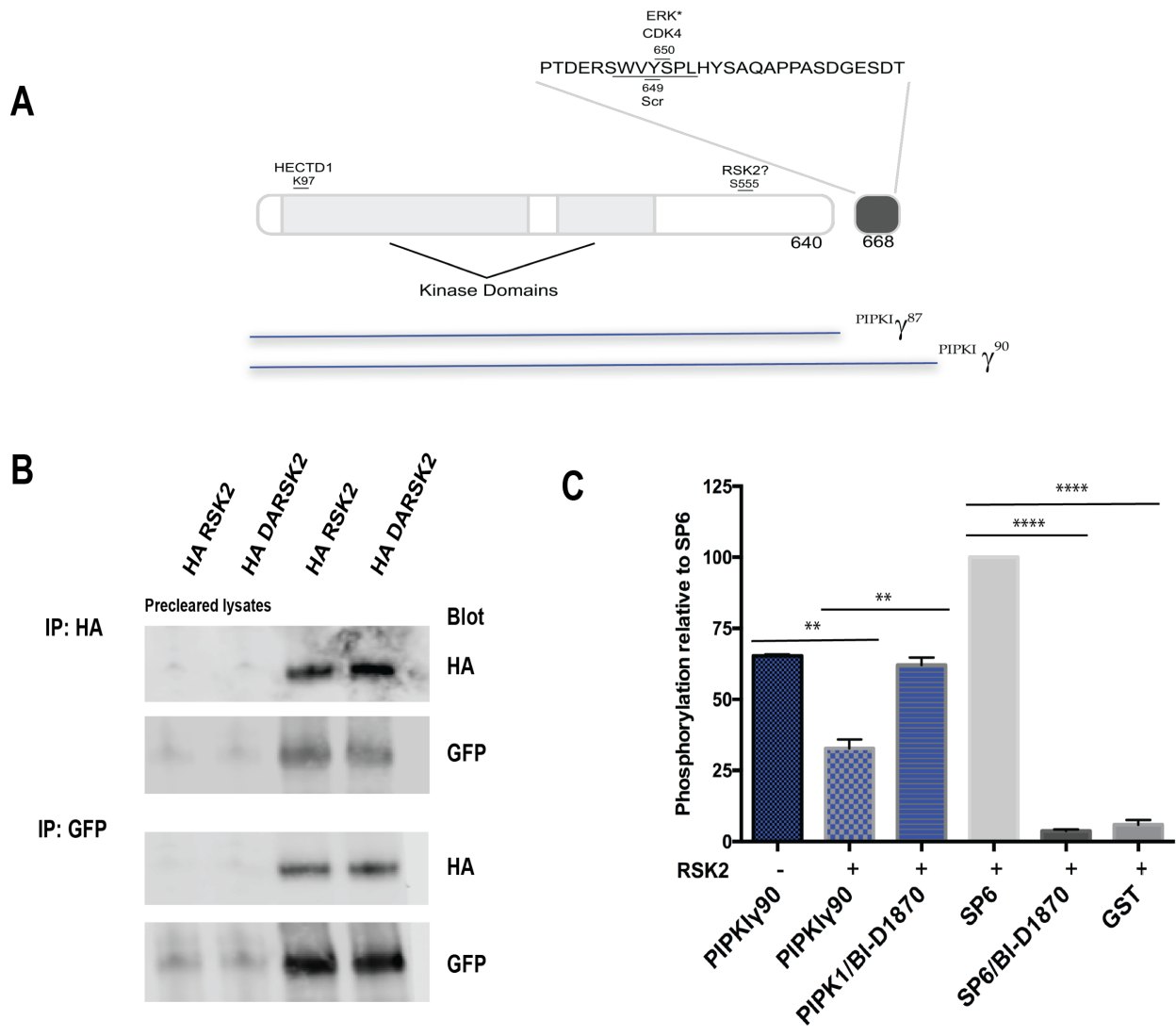


FIGURE 5.1 PIPK1 $\gamma^{90}$  IS A SUBSTRATE OF RSK2

5.1 (A) Diagram of PIPK1 $\gamma$  splice variants. The last 25 amino acids in PIPK1 $\gamma$ 90 target the kinase to focal adhesions. (B) PIPK1 $\gamma$ 90 coimmunoprecipitates with of wild-type and dominant active RSK2 and the reverse immunoprecipitation. (C) Recombinant PIPK1 $\gamma$ 90 was incubated alone, with purified active RSK2 alone, and with purified active RSK2 and RSK2 inhibitor BI-D1870. SP6 substrate served as a positive control for purified active RSK2 and RSK2 inhibitor BI-D1870. Lack of phosphorylation with purified GST indicates that purified active RSK2 does not contribute to the phosphorylation signal.

PIPK1 $\gamma$ 90

RSK2

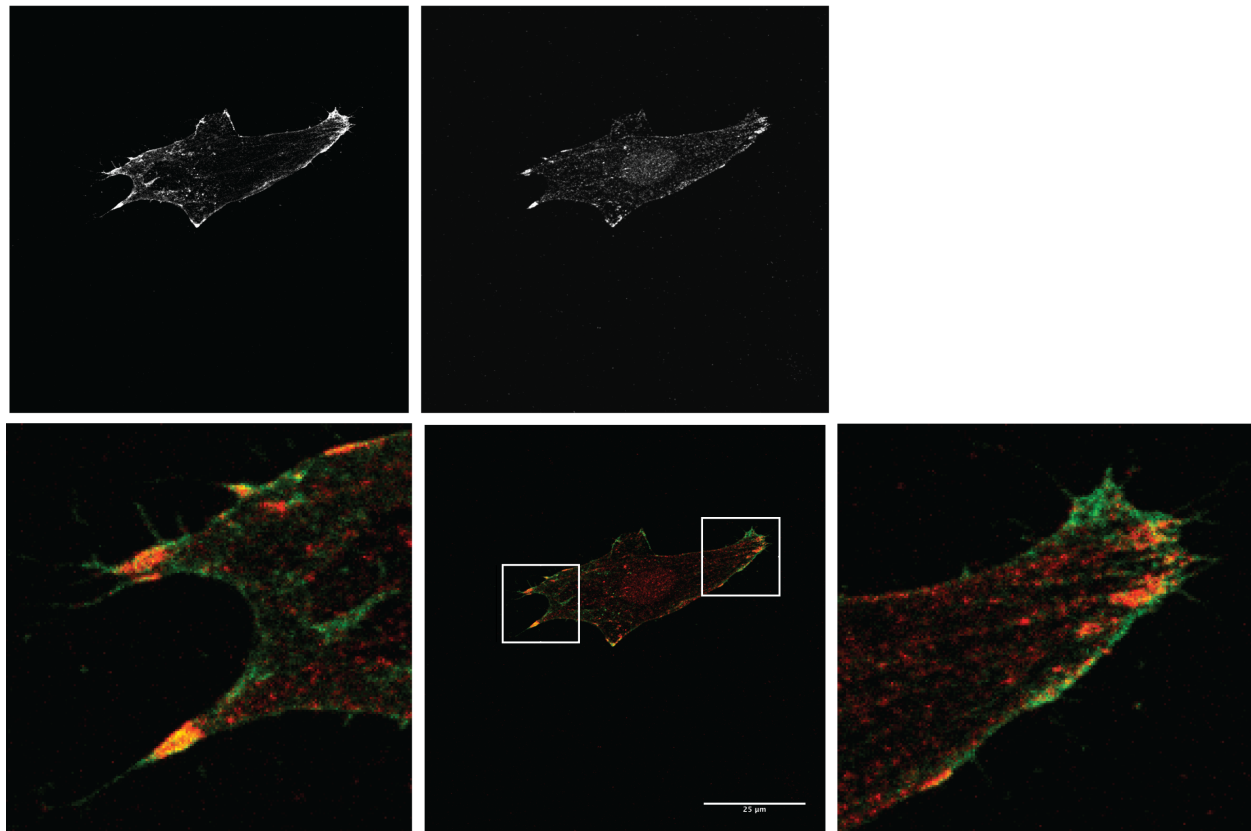


FIGURE 5.2 COLOCAZIATION OF PIPK1 $\gamma$ 90 AND RSK2

5.2 GFP- PIPK1 $\gamma$ 90 was expressed in U373MG cells. The cells were stimulated with EGF (100 ng/ml) for 30 minutes, then fixed and stained for RSK2.

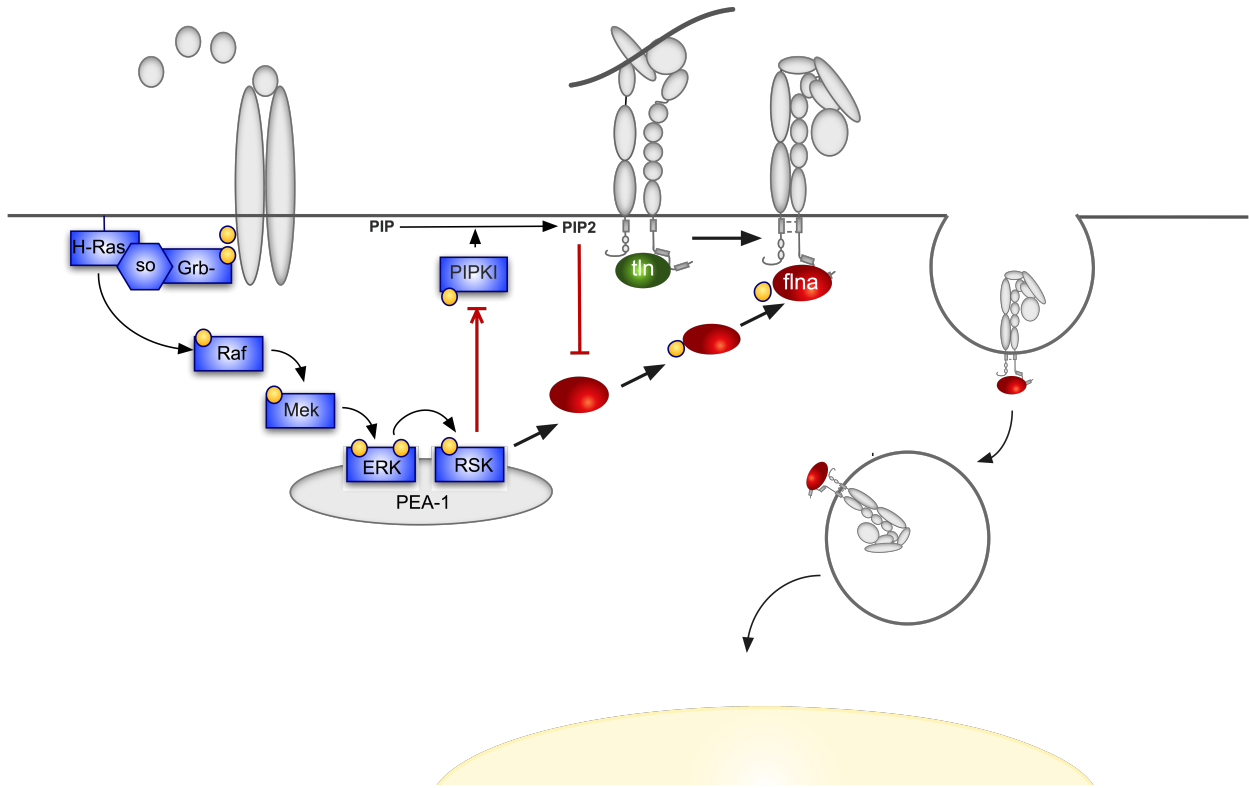


FIGURE 5.3 RSK2 REGULATES CELL ADHESION TO PROMOTE MIGRATION THROUGH PHOSPHORYLATION OF FILAMINA AND PIPK1 $\gamma$ 90.

5.3 Model. PEA-15 scaffolding of ERK and RSK2 activates the latter in response to activation of H-RAS. RSK2 translocates to the plasma membrane where it phosphorylates PIPK1 $\gamma$ 90. Inhibition of PIPK1 $\gamma$ 90 reduces the local pool of PIP<sub>2</sub> at the plasma membrane and as a consequence talin becomes destabilized on the integrin tail and inhibition of filaminA is released. RSK2 phosphorylates filaminA, which displaces talin on the integrin tail. The integrin activating complex disassociates and activated ERK phosphorylates PIPK1 $\gamma$ 90 to prevent reactivation of PIPK1 $\gamma$ 90 by Src. The deactivated integrin is endocytosed in response to microtubule induce cell polarity and is sorted to the early endosomes.

## APPENDIX

### PRIMERS DESIGNED FOR THIS STUDY

#### **Integrin**

$\beta$ 1 NPxA<sub>Distal</sub> F

CTG TGG TCA ATC CGA AGG CTG AGG GAA AAT GAT GAC CTA GGC CGG

$\beta$ 1 NPxA<sub>Distal</sub> R

CGG CTT CCG GCC TAG GTC ATC ATT TTC CCT CAG CCT TCG GAT TGA CC

$\beta$ 1 NPxA/NPxA F

CAG TGA CAA CTG TGG TCA ATC CTA AAG CTG AGG GAA AAT GAT GAG GAT CC

$\beta$ 1 NPxA/NPxA R

GCA GCC GGA TCC TCA TCA TTT TCC CTC AGC TTT AGG ATT GAC CAC AG

$\beta$ 7 NPxA F

GCA GGA CAG TAA TCC TCT CGC CAA AAG TGC CAT CAC GAC CAC C

$\beta$ 7 NPxA R

GCG AGG ATT GAT GGT GGT CGT GAT GGC ACT TTT GGC GAG AGG ATT ACT GTC

#### **PIP1 $\gamma$ 90**

264 Peptide F

ACC GTC ATG CAC AAG G

264 Peptide R

GAT CTT GAA ACT TTC CAG GAC

402 Peptide F

GGC GTG CAC AAC ATC GAC C

402 Peptide R

CCC ATC GTG GAC GAG GGC CTT

D253 F

GCG TGG TCA AGA TGC ACC TCA AGT TCG CCC TCA AGG GCT C

D253 R

CCG CTT GTA GGT GGA GCC CTT GAG GGC GAA CTT GAG GTG C

S555A F

GCG GTA CAG GCG GCG CAC ACA GGC GTC TGG ACA GGA TGG

S555A R

GGC CTG CCA TCC TGT CCA GAC GCC TGT GTG CGC CGC CTG

S555D F

GCG GTA CAG GCG GCG CAC ACA GGA CTC TGG ACA GGA TGG

S555D R

GGC CTG CCA TCC TGT CCA GAG TCC TGT GTG CGC CGC CTG

S555E F

GCG GTA CAG GCG GCG CAC ACA GGA GTC TGG ACA GGA TGG

S555E R

GGC CTG CCA TCC TGT CCA GAC TCC TGT GTG CGC CGC CTG

Y649R F

GCT GGG TGT ACT CCC CGC TCC ACT TTA GCG CCC AGG

Y649R R

GGC CGG GGG GGC CTG GGC GCT AAA GTG GAG CGG GGA

### **UniRapR RSK2 (Y707A)**

UniRapR RSK2<sub>CTKD</sub> Mega Primer F

TCA TAC TCC GTT TGT AAG AGA TGT ATA CAT

UniRapR RSK2<sub>CTKD</sub> Mega Primer R

ATC AAT AAT CTT CAC GGC AAA CTC CAT GTT

UniRapR RSK2 (pKH3) Gibson Assembly F1 F

CGA TGT TCC AGA TTA CGC TGG ATC C

UniRapR RSK2 (pKH3) Gibson Assembly F3 R

GCG GCC ATC GAT TGA ATT CGG ATC C

UniRapR RSK2<sub>CTKD</sub> Gibson Assembly F1 R

AGT GCA CCA CGC AGG TAC CTG GTC CAT GTA TAC ATC TCT TAC AAA CGG AG

UniRapR RSK2<sub>CTKD</sub> Gibson Assembly F2 F

CTC CGT TTG TAA GAG ATG TAT ACA TGG ACC AGG TAC CTG CGT GGT GCA CT

UniRapR RSK2<sub>CTKD</sub> Gibson Assembly F2 R

TAA TCT TCA CGG CAA ACT CCA TGT TTC CGG GAC CTT CCA GTT TTA GAA GC

UniRapR RSK2<sub>CTKD</sub> Gibson Assembly F3 F

GCT TCT AAA ACT GGA AGG TCC CGG AAA CAT GGA GTT TGC CGT GAA GAT TA

UniRapR RSK2<sub>NTKD</sub> Gibson Assembly F1R

AGT GCA CCA CGC AGG TAC CTG GTC CGA TTT TTT TAA CTA AGA AAA CCT TT

UniRapR RSK2<sub>NTKD</sub> Gibson Assembly F2 F

AAA GGT TTT CTT AGT TAA AAA AAT CGG ACC AGG TAC CTG CGT GGT GCA CT

UniRapR RSK2<sub>NTKD</sub> Gibson Assembly F2 R

Check should be same as CTKD

UniRapR RSK2<sub>NTKD</sub> Gibson Assembly F3 F

GCT TCT AAA ACT GGA AGG TCC CGG AGA TGC TAG ACA GCT TTA TGC CAT GA

## REFERENCES

1. Hynes, R.O. Integrins: a family of cell surface receptors. *Cell* **48**, 549-554 (1987).
2. Hynes, R.O. The emergence of integrins: a personal and historical perspective. *Matrix Biol* **23**, 333-340 (2004).
3. Ali, I.U., Mautner, V., Lanza, R. & Hynes, R.O. Restoration of normal morphology, adhesion and cytoskeleton in transformed cells by addition of a transformation-sensitive surface protein. *Cell* **11**, 115-126 (1977).
4. Yamada, K.M., Yamada, S.S. & Pastan, I. Cell surface protein partially restores morphology, adhesiveness, and contact inhibition of movement to transformed fibroblasts. *Proc Natl Acad Sci U S A* **73**, 1217-1221 (1976).
5. Pierschbacher, M.D. & Ruoslahti, E. Cell attachment activity of fibronectin can be duplicated by small synthetic fragments of the molecule. *Nature* **309**, 30-33 (1984).
6. Damsky, C.H., Knudsen, K.A., Bradley, D., Buck, C.A. & Horwitz, A.F. Distribution of the cell substratum attachment (CSAT) antigen on myogenic and fibroblastic cells in culture. *J Cell Biol* **100**, 1528-1539 (1985).
7. Chen, W.T., Hasegawa, E., Hasegawa, T., Weinstock, C. & Yamada, K.M. Development of cell surface linkage complexes in cultured fibroblasts. *J Cell Biol* **100**, 1103-1114 (1985).
8. Tamkun, J.W. *et al.* Structure of integrin, a glycoprotein involved in the transmembrane linkage between fibronectin and actin. *Cell* **46**, 271-282 (1986).
9. Hynes, R.O. Integrins: bidirectional, allosteric signaling machines. *Cell* **110**, 673-687 (2002).
10. Adair, B.D. & Yeager, M. Three-dimensional model of the human platelet integrin alpha IIb beta 3 based on electron cryomicroscopy and x-ray crystallography. *Proc Natl Acad Sci U S A* **99**, 14059-14064 (2002).
11. Vinogradova, O., Haas, T., Plow, E.F. & Qin, J. A structural basis for integrin activation by the cytoplasmic tail of the alpha IIb-subunit. *Proc Natl Acad Sci U S A* **97**, 1450-1455 (2000).

12. Hughes, P.E., O'Toole, T.E., Ylanne, J., Shattil, S.J. & Ginsberg, M.H. The conserved membrane-proximal region of an integrin cytoplasmic domain specifies ligand binding affinity. *J Biol Chem* **270**, 12411-12417 (1995).
13. Hughes, P.E. *et al.* Breaking the integrin hinge. A defined structural constraint regulates integrin signaling. *J Biol Chem* **271**, 6571-6574 (1996).
14. Sethi, T., Ginsberg, M.H., Downward, J. & Hughes, P.E. The Small GTP-binding Protein R-Ras Can Influence Integrin Activation by Antagonizing a Ras/Raf-initiated Integrin Suppression Pathway. *Molecular Biology of the Cell* **10**, 1799-1809 (1999).
15. Zhang, Z., Vuori, K., Wang, H.-G., Reed, J.C. & Ruoslahti, E. Integrin Activation by R-ras. *Cell* **85**, 61-69.
16. Lafuente, E.M., A.F.L. van Puijenbroek, A., Krause, M., Carman, C.V., Freeman, G.J., Berezovskaya, A., Constantine, E., Springer, T.A. & Gertler, F.B.B., V.A. RIAM, an Ena/VASP and Profilin ligand, interacts with Rap1-GTP and mediates Rap1-induced adhesion. *Developmental Cell* **7**, 585-595 (2004).
17. Lee, H.-S., Lim, C.J., Puzon-McLaughlin, W., Shattil, S.J. & Ginsberg, M.H. RIAM Activates Integrins by Linking Talin to Ras GTPase Membrane-targeting Sequences. *The Journal of Biological Chemistry* **284**, 5119-5127 (2009).
18. Lafuente, E.M. *et al.* RIAM, an Ena/VASP and Profilin ligand, interacts with Rap1-GTP and mediates Rap1-induced adhesion. *Dev Cell* **7**, 585-595 (2004).
19. Han, J. *et al.* Reconstructing and deconstructing agonist-induced activation of integrin alphaIIb beta3. *Curr Biol* **16**, 1796-1806 (2006).
20. Schramp, M., Hedman, A., Li, W., Tan, X. & Anderson, R. PIP Kinases from the Cell Membrane to the Nucleus. *Subcell Biochem* **58**, 25-59 (2012).
21. Ling, K., Doughman, R.L., Firestone, A.J., Bunce, M.W. & Anderson, R.A. Type I gamma phosphatidylinositol phosphate kinase targets and regulates focal adhesions. *Nature* **420**, 89-93 (2002).
22. Martel, V. *et al.* Conformation, localization, and integrin binding of talin depend on its interaction with phosphoinositides. *J Biol Chem* **276**, 21217-21227 (2001).
23. Wang, J.H. Pull and push: talin activation for integrin signaling. *Cell Res* **22**, 1512-1514 (2012).

24. Karaköse, E., Schiller, H.B. & Fässler, R. The kindlins at a glance. *Journal of Cell Science* **123**, 2353-2356 (2010).
25. Calderwood, D.A., Campbell, I.D. & Critchley, D.R. Talins and kindlins: partners in integrin-mediated adhesion. *Nat Rev Mol Cell Biol* **14**, 503-517 (2013).
26. Bouvard, D., Pouwels, J., De Franceschi, N. & Ivaska, J. Integrin inactivators: balancing cellular functions in vitro and in vivo. *Nat Rev Mol Cell Biol* **14**, 430-442 (2013).
27. Rantala, J.K. *et al.* SHARPIN is an endogenous inhibitor of beta1-integrin activation. *Nature Cell Biology* **13**, 1315-1324 (2011).
28. Legate, K.R. & Fässler, R. Mechanisms that regulate adaptor binding to  $\beta$ -integrin cytoplasmic tails. *Journal of Cell Science* **122**, 187-198 (2009).
29. Calderwood, D.A., Zent, R., Grant, R., Rees, D.J., Hynes, R.O., & Ginsberg, M.H. The Talin head domain binds to integrin beta subunit cytoplasmic tails and regulates integrin activation. *Journal of Biological Chemistry* **274**, 28071-28074 (1999).
30. Margadant, C., Kreft M., Jan de Groot, D., Norman, J.C. and Sonnenberg, A. Distinct roles of talin and kindlin in regulating integrin  $\alpha 5\beta 1$  function and trafficking. *Current Biology* **22**, 1-10 (2012).
31. Kiema, T., Lad, Y., Jiang, P., Oxley, C.L., Baldassarre, M., Wegener, K.L., Campbell, I.D., Ylanne, J., & Calderwood, D.A. The molecular basis of filamin binding to integrins and competition with talin. *Molecular cell* **21**, 337-347 (2006).
32. Nevo, J. *et al.* Mammary-derived growth inhibitor (MDGI) interacts with integrin  $[\alpha]$ -subunits and suppresses integrin activity and invasion. *Oncogene* **29**, 6452-6463 (2010).
33. Lauffenburger, D.A. & Horwitz, A.F. Cell migration: a physically integrated molecular process. *Cell* **84**, 359-369 (1996).
34. Ridley, A.J. *et al.* Cell migration: integrating signals from front to back. *Science* **302**, 1704-1709 (2003).
35. Vicente-Manzanares, M., Webb, D.J. & Horwitz, A.R. Cell migration at a glance. *J Cell Sci* **118**, 4917-4919 (2005).
36. Vicente-Manzanares, M., Choi, C.K. & Horwitz, A.R. Integrins in cell migration – the actin connection. *Journal of Cell Science* **122**, 199-206 (2009).

37. Amano, M. *et al.* Phosphorylation and activation of myosin by Rho-associated kinase (Rho-kinase). *J Biol Chem* **271**, 20246-20249 (1996).
38. Mitra, S.K., Hanson, D.A. & Schlaepfer, D.D. Focal adhesion kinase: in command and control of cell motility. *Nat Rev Mol Cell Biol* **6**, 56-68 (2005).
39. Kiyokawa, E. *et al.* Activation of Rac1 by a Crk SH3-binding protein, DOCK180. *Genes Dev* **12**, 3331-3336 (1998).
40. Parsons, J.T., Martin, K.H., Slack, J.K., Taylor, J.M. & Weed, S.A. Focal adhesion kinase: a regulator of focal adhesion dynamics and cell movement. *Oncogene* **19**, 5606-5613 (2000).
41. Huttenlocher, A. & Horwitz, A.R. Integrins in Cell Migration. *Cold Spring Harbor Perspectives in Biology* **3**, a005074 (2011).
42. Ezratty, E.J., Partridge, M.A. & Gundersen, G.G. Microtubule-induced focal adhesion disassembly is mediated by dynamin and focal adhesion kinase. *Nat Cell Biol* **7**, 581-590 (2005).
43. Nagano, M., Hoshino, D., Koshikawa, N., Akizawa, T. & Seiki, M. Turnover of focal adhesions and cancer cell migration. *International Journal of Cell Biology* **2012** (2012).
44. Ilic, D. *et al.* Reduced cell motility and enhanced focal adhesion contact formation in cells from FAK-deficient mice. *Nature* **377**, 539-544 (1995).
45. Nader, G.P.F., Ezratty, E.J. & Gundersen, G.G. FAK, talin and PIPKI[gamma] regulate endocytosed integrin activation to polarize focal adhesion assembly. *Nat Cell Biol* **18**, 491-503 (2016).
46. Nagano, M., Hoshino, D., Koshikawa, N., Akizawa, T. & Seiki, M. Turnover of focal adhesions and cancer cell migration. *Int J Cell Biol* **2012**, 310616 (2012).
47. Erikson, E. & Maller, J.L. A protein kinase from *Xenopus* eggs specific for ribosomal protein S6. *Proceedings of the National Academy of Sciences* **82**, 742-746 (1985).
48. Julien, L.A. & Roux, Philippe P. RSK3. *UCSD-Nature Molecule Pages* (2007).
49. Romain, L., Seckl, M.J. & Pardo, O.E. The p90 RSK Family Members: Common Functions and Isoform Specificity. *Cancer Research* **73**, 5301-5308 (2013).
50. Roux, Philippe P. RSK4. *UCSD-Nature Molecule Pages* (2007).
51. Roux, Philippe P. & Blenis, J. RSK1. *UCSD-Nature Molecule Pages* (2007).

52. Sulzmaier, F.J. & Ramos, J.W. RSK isoforms in cancer cell invasion and metastasis. *Cancer research* **73**, 6099-6105 (2013).
53. Wassarman, D.A., Solomon, N.M. & Rubin, G.M. The *Drosophila melanogaster* ribosomal S6 kinase II-encoding sequence. *Gene* **144**, 309-310 (1994).
54. Romeo, Y., Zhang, X. & Roux, Philippe P. Regulation and function of the RSK family of protein kinases. *Biochemical Journal* **441**, 553-569 (2012).
55. Carriere, A., Ray, H., Blenis, J. & Roux, Philippe P. The RSK factors of activating the Ras/MAPK signaling cascade. *Frontiers in Bioscience* **13**, 4258-4275 (2008).
56. Anjum, R.B., J. The RSK family of kinases: emerging roles in cellular signalling. *Nature Reviews Molecular Cell Biology* **9**, 747-758 (2008).
57. Dalby, K.N., Morrice, N., Caudwell, F.B., Avruch, J. & Cohen, P. Identification of Regulatory Phosphorylation Sites in Mitogen-activated Protein Kinase (MAPK)-activated Protein Kinase-1a/p90 rsk That Are Inducible by MAPK. *Journal of Biological Chemistry* **273**, 1496-1505 (1998).
58. Vaidyanathan, H. *et al.* ERK MAP kinase is targeted to RSK2 by the phosphoprotein PEA-15. *Proceedings of the National Academy of Sciences of the United States of America* **104**, 19837-19842 (2007).
59. Richards, S.A., Dreisbach, V.C., Murphy, L.O. & Blenis, J. Characterization of Regulatory Events Associated with Membrane Targeting of p90 Ribosomal S6 Kinase 1. *Molecular and Cellular Biology* **21**, 7470-7480 (2001).
60. Doehn, U., Gammeltoft, S., Shen, S.-H. & Jensen, Claus J. p90 ribosomal S6 kinase 2 is associated with and dephosphorylated by protein phosphatase 2C $\delta$ . *Biochemical Journal* **382**, 425-431 (2004).
61. Leighton, I.A., Dalby, K.N., Barry Caudwell, F., Cohen, P.T.W. & Cohen, P. Comparison of the specificities of p70 S6 kinase and MAPKAP kinase-1 identifies a relatively specific substrate for p70 S6 kinase: the N-terminal kinase domain of MAPKAP kinase-1 is essential for peptide phosphorylation. *FEBS Letters* **375**, 289-293 (1995).
62. Lara, R., Mauri, F.A., Taylor, H., Derua, R., Shia, A., Gray, C., Nicols, A., Shiner, R.J., Schofield, E., Bates, P.A., Waelkens, E., Dallman, M., Lamb, J., Zicha, D., Downward, J.,

- Seckl, M.J., & Pardo, O.E. An siRNA screen identifies RSK1 as a key modulator of lung cancer metastasis. *Oncogene* **30**, 3513-3521 (2011).
63. Chen, R.H., Abate, C. & Blenis, J. Phosphorylation of the c-Fos transrepression domain by mitogen-activated protein kinase and 90-kDa ribosomal S6 kinase. *Proceedings of the National Academy of Sciences of the United States of America* **90**, 10952-10956 (1993).
  64. Brüning, J.C. *et al.* Ribosomal subunit kinase-2 is required for growth factor-stimulated transcription of the c-Fos gene. *Proceedings of the National Academy of Sciences of the United States of America* **97**, 2462-2467 (2000).
  65. De Cesare, D., Jacquot, S., Hanauer, A. & Sassone-Corsi, P. Rsk-2 activity is necessary for epidermal growth factor-induced phosphorylation of CREB protein and transcription of c-fos gene. *Proceedings of the National Academy of Sciences of the United States of America* **95**, 12202-12207 (1998).
  66. Deak, M., Clifton, A.D., Lucocq, L.M. & Alessi, D.R. Mitogen- and stress-activated protein kinase-1 (MSK1) is directly activated by MAPK and SAPK2/p38, and may mediate activation of CREB. *The EMBO Journal* **17**, 4426-4441 (1998).
  67. Pierrat, B., Correia, J.d.S., Mary, J.-L., Tomás-Zuber, M. & Lesslauer, W. RSK-B, a Novel Ribosomal S6 Kinase Family Member, Is a CREB Kinase under Dominant Control of p38 $\alpha$  Mitogen-activated Protein Kinase (p38 $\alpha$ MAPK). *Journal of Biological Chemistry* **273**, 29661-29671 (1998).
  68. Clark, D.E. *et al.* The Serine/Threonine Protein Kinase, p90 Ribosomal S6 Kinase, Is an Important Regulator of Prostate Cancer Cell Proliferation. *Cancer Research* **65**, 3108-3116 (2005).
  69. Smith, J.A. *et al.* Identification of the First Specific Inhibitor of p90 Ribosomal S6 Kinase (RSK) Reveals an Unexpected Role for RSK in Cancer Cell Proliferation. *Cancer Research* **65**, 1027-1034 (2005).
  70. Chen, R.H., Juo, P.C., T., C. & Blenis, J. Phosphorylation of c-Fos at the C-terminus enhances its transforming activity. *Oncogene* **12**, 1493-1502 (1996).

71. Murphy, L.O., Smith, S., Chen, R.-H., Fingar, D.C. & Blenis, J. Molecular interpretation of ERK signal duration by immediate early gene products. *Nat Cell Biol* **4**, 556-564 (2002).
72. David, J.-P. *et al.* Essential role of RSK2 in c-Fos-dependent osteosarcoma development. *The Journal of Clinical Investigation* **115**, 664-672.
73. Fujita, N., Sato, S. & Tsuruo, T. Phosphorylation of p27Kip1 at Threonine 198 by p90 Ribosomal Protein S6 Kinases Promotes Its Binding to 14-3-3 and Cytoplasmic Localization. *Journal of Biological Chemistry* **278**, 49254-49260 (2003).
74. Roux, P.P., Ballif, B.A., Anjum, R., Gygi, S.P. & Blenis, J. Tumor-promoting phorbol esters and activated Ras inactivate the tuberous sclerosis tumor suppressor complex via p90 ribosomal S6 kinase. *Proceedings of the National Academy of Sciences of the United States of America* **101**, 13489-13494 (2004).
75. Anjum, R., Roux, P.P., Ballif, B.A., Gygi, S.P. & Blenis, J. The tumor suppressor DAP kinase is a target of RSK-mediated survival signaling. *Curr. Biol.* **15**, 1762-1767 (2005).
76. Bonni, A. Cell survival promoted by the Ras-MAPK signaling pathway by transcription-dependent and -independent mechanisms. *Science* **286**, 1358-1362 (1999).
77. Shimamura, A., Ballif, B.A., Richards, S.A. & Blenis, J. Rsk1 mediates a MEK-MAP kinase cell survival signal. *Curr. Biol.* **10**, 127-135 (2000).
78. Tan, Y., Ruan, H., Demeter, M.R. & Comb, M.J. p90RSK blocks Bad-mediated cell death via a protein kinase C-dependent pathway. *J. Biol. Chem.* **274**, 34859-34867 (1999).
79. Buck, M., Poli, V., Hunter, T. & Chojkier, M. C/EBP[beta] phosphorylation by RSK creates a functional XEXD caspase inhibitory box critical for cell survival. *Mol. Cell* **8**, 807-816 (2001).
80. Ghoda, L., Lin, X. & Greene, W.C. The 90-kDa ribosomal S6 kinase (pp90rsk) phosphorylates the N-terminal regulatory domain of I[kappa]B[alpha] and stimulates its degradation in vitro. *J. Biol. Chem.* **272**, 21281-21288 (1997).
81. Schouten, G.J. I[kappa]B [alpha] is a target for the mitogen-activated 90 kDa ribosomal S6 kinase. *EMBO J.* **16**, 3133-3144 (1997).

82. Hanauer, A. & Young, I.D. Coffin-Lowry syndrome: clinical and molecular features. *Journal of Medical Genetics* **39**, 705-713 (2002).
83. David, J.-P. *et al.* Essential role of RSK2 in c-Fos-dependent osteosarcoma development. *Journal of Clinical Investigation* **115**, 664-672 (2005).
84. Dumont, J., Umbhauer, M., Rassinier, P., Hanauer, A. & Verlhac, M.-H. p90Rsk is not involved in cytostatic factor arrest in mouse oocytes. *The Journal of Cell Biology* **169**, 227-231 (2005).
85. Smith, J.A., Maloney, D.J., Hecht, S.M. & Lannigan, D.A. Structural basis for the activity of the RSK-specific inhibitor, SL0101. *Bioorganic & Medicinal Chemistry* **15**, 5018-5034 (2007).
86. Nguyen, T.L. Targeting RSK: An Overview of Small Molecule Inhibitors. *Anti-Cancer Agents in Medicinal Chemistry- Anti-Cancer Agents* **8**, 710-716 (2008).
87. Sapkota, Gopal P. *et al.* BI-D1870 is a specific inhibitor of the p90 RSK (ribosomal S6 kinase) isoforms in vitro and in vivo. *Biochemical Journal* **401**, 29-38 (2007).
88. Cohen, M.S., Zhang, C., Shokat, K.M. & Taunton, J. Structural Bioinformatics-Based Design of Selective, Irreversible Kinase Inhibitors. *Science (New York, N.Y.)* **308**, 1318-1321 (2005).
89. Mizejewski, G.J. Role of Integrins in Cancer: Survey of Expression Patterns. *Proceedings of the Society for Experimental Biology and Medicine* **222**, 124-138 (1999).
90. Hood, J.D. & Cheresch, D.A. Role of integrins in cell invasion and migration. *Nat Rev Cancer* **2**, 91-100 (2002).
91. Gawecka, J.E., Young-Robbins, S. S., Sulzmaier, F. J., Caliva, M. J., Heikkilä, M. M., Matter, M. L., & Ramos, J. W. RSK2 protein suppresses integrin activation and fibronectin matrix assembly and promotes cell migration. *Journal of Biological Chemistry* **287**, 43424-43437 (2012).
92. Hynes, R.O. Integrins: a family of cell surface receptors. *Cell* **48**, 549-554 (1987).
93. Hynes, R.O. Integrins: bidirectional, allosteric signaling machines. *Cell* **110**, 673-687 (2002).

94. Friedl, P. & Wolf, K. Tumour-cell invasion and migration: diversity and escape mechanisms. *Nat Rev Cancer* **3**, 362-374 (2003).
95. Lauffenburger, D.A. & Horwitz, A.F. Cell migration: a physically integrated molecular process. *Cell* **84**, 359-369 (1996).
96. Hughes, P.E. *et al.* Suppression of integrin activation: a novel function of a Ras/Raf-initiated MAP kinase pathway. *Cell* **88**, 521-530 (1997).
97. Jeffrey, K.L., Camps, M., Rommel, C. & Mackay, C.R. Targeting dual-specificity phosphatases: manipulating MAP kinase signalling and immune responses. *Nat Rev Drug Discov* **6**, 391-403 (2007).
98. Liu, Y., Shepherd, E.G. & Nelin, L.D. MAPK phosphatases [mdash] regulating the immune response. *Nat Rev Immunol* **7**, 202-212 (2007).
99. Hughes, P.E., Oertli, B., Hansen, M., Chou, F.-L., Willumsen, B. M., & Ginsberg, M. H. Suppression of integrin activation by activated Ras or Raf does not correlate with bulk activation of ERK MAP kinase. . *Molecular Biology of the Cell* **13**, 2256-2265 (2002).
100. Flanagan, L.A. Filamin A, the Arp2/3 complex, and the morphology and function of cortical actin filaments in human melanoma cells. *J. Cell Biol.* **155**, 511-517 (2001).
101. Zeniou, M., Ding, T., Trivier, E. & Hanauer, A. Expression analysis of RSK gene family members: the RSK2 gene, mutated in Coffin-Lowry syndrome, is prominently expressed in brain structures essential for cognitive function and learning. *Hum Mol Genet* **11**, 2929-2940 (2002).
102. Yong-Yeon CHO, M.-h.l., cheol-jung lee, ke yao, hye suk lee, ann m. bode, zigang dong Rsk2 as a key regulator in human skin cancer. *Carcinogenesis* **33**, 2529-2537 (2012).
103. Anjum, R. & Blenis, J. The RSK family of kinases: emerging roles in cellular signalling. *Nat Rev Mol Cell Biol* **9**, 747-758 (2008).
104. Kang, S. & Chen, J. Targeting RSK2 in human malignancies. *Expert Opin Ther Targets* **15**, 11-20 (2011).
105. Lara, R. *et al.* An siRNA screen identifies RSK1 as a key modulator of lung cancer metastasis. *Oncogene* **30**, 3513-3521 (2011).

106. Pfaff, M., Liu, S., Erle, D.J. & Ginsberg, M.H. Integrin beta cytoplasmic domains differentially bind to cytoskeletal proteins. *J Biol Chem* **273**, 6104-6109 (1998).
107. Woo, M.S., Ohta, Y., Rabinovitz, I., Stossel, T.P. & Blenis, J. Ribosomal S6 kinase (RSK) regulates phosphorylation of filamin A on an important regulatory site. *Mol Cell Biol* **24**, 3025-3035 (2004).
108. Ohta, Y. & Hartwig, J.H. Phosphorylation of actin-binding protein 280 by growth factors is mediated by p90 ribosomal protein S6 kinase. *J Biol Chem* **271**, 11858-11864 (1996).
109. Ezratty, E.J., Partridge, M.A. & Gundersen, G.G. Microtubule-induced focal adhesion disassembly is mediated by dynamin and focal adhesion kinase. *Nature Cell Biology* **7**, 581-590 (2005).
110. van der Flier, A. & Sonnenberg, A. Structural and functional aspects of filamins. *Biochimica et Biophysica Acta (BBA) - Molecular Cell Research* **1538**, 99-117 (2001).
111. Shao, Q.-Q. *et al.* Filamin A: Insights into its Exact Role in Cancers. *Pathology & Oncology Research* **22**, 245-252 (2016).
112. Bedolla, R.G. *et al.* Nuclear vs Cytoplasmic localization of Filamin A in Prostate Cancer: Immunohistochemical Correlation with Metastases. *Clinical cancer research : an official journal of the American Association for Cancer Research* **15**, 788-796 (2009).
113. van der Flier, A. & Sonnenberg, A. Structural and functional aspects of filamins. *Biochim Biophys Acta* **1538** (2001).
114. Bedolla, R.G. *et al.* Nuclear versus cytoplasmic localization of filamin A in prostate cancer: immunohistochemical correlation with metastases. *Clin Cancer Res* **15** (2009).
115. Karginov, A.V. & Hahn, K.M. Allosteric activation of kinases: Design and application of RapR kinases. *Current Protocols in Cell Biology* **CHAPTER**, Unit-14.13. (2011).
116. Wombacher, R. *et al.* Live-cell super-resolution imaging with trimethoprim conjugates. *Nat. Methods* **7**, 717-719 (2010).
117. Sathornsumetee, S., Rich, J.N. & Reardon, D.A. Diagnosis and Treatment of High-Grade Astrocytoma. *Neurologic Clinics* **25**, 1111-1139 (2007).

118. Ostrom, Q.T. *et al.* CBTRUS Statistical Report: Primary Brain and Central Nervous System Tumors Diagnosed in the United States in 2008-2012. *Neuro-Oncology* **17**, iv1-iv62 (2015).
119. Alcantara Llaguno, S. *et al.* Malignant astrocytomas originate from neural stem/progenitor cells in a somatic tumor suppressor mouse model. *Cancer Cell* **15**, 45-56 (2009).
120. Ignatova, T.N. *et al.* Human cortical glial tumors contain neural stem-like cells expressing astroglial and neuronal markers in vitro. *Glia* **39**, 193-206 (2002).
121. Wen, P.Y. & Kesari, S. Malignant gliomas in adults. *N Engl J Med* **359**, 492-507 (2008).
122. Choucair, A.K. *et al.* Development of multiple lesions during radiation therapy and chemotherapy in patients with gliomas. *J Neurosurg* **65**, 654-658 (1986).
123. Bartek, J., Jr. *et al.* Key concepts in glioblastoma therapy. *J Neurol Neurosurg Psychiatry* **83**, 753-760 (2012).
124. Nakada, M. *et al.* Molecular targets of glioma invasion. *Cell Mol Life Sci* **64**, 458-478 (2007).
125. Winkler, F. *et al.* Imaging glioma cell invasion in vivo reveals mechanisms of dissemination and peritumoral angiogenesis. *Glia* **57**, 1306-1315 (2009).
126. Giese, A., Bjerkvig, R., Berens, M.E. & Westphal, M. Cost of migration: invasion of malignant gliomas and implications for treatment. *J Clin Oncol* **21**, 1624-1636 (2003).
127. Zhong, J., Paul, A., Kellie, S.J. & O'Neill, G.M. Mesenchymal migration as a therapeutic target in glioblastoma. *J Oncol* **2010**, 430142 (2010).
128. Hynes, R.O. Integrins: bidirectional, allosteric signaling machines. *Cell* **110**, 673-687 (2002).
129. D'Abaco, G.M. & Kaye, A.H. Integrins: Molecular determinants of glioma invasion. *Journal of Clinical Neuroscience* **14**, 1041-1048 (2007).
130. Gingras, M.-c., Roussel, E., Bruner, J.M., Branch, C.D. & Moser, r.P. Comparison of cell adhesion molecule expression between glioblastoma multiforme and autologous normal brain tissue. *Journal of Neuroimmunology* **57**, 143-153.
131. Paulus, W., Baur, I., Beutler, A.S. & Reeves, S.A. Diffuse brain invasion of glioma cells requires beta 1 integrins. *Lab. Invest.* **75**, 819-826 (1996).

132. Paulus, W., Baur, I., Schuppan, D. & Roggendorf, W. Characterization of integrin receptors in normal and neoplastic human brain. *The American Journal of Pathology* **143**, 154-163 (1993).
133. Rooprai, H.K. *et al.* The role of integrin receptors in aspects of glioma invasion in vitro. *International Journal of Developmental Neuroscience* **17**, 613-623 (1999).
134. Friedlander, D.R. *et al.* Migration of Brain Tumor Cells on Extracellular Matrix Proteins in Vitro Correlates with Tumor Type and Grade and Involves  $\alpha v$  and  $\beta 1$  Integrins. *Cancer Research* **56**, 1939-1947 (1996).
135. Ramos, J.W. The regulation of extracellular signal-regulated kinase (ERK) in mammalian cells. *Int J Biochem Cell Biol* **40**, 2707-2719 (2008).
136. Santarpia, L., Lippman, S.M. & El-Naggar, A.K. Targeting the MAPK-RAS-RAF signaling pathway in cancer therapy. *Expert Opin Ther Targets* **16**, 103-119 (2012).
137. Gawecka, J.E. *et al.* RSK2 Suppresses Integrin Activation and Fibronectin Matrix Assembly and Promotes Cell Migration. *J Biol Chem* (2012).
138. Frodin, M. & Gammeltoft, S. Role and regulation of 90 kDa ribosomal S6 kinase (RSK) in signal transduction. *Mol. Cell. Endocrinol.* **151**, 65-77 (1999).
139. Lin, J.-X., Spolski, R. & Leonard, W.J. Critical role for Rsk2 in T-lymphocyte activation. *Blood* **111**, 525-533 (2008).
140. Clark, D.E. The serine/threonine protein kinase, p90 ribosomal S6 kinase, is an important regulator of prostate cancer cell proliferation. *Cancer Res.* **65**, 3108-3116 (2005).
141. Cho, Y.-Y. *et al.* Ribosomal S6 Kinase 2 Is a Key Regulator in Tumor Promoter-Induced Cell Transformation. *Cancer research* **67**, 8104 (2007).
142. Doehn, U. *et al.* RSK is a principal effector of the RAS-ERK pathway for eliciting a coordinate, pro-motile/invasive gene program and phenotype in epithelial cells. *Molecular cell* **35**, 511-522 (2009).
143. Kang, S. *et al.* p90 ribosomal S6 kinase 2 promotes invasion and metastasis of human head and neck squamous cell carcinoma cells. *The Journal of Clinical Investigation* **120**, 1165-1177.

144. Feng, Y. *et al.* Filamin A (FLNA) is required for cell-cell contact in vascular development and cardiac morphogenesis. *Proc Natl Acad Sci USA* **103** (2006).
145. Feng, Y. & Walsh, C.A. The many faces of filamin: a versatile molecular scaffold for cell motility and signalling. *Nat Cell Biol* **6** (2004).
146. Popowicz, G.M., Schleicher, M., Noegel, A.A. & Holak, T.A. Filamins: promiscuous organizers of the cytoskeleton. *Trends Biochem Sci* **31** (2006).
147. Xu, Y. *et al.* Filamin A regulates focal adhesion disassembly and suppresses breast cancer cell migration and invasion. *J Exp Med* **207** (2010).
148. Kiema, T. *et al.* The molecular basis of filamin binding to integrins and competition with talin. *Mol Cell* **21** (2006).
149. Li, A. *et al.* Genomic Changes and Gene Expression Profiles Reveal That Established Glioma Cell Lines Are Poorly Representative of Primary Human Gliomas. *American Association for Cancer Research* **6**, 21-30 (2008).
150. Galli, R. *et al.* Isolation and Characterization of Tumorigenic, Stem-like Neural Precursors from Human Glioblastoma. *Cancer Research* **64**, 7011-7021 (2004).
151. Lee, J. *et al.* Tumor stem cells derived from glioblastomas cultured in bFGF and EGF more closely mirror the phenotype and genotype of primary tumors than do serum-cultured cell lines. *Cancer Cell* **9**, 391-403.
152. Kruskal, W.H. & Wallis, W.A. Use of Ranks in One-Criterion Variance Analysis. *Journal of the American Statistical Association* **47**, 583-621 (1952).
153. McDonald, J. Handbook of Biological statistics. *Sparky House Publishing* (2008).
154. Huse, J.T. & Holland, E.C. Targeting brain cancer: advances in the molecular pathology of malignant glioma and medulloblastoma. *Nat Rev Cancer* **10**, 319-331 (2010).
155. Shattil, S.J., Kim, C. & Ginsberg, M.H. The final steps of integrin activation: the end game. *Nature reviews. Molecular cell biology* **11**, 288-300 (2010).
156. Caswell, P.T. & Norman, J.C. Integrin Trafficking and the Control of Cell Migration. *Traffic* **7**, 14-21 (2006).
157. Ramsay, A.G. *et al.* HS1-Associated Protein X-1 Regulates Carcinoma Cell Migration and Invasion via Clathrin-Mediated Endocytosis of Integrin  $\alpha\beta 6$ . *Cancer Research* **67**, 5275-5284 (2007).

158. Caswell, P.T., Vadrevu, S. & Norman, J.C. Integrins: masters and slaves of endocytic transport. *Nat Rev Mol Cell Biol* **10**, 843-853 (2009).
159. Steinberg, F., Heesom, K.J., Bass, M.D. & Cullen, P.J. SNX17 protects integrins from degradation by sorting between lysosomal and recycling pathways. *The Journal of Cell Biology* **197**, 219-230 (2012).
160. Stehbens, S. & Wittmann, T. Targeting and transport: How microtubules control focal adhesion dynamics. *The Journal of Cell Biology* **198**, 481-489 (2012).
161. Ivaska, J., Whelan, R.D.H., Watson, R. & Parker, P.J. PKC $\epsilon$  controls the traffic of  $\beta$ 1 integrins in motile cells. *The EMBO Journal* **21**, 3608-3619 (2002).
162. Roberts, M., Barry, S., Woods, A., van der Sluijs, P. & Norman, J. PDGF-regulated rab4-dependent recycling of  $\alpha$ v $\beta$ 3 integrin from early endosomes is necessary for cell adhesion and spreading. *Current Biology* **11**, 1392-1402.
163. Li, J. *et al.* Phosphorylation of ACAP1 by Akt Regulates the Stimulation-Dependent Recycling of Integrin  $\alpha$ 5 $\beta$ 1 to Control Cell Migration. *Developmental Cell* **9**, 663-673 (2005).
164. Bridgewater, R.E., Norman, J.C. & Caswell, P.T. Integrin trafficking at a glance. *Journal of Cell Science* **125**, 3695-3701 (2012).
165. Gawecka, J.E. *et al.* PEA15 impairs cell migration and correlates with clinical features predicting good prognosis in neuroblastoma. *International journal of cancer. Journal international du cancer* **131**, 1556-1568 (2012).
166. Glading, A., Koziol, J.A., Krueger, J. & Ginsberg, M.H. PEA-15 Inhibits Tumor Cell Invasion by Binding to Extracellular Signal-Regulated Kinase 1/2. *Cancer Research* **67**, 1536-1544 (2007).
167. Lee, J. *et al.* PEA-15 unphosphorylated at both serine 104 and serine 116 inhibits ovarian cancer cell tumorigenicity and progression through blocking  $\beta$ -catenin. *Oncogenesis* **1**, e22 (2012).
168. Janouskova, H. *et al.* Integrin  $\alpha$ 5 $\beta$ 1 Plays a Critical Role in Resistance to Temozolomide by Interfering with the p53 Pathway in High-Grade Glioma. *Cancer Research* **72**, 3463-3470 (2012).

169. Martinkova, E. *et al.*  $\alpha 5\beta 1$  integrin antagonists reduce chemotherapy-induced premature senescence and facilitate apoptosis in human glioblastoma cells. *International Journal of Cancer* **127**, 1240-1248 (2010).
170. Serres, E. *et al.* Fibronectin expression in glioblastomas promotes cell cohesion, collective invasion of basement membrane in vitro and orthotopic tumor growth in mice. *Oncogene* **33**, 3451-3462 (2014).
171. Trecia, A. *et al.* Protein Kinase B/Akt Binds and Phosphorylates PED/PEA-15, Stabilizing Its Antiapoptotic Action. *Molecular and Cellular Biology* **23**, 4511-4521 (2003).
172. von Kriegsheim, A. *et al.* Cell fate decisions are specified by the dynamic ERK interactome. *Nature cell biology* **11**, 10.1038/ncb1994 (2009).
173. King, S.J. *et al.*  $\beta 1$  integrins regulate fibroblast chemotaxis through control of N-WASP stability. *The EMBO Journal* **30**, 1705-1718 (2011).
174. Galan, J.A. *et al.* Phosphoproteomic analysis identifies the tumor suppressor PDCD4 as a RSK substrate negatively regulated by 14-3-3. *Proceedings of the National Academy of Sciences* **111**, E2918-E2927 (2014).
175. Clark, M.J. *et al.* U87MG Decoded: The Genomic Sequence of a Cytogenetically Aberrant Human Cancer Cell Line. *PLoS Genetics* **6**, e1000832 (2010).
176. Sulzmaier, F.J., Opoku-Ansah, J. & Ramos, J.W. Phosphorylation is the switch that turns PEA-15 from tumor suppressor to tumor promoter. *Small GTPases* **3**, 173-177 (2012).
177. Siegrist, S.E. & Doe, C.Q. Microtubule-induced cortical cell polarity. *Genes & Development* **21**, 483-496 (2007).
178. Xie, X. *et al.* Bisphosphorylated PEA-15 Sensitizes Ovarian Cancer Cells to Paclitaxel by Impairing the Microtubule-Destabilizing Effect of SCLIP. *Molecular cancer therapeutics* **12**, 1099-1111 (2013).
179. Vinci, M. *et al.* Advances in establishment and analysis of three-dimensional tumor spheroid-based functional assays for target validation and drug evaluation. *BMC Biology* **10**, 1-21 (2012).

180. Pfaff, M., Liu, S., Erle, D.J. & Ginsberg, M.H. Integrin beta cytoplasmic domains differentially bind to cytoskeletal proteins. *Journal of Biological Chemistry* **273**, 6104-6109 (1998).
181. Schramp, M., Hedman, A., Li, W., Tan, X. & Anderson, R. PIP Kinases from the Cell Membrane to the Nucleus. *Subcell Biochem* **58**, 25-59 (2012).
- . *Subcellular Biochemistry* **58**, 25-59 (2012).
182. van den Bout, I. & Divecha, N. PIP5K-driven PtdIns(4,5)P<sub>2</sub> synthesis: regulation and cellular functions. *Journal of Cell Science* **122**, 3837-3850 (2009).
183. Lee, S.Y. *et al.* Regulation of the interaction between PIPK $\gamma$  and talin by proline-directed protein kinases. *The Journal of Cell Biology* **168**, 789-799 (2005).
184. Coló, G.P. *et al.* Focal adhesion disassembly is regulated by a RIAM to MEK-1 pathway. *Journal of Cell Science* **125**, 5338-5352 (2012).
185. Wang, J.-h. Pull and push: Talin activation for integrin signaling. *Cell Research* **22**, 1512-1514 (2012).